AD 273 170

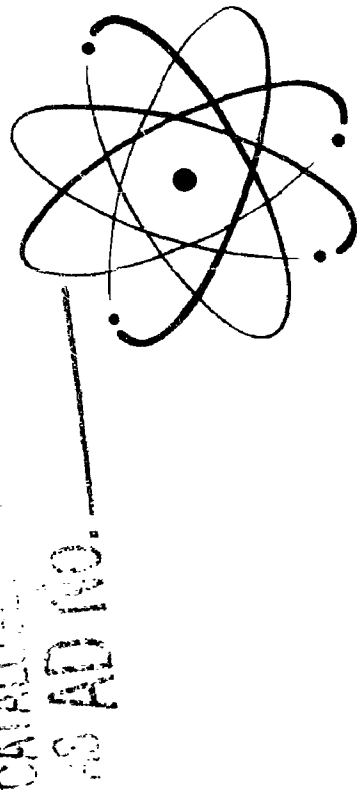

INTERIM ENGINEERING REPORT NO. 3

Research and Investigation on Radiation Resistant, High Temperature Thermionic Circuitry

Period Covered - October 1, 1961 - December 31, 1961

Project Engineer - Fred J. Schmidt
Advanced Development Engineering

AF 33(616)-8096

"The applied research reported in this document has been made possible through support and sponsorship extended by the Electronic Technology (WWRNE) Laboratory of the Wright Air Development Division, under Contract AF 33(616)-8096. It is published for technical information only, and does not necessarily represent recommendations or conclusions of the sponsoring agency."

RECEIVING TUBE DEPARTMENT

GENERAL ELECTRIC

OWENSBORO, KENTUCKY

A B S T R A C T

The present report covers the experimental work conducted during the third quarter of a planned six-quarter program directed toward the development of high temperature, nuclear radiation resistant, integrated thermionic circuitry of high efficiency and long life.

TIMM tube research and development efforts were continued in the areas of electrical and mechanical design, materials and assembly processing, component evaluation and module fabrication.

Investigation programs for the improvement of grid tensioning methods, development of grid transparency measuring devices, and a better understanding of the problem of low contact potential to the grid electrode were continued and results are reported.

Low capacitance diodes have been designed and fabricated with experimental values of capacitance being 58 per cent of conventional TIMM diode capacitance. Programs of investigation have been initiated to design and fabricate a zero contact potential diode and a triple section series diode to satisfy contract circuitry requirements.

Shock test and life test data for TIMM diodes and triodes are presented.

Investigation of tungsten, platinum, rhodium and carbon resistive films for TIMM resistor application is continuing. Ground surface substrates have been evaluated for possible advantages to be realized from depositing thin films on relatively smooth surfaces. Low capacitance units and units in the order of 470K ohms have been fabricated for contract circuitry. Life data are presented for carbon and metal film resistors.

The program of investigation relating to high temperature conductivity of TIMM ceramic-metal capacitors is progressing. Measurable voltages have been obtained from stacked capacitors after subjecting the units to operating temperature and voltage. Spontaneous polarization, polarization

reversal and the change in the slope of conductivity versus the reciprocal of absolute temperatures have been verified for stacked units. It is postulated that titanium is being injected into the ceramic during the sealing cycle and the boundary area at the ceramic metal interface can then act as a titanium concentration cell. Estimated activation energies match the requirements for the Ti-TiO_2 cell theory.

The design of a stacked capacitor utilizing deposited film electrodes is complete. The unit will be used primarily for evaluation of new film type electrode materials. Variable capacitors have been fabricated, utilizing a new mechanical design, with values ranging from 3.5 to 17.0 picofarads.

Inductor test units have been designed for investigating conductor winding wire and winding wire insulations. Fabricated units have been evaluated at room temperature and over a range of temperatures from 25 C to 580 C. Q and inductance data are presented for units before and after encapsulation.

The investigation of a chromium plus nickel electroplate to prevent contamination and embrittlement of titanium at 580 C was continued this period and results are reported. Brazing materials and methods for module construction, welding and brazing techniques for module electrical interconnections, titanium-clad refractory metals for grid application and the use of oxidation-resistant electrode materials are discussed.

TIMM circuit development programs were directed toward the investigation of half adder, pulse shaper, r-f amplifier oscillator, shift register and four-input Nor circuitry. In addition to performance data for all circuitry listed above, stacking and wiring diagrams and component lug configurations for the half-adder, shift register and four-input Nor circuits are presented. A discussion of the word generator display unit prepared for the contract review meeting is included.

TABLE OF CONTENTS

TABLE OF CONTENTS (continued)

TABLE OF CONTENTS (continued)

LIST OF ILLUSTRATIONS

LIST OF ILLUSTRATIONS (continued)

LIST OF ILLUSTRATIONS (continued)

LIST OF ILLUSTRATIONS (continued)

LIST OF TABLES

TUBE DEVELOPMENT

The efforts of the Tube Development Group for this quarter were again concentrated in the following general areas:

1. Electrical Design
2. Mechanical Design
3. Tube Processing
4. Testing Methods
5. Test Results
6. Module Fabrication

Electrical Design - Triode

In an effort to achieve the maximum transconductance possible in a 0.325" diameter TIMM triode, a fine mesh grid which represents the smallest wire size and the greatest number of lines per inch which can be successfully photoetched from 0.001" titanium was designed. This grid had a mesh pattern with 0.001" wires spaced 0.003" center to center in one direction and 0.050" in the other direction. The first grids of this design received from the manufacturer had two major defects: (Illustrated in Figure 1A)

1. Very thin lateral wires at the inside edge of the solid titanium ring.
2. Low transparency of the grid mesh caused by the wires being too wide and the openings being too narrow. The transparency was as low as 30% on some grids whereas the design center was 66%.

A new master to correct the defects of the first grids was designed. This design is illustrated in Figure 1B. Grids from the new master were received and inspected. The wires were now uniform in width and the transparency was close to its specified value.

To compare this new mesh of 0.003" by 0.050" wire spacings with the previously used mesh having a wire spacing of 0.007" , triodes were built, processed

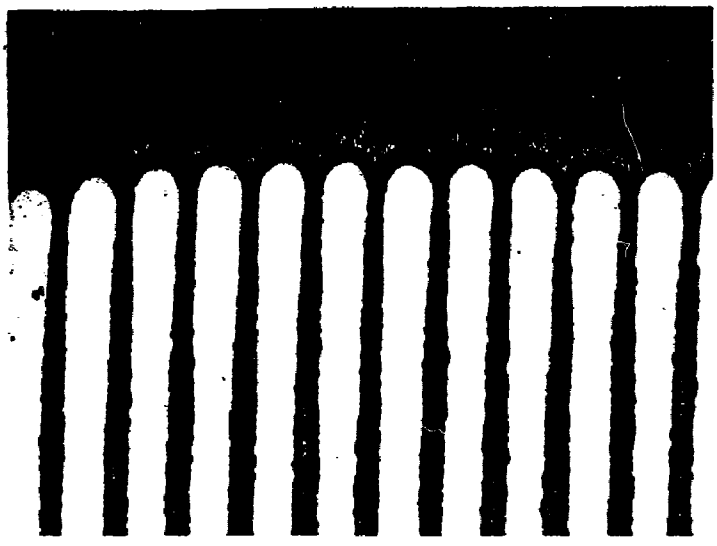

First Sample of Grid With .003"x.050" Mesh

Figure 1A

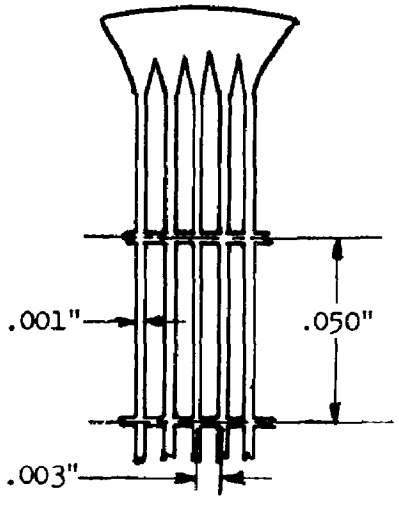

.003"x.050" Mesh Pattern

Figure 1B

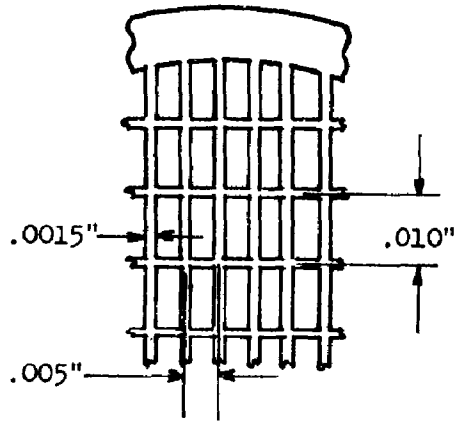

.005"x.010" Mesh Pattern

Figure 1C

and tested for amplification factor and transconductance. In these tests, plate voltage was set to 15.0 volts and the grid voltage was adjusted for a 1.0 milliampere plate current. Data from these tests are shown in Table 1.

Another grid which had been used successfully is one with a wire pattern of 0.005" by 0.010" shown in Figure 1C.

Circuit Requirements

At the present time, the computer circuits being developed for the Air Force Contract appear to require a higher level of plate current and a sharper cutoff than has been obtained with a tube using any of these three grids. For example, where these circuits require plate currents over 1.25 milliamperes at plate voltage of 5.0 volts and a grid voltage of 2.5 volts, the highest plate current consistently obtained to date has been approximately 1.0 milliampere. A few tubes have exceeded this level at the expense of cutoff. Where the circuits require a level of plate current at cutoff below 100 microamps, at 11.5 volts on the plate and zero volts on the grid, the tubes which have an adequate plate current at 5.0 volts will still have as high as 400 microamps at cutoff conditions. Data on recent representative tubes using the 0.005" x 0.010" grid mesh are shown in Table 2.

Triode plate family curves comparing the 0.007" by 0.007" mesh, the 0.005" by 0.010" mesh, and the 0.003" by 0.050" mesh are shown in Figure 2. As can be noted, the 0.003" by 0.050" mesh has the highest transconductance and mu of the three. Also in evidence in these curves is the high grid current at 2.5 volts grid voltage in tube #5054 which has a 0.003" by 0.050" grid. This will be discussed later in this report.

Transconductance and Amplification Factor (μ) Measurements Comparing 0.007" and 0.003" x 0.050" Grid Mesh

Test Conditions: E_p = 15.0 volts
I_p = 1.0 ma

0.007" x 0.007" Mesh Grid

Tube No.	Amplification Factor	Transconductance (μmhos)
4334	4.0	1030
4269	7.7	1620
4270	6.4	1330
4202	5.4	1250
4279	8.6	1540
4256	7.0	1460
4251	7.5	1580
4393	9.0	1390
4246	10.0	1810
4253	8.4	1620
Average	7.4	1460

0.003" x 0.050" Mesh Grid

4912	22.8	3460
4943	23.9	3560
4937	31.7	3960
4896	22.2	3340
4978	35.7	3480
4934	36.0	4250
4941	18.3	3230
4887	35.9	3970
4907	33.7	3900
4865	27.2	3660
Average	28.7	3680

TABLE 1

Tube No.	I_{p_1}	I_{p_3}
6647	0.8 ma	20 μa
6648	1.2	175
6653	.7	30
6654	1.3	200
6656	1.0	100
6657	1.1	250
6659	0.9	100
6664	0.95	40
6674	0.75	40
6675	1.55	550
6685	1.40	400
6703	1.50	650

Test Conditions: I_{p1} - E_p = 5.0v E_g = +2.5v

I_{p3} - E_p = 11.5v E_g = 0

TABLE 2

Triode Switch Tube Currents

These plate families illustrate that a triode which will satisfy the circuit requirements must have both a higher transparency grid to raise the plate current and a higher transconductance and mu to improve plate current cutoff than has been achieved with tubes using either the 0.005" by 0.010" or the 0.007" by 0.007" grid. Although a tube with the 0.003" by 0.050" grid will have a satisfactory cutoff, the transparency of this grid is apparently too low to allow a satisfactory level of plate current. It is believed that the proper grid mesh spacing lies somewhere between that of the 0.003" by 0.050" and the 0.005" by 0.010" grid mesh.

Theoretical Calculations

A study of formula which give the relationship of tube characteristics to tube parameters showed that the spacings being used were slightly out of range of the formula. However, the theoretical tube characteristics of a triode using the 0.003" by 0.050" grid and "in range" spacings were calculated.

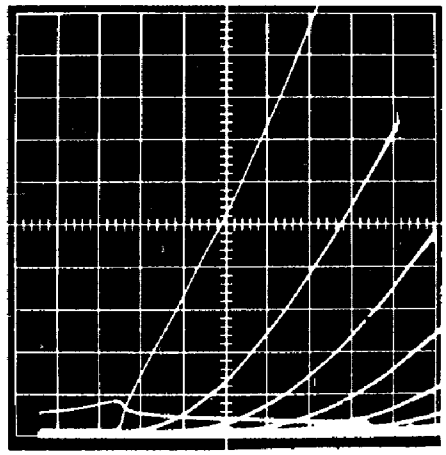

Tube #6031 .007"x.007" mesh

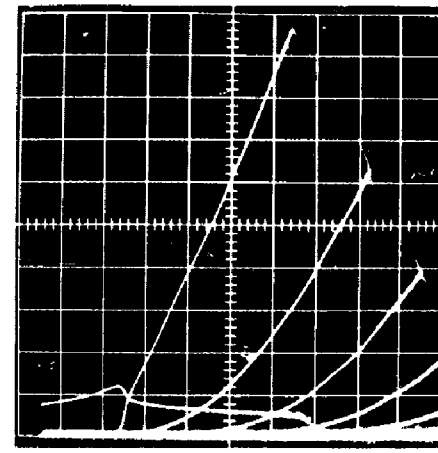

Tube #6120 .005"x.010" mesh

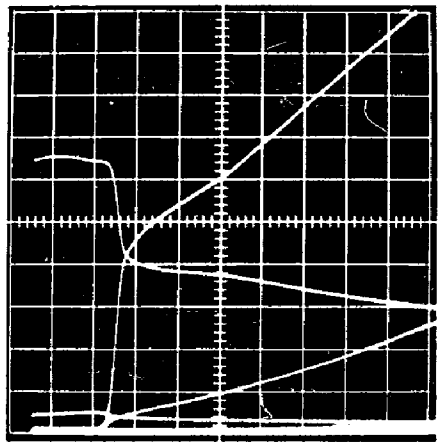

Tube #5054 .003"x.050" mesh

Test Conditions

Horizontal Scale - 1 volt / Div.

Vertical Scale - .2 ma / Div.

Grid Voltage - +2.5 volts max.

- .5 volt / step

Plate current is diagonal trace

Grid current is horizontal trace

Plate Families of Triodes Comparing Grid Mesh Patterns

Figure 2

The following expressions were used:

$$\mu = 2\,Nb\,0.266.8\,Nd + 680\,(Nd)^5 \quad *$$

Where N = Grid turns per unit length

b = Grid to plate spacing

d = Grid wire diameter

$$G_m = \frac{264\,S^{2/3}\,i_B^{1/3}}{1+\frac{1}{\mu}\quad\frac{1}{\mu}\,(\frac{4b}{3a})\,a^{4/3}} \quad \mu\text{mhos} \quad **$$

Where S = Cathode surface area

i_B = Plate current

μ = Amplification factor

a = Cathode to grid spacing

b = Grid to plate spacing

* E.W. Herold "Empirical Formula for Amplification Factor" Proc. I.R.E., Vol. 35 - Page 493, May 1947.

** W. G. Dow, Fundamentals of Engineering Electronics, Page 145, Wiley, 1952.

These expressions are not reliable for grid to cathode spacings smaller than the grid pitch, because the close proximity of the grid causes the amplification factor to vary along the surface of the cathode.

Table 1 illustrated that the experimental values of amplification factor and transconductance obtained were 28.7 and 3680 micromhos respectively, (ten tube average), as compared to the theoretical values of 50 and 4850 micromhos.

These discrepancies may be due to several reasons. The grid to cathode spacings actually used in the tubes are slightly closer than that assumed in the calculations, the cathode emission may be nonuniform along the surface making the effective cathode area smaller than the actual area and the grid transparency may differ from grid to grid.

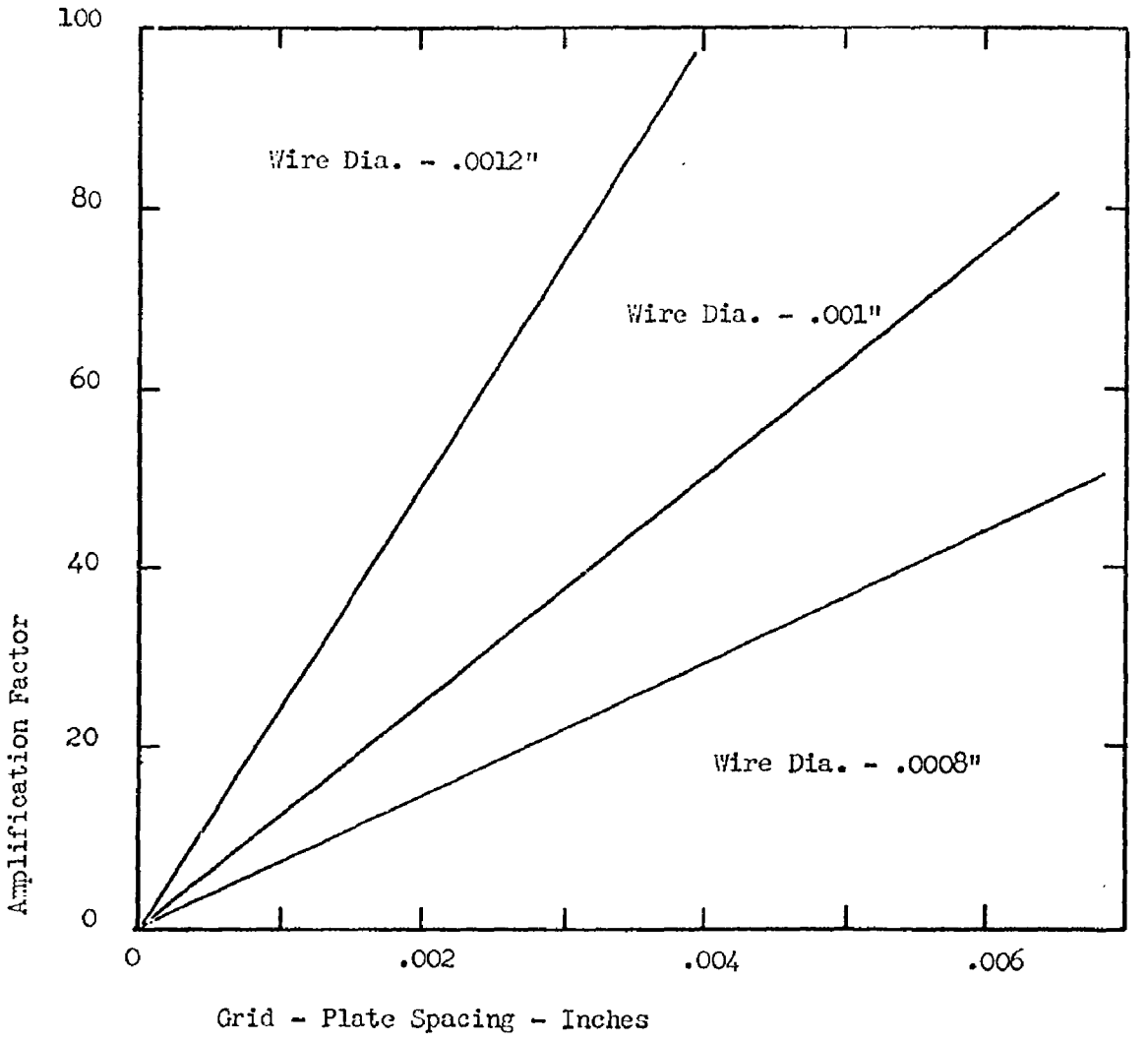

Amplification Factor Vs. Grid
Plate Spacing

Grid Mesh .003" x .050"

Figure 3

Although the computed tube characteristics are somewhat in error, it is believed that valuable information has been gained, in that the degree of dependence of the electrical characteristics upon the mechanical parameters has been demonstrated. This information facilitates the prediction of how much the experimentally observed characteristics will change when constructional changes are made in the tube. Using this technique, a new grid is being designed. It is anticipated that tubes using this grid will meet the circuit requirements.

The range of values of amplification factor which may be expected in a tube which has a 0.003" by 0.050" grid with various grid wire diameters and plate spacings was calculated using the formula by Herold and shown graphically in Figure 3. This graph shows the wide variations which may be expected when the grid wire diameter is varied a small amount. Table 1 also illustrates the wide variations in mu obtained in the experimental tubes. This may be due to slight variations in grid transparency.

Grid Measurement Techniques

In an effort to eliminate improperly etched and formed grids of any design, an optical device was designed to provide a means of measuring the transparency of each grid before it is used. A schematic drawing of this instrument is shown in Figure 4. A light source is located in one end of a black walled collimator tube and a calibrated photocell is located at the other end. The photocell is connected to associated metering equipment. The grid is inserted into the machined slot midway between the two ends and the amount of light transmitted is measured. It is anticipated that proper calibration of the unit will allow selective sorting of grids for use in the triode investigation programs being conducted.

OPTICAL GRID TRANSPARENCY MEASUREMENT DEVICE

(Preliminary Design)

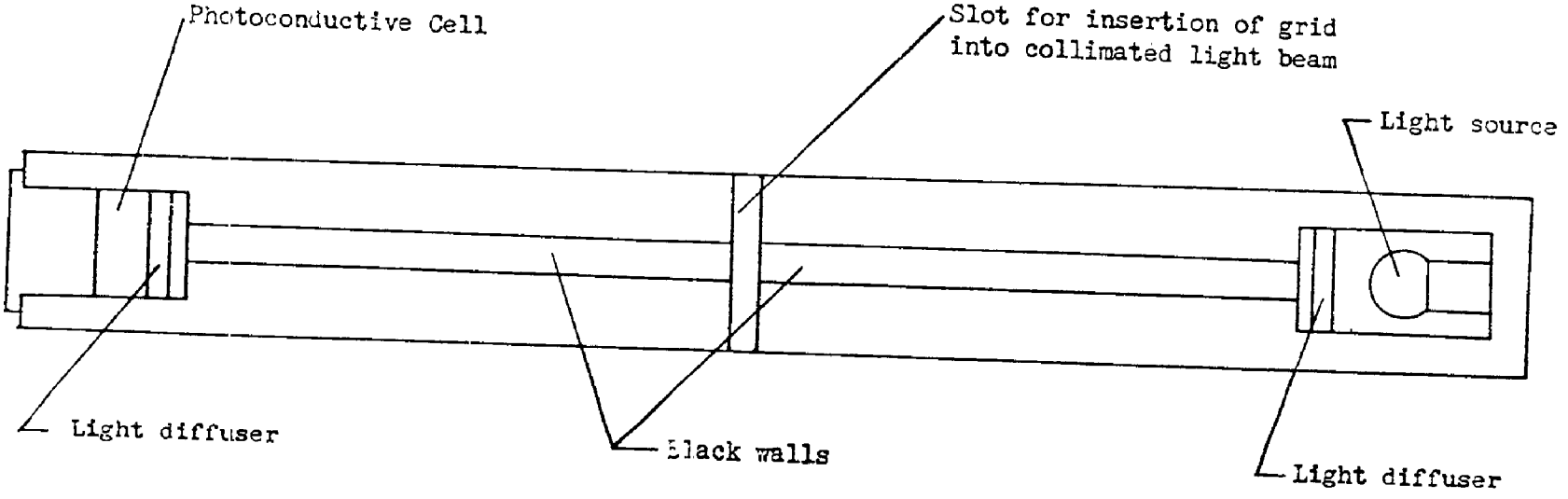

Figure 4

Contact Potential

Another circuit requirement is low grid current at positive grid voltages. Grid current is dependent upon the difference between the applied voltage and the contact potential. When the contact potential between the grid and the cathode is low, the tube draws too much grid current and causes loading in the grid circuit.

Although the reasons for low contact potential are not thoroughly understood and may be dependent upon tube processing, cathode coating, grid material, or grid thickness, contact potential controls some electrical characteristics of the tube and so these considerations will be discussed in this section of the report.

In addition to causing the grid current level to be too high, an erratic contact potential level will cause an erratic level of plate current even though all other tube parameters are equal. This results from the effective bias of the tube being the difference between the applied bias and the contact potential. For example, if 2.5 volts positive bias is applied to grids of two mechanically identical tubes, one of which has a contact potential of 2.3 volts and the other one a contact potential of 1.5 volts, the effective grid bias would be 0.2 volts on the first tube and 0.8 volts on the other. The plate current then would be higher for the first tube, even though the applied voltages were equal.

The effect these variations of contact potential have on plate current is greater in tubes which have higher levels of transconductance. This effect on plate current is shown in the distributions of plate current and contact potential for two different grids illustrated in Figure 5.

In tubes having a 0.007" by 0.007" grid mesh, a transconductance of 1450 micromhos and contact potentials varying between 1.8 and 2.4 volts,

CONTACT POTENTIAL AND PLATE CURRENT DISTRIBUTIONS

Test Conditions:

Contact Potential - E_p = 0, I_g = 10 μa
Plate Current - E_p = 7 0, E_g = +2.5

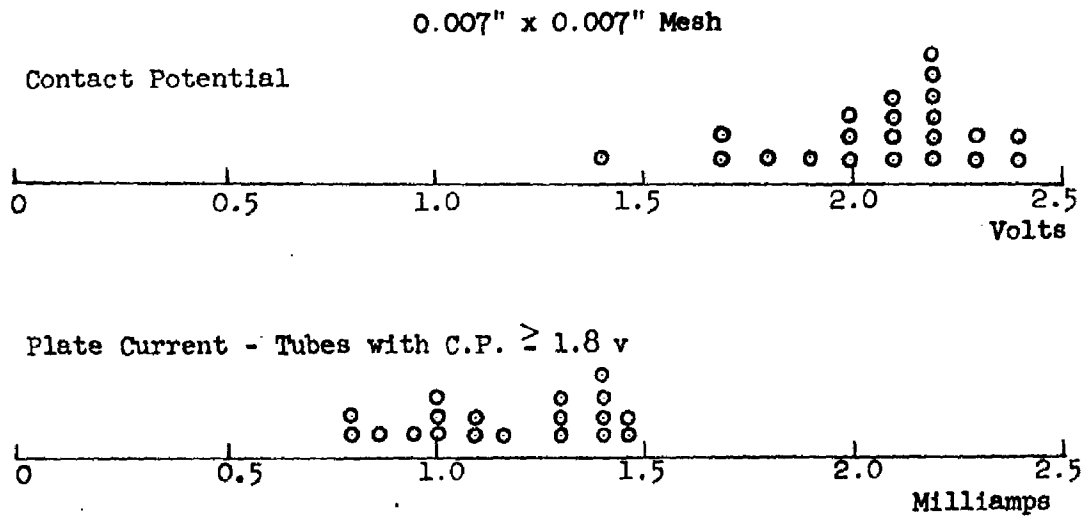

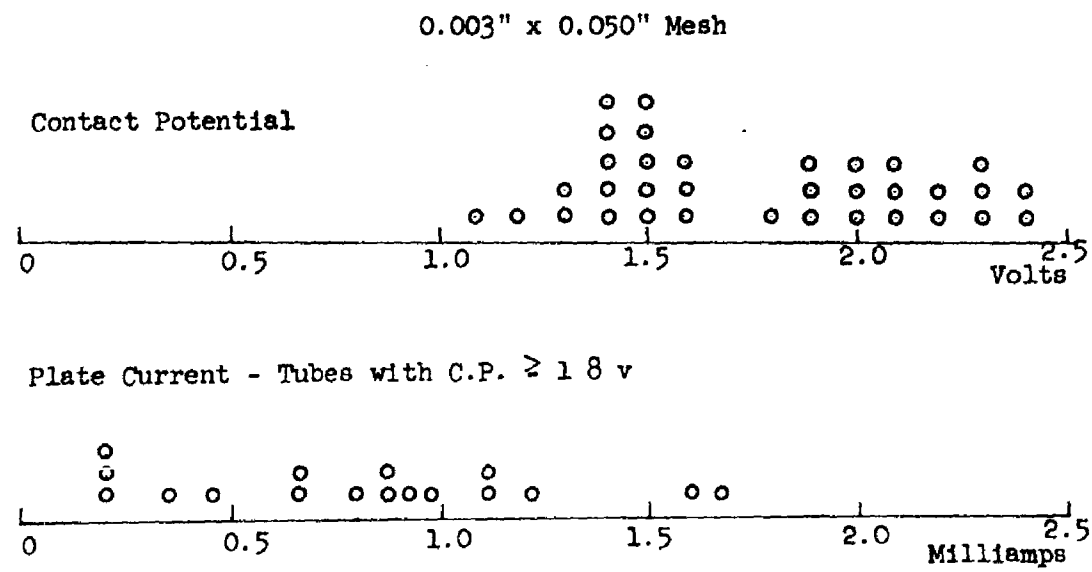

Figure 5

the plate current spread is 0.75 to 1.45 milliamperes. When tubes with the 0.003" by 0.050" grid and a transconductance of 3680 micromhos have the same variations of contact potential, the plate current spread is from 0.2 to 1.65 milliamperes. As can be noted, the spread in plate current is approximately proportional to the transconductance. Although the distributions show tubes with contact potentials below 1.8 volts, only those tubes exhibiting 1.8 volts or over were shown in the plate current distributions.

One factor that may affect contact potential is the grid thickness. This factor will be closely observed when grids of several different thickness materials, all from the same melt of titanium and etched by the same supplier, have been obtained. Available data shown in Figure 5 indicate that the 0.003" by 0.050" mesh which is 0.001" thick has a wider spread of contact potentials than the 0.007" by 0.007" grid which is .0015" thick. Data from Table 3 also indicate this same trend.

Tube No.	Mesh	Thickness	Contact Potential
4721	0.007" x 0.007"	0.0015"	2.35 volts
4741	"	"	2.15
4745	"	"	2.3
4727	"	0.001	1.14
4729	"	"	1.27
4730	"	"	1.68
4733	0.003" x 0.050"	"	1.7
4735	"	"	2.04
4737	"	"	1.48
4739	"	"	1.33
4756	"	"	1.47
4757	"	"	1.75
4759	"	"	1.71

TABLE 3

It is believed that the thinner materials are more prone to become contaminated during processing and thus change in work function. The

nature of this contamination is not understood. Grids with poor contact potential have been analyzed using mass spectrometer, spectrograph, and x-ray diffraction techniques with no positive results. Analysis work will continue in an effort to identify the contaminants causing trouble.

Previous tests have indicated that there is some tendency for thick cathode coating to reduce the contact potential. It is believed that areas of thick cathode coating could also cause low contact potential.

One attempt to achieve a more uniform cathode coating involved the application of a more than usual amount of coating having a lower ratio of carbonates to vehicle. This coating was applied to diode cathodes in four different carbonate concentrations ranging from 8% to 20% H1-1R-3 coating (Strontium 70/Barium 30) in reagent grade acetone. Table 4 presents initial tube data obtained from these tests.

Coating Concentration	Is	Contact Potential
8%	7.3 ma	2.4 volts
10%	7.6	2.5
15%	5.9	2.6
20%	8.6	2.4

Effect on Diode Characteristics of Cathode Coating Concentrations-Median Value of Each Lot

TABLE 4

From these tests, it was concluded that there was little significant difference in the effect of coating concentration when applied to diode cathodes. The life test on the diodes will be reported later in this report. It is believed these tests would have shown larger differences between lots if they had been performed on triodes. After a few tests, this method of coating was discontinued because the larger amount of coating mix required would not remain on the cathode. Many tubes had coating on the titanium stud supporting the cathode which further reduced the contact potential.

An improved method of keeping the cathode coating in suspension is now being used. Instead of mixing the coating just prior to use, the coating is now continuously stirred during the cathode coating operation. This technique appears to produce a much more uniform coating; tests are being run to determine the effects on tube characteristics.

Electrical Design - Diode

Three new diode designs were investigated this quarter:

1. Low capacitance diode
2. Zero contact potential diode
3. Multiple series diode for high contact potential

Low Capacitance Diode

At the request of the circuit group, the feasibility of reducing the interelectrode capacitance of the conventional TIMM diode to half its present value was studied. The circuit requirements for the diode are such that a reduction of perveance can be tolerated.

Through an analysis of the present diode, it was determined that 44% of the capacitance is active (anode to cathode) and the rest, 56%, is passive (in the seal area). Since a reduction of perveance can be tolerated, the spacing between the anode and cathode was increased from 0.002" to 0.003". This reduced the perveance by approximately 50% and the active capacitance to 67% of its former value.

The passive capacitance was reduced by the use of a thicker insulator between the cathode and the anode. This was changed from 0.015" to 0.035" and reduced the passive capacitance to 43% of its former value.

The calculated total capacitance of the low capacitance diode is 54% that of the conventional diode. Tubes having this type construction were made; capacitance measurements of these diodes are compared to those of regular diodes in Table 5.

Standard Diode		Reduced Capacitance Diode	
0.015" Insulator 0.002" K - A Spacing		0.035" Insulator 0.003" K - A Spacing	
Tube No.	Capacitance	Tube No.	Capacitance
5028	6.9 pf	3606	4.1 pf
5032	6.8	3609	3.85
5034	6.9	3608	3.9

TABLE 5

Diode Capacitance Measurements

The experimental value of the capacitance reduction is 58% of the conventional diode capacitance while the calculated value is 54%.

Some of these diodes were given to the Circuit Group for their evaluation.

Zero Contact Potential Diode

The Circuit Group also requested a diode with zero contact potential to use as an RF mixer. Since the materials used in the conventional diode consistently resulted in a high contact potential, it was realized that a material change was necessary. Work performed some years ago at the General Electric Research Laboratories, Schenectady, New York, indicated that tubes with a slightly more active cathode substrate material than platinum would deposit excessive amounts of barium or strontium on the anode and so reduce its work function to that of the cathode after operating for a few hours. One cathode material suggested was tungsten powder on the cathode substrate. Preliminary attempts to use the powder failed because of poor adherence of the powder to the base. Likewise, tungsten foil would not maintain a flat surface because of the diffenence in temperature coefficients of expansion. Further work will include the investigation of other anode materials, as well as different cathode materials.

Series Diode

Some circuits require that a diode not conduct until the voltage across it exceeds six or more volts. Since this is considerably more than the highest theoretical contact potential for a single diode, multiple units were designed. A triple unit is shown in Figure 6A. The center electrodes serve as an anode of one section as well as a cathode for the adjacent section, thereby reducing weight and volume over the same number of single units connected in series. The electrical characteristics of this triple series diode compared to those of a conventional diode are shown in the curves displayed in Figure 6B.

Mechanical Design

Electrode Studs

Anode and cathode studs have previously been fabricated by welding several layers of titanium discs to the approximate required height and then swaging or pressing to the finished size. There were many problems connected with this method of stud making:

1. It was necessary to keep on hand identified and separated many different size discs.
2. The welding together of many layers of material formed the possibility of enclosing and rendering unremovable contaminants on the surface of these discs which would later migrate out of the areas between studs into the tube and cause emission or leakage problems.
3. Parts sized by swaging would change size during processing, making it difficult to predict tube spacings.

It is postulated that the emission level of the triode, usually lower than that of the diode, is affected by seal products from the nickel-titanium eutectic or its reaction with the insulator, formed when the tube seal is made. Since the triode has all four seals exposed to the interior of the tube, instead of two as in the diode, more seal products are formed and can enter the evacuated region of the tube.

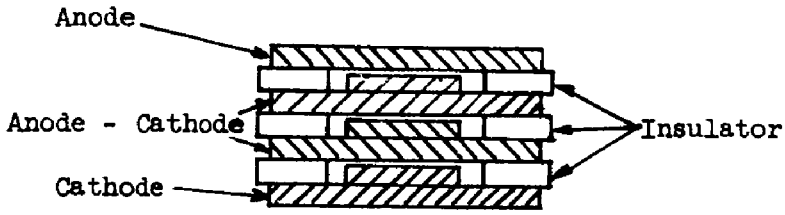

Cross Section of Triple Series Diode

Figure 6A

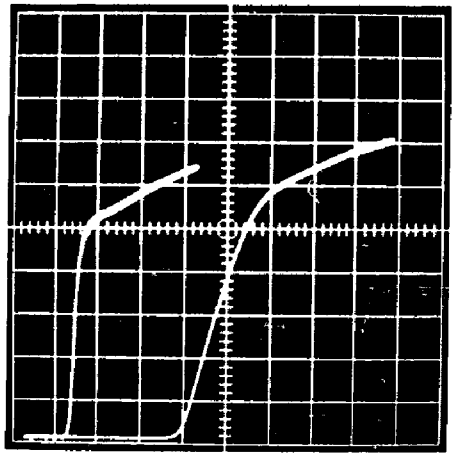

Horizontal Scale - 2 Volts / Div.

Vertical Scale - 2 Ma. / Div.

Left Trace - Single Section Diode

Right Trace - Triple Section Diode

Diode I_p Vs. E_p

Figure 6B

Anode and cathode studs suitable for fabrication on an automatic screw machine were designed. Recently constructed triodes have these studs incorporated in their design. Figure 7A illustrates the cathode stud and its relationship to the ceramic insulator.

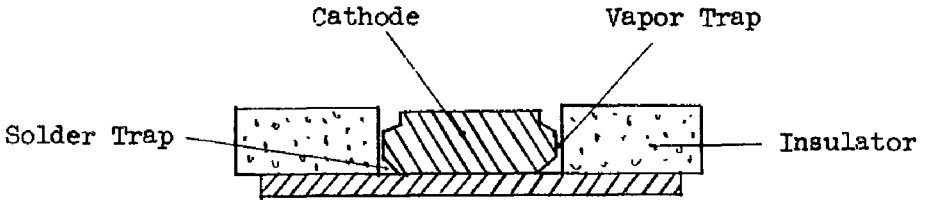

Figure 7A
Cross Section of Machined Stud and Insulator

These studs fit the ceramic insulator more closely than the studs previously used. With this design, it is expected that seal products which may enter the tube during sealing will be trapped or gettered by the hot titanium stud before they can penetrate to the active surface areas of the cathode, grid and anode. Usually the close spacing of an electrode stud to the ceramic insulator results in solder being drawn up along the stud by capillary action during the sealing operation. To prevent this, the lower edge of the stud is beveled to form an enclosure designed to trap any solder which may be forced into the tube at sealing.

The anode stud is similar to the cathode stud with the exception that the active face is slightly smaller in diameter to allow a larger anode to grid electrode clearance.

Attempts are being made to machine these one-piece studs to the proper size and thereby eliminate the swaging operation formerly necessary for sizing. These one-piece studs remain nearly constant in size throughout the processing steps.

Controlled tests to determine the value of the solder and vapor trap have not been made. It has been observed, however, that the general level of emission of the triodes is considerably higher than it has been in the past. A photograph of tubes using these studs is shown in Figure 7B and 7C.

Grid Electrode

The second quarterly report described preliminary tests of a grid electrode which would stretch the titanium grid while the seal was being made. A cross-section of the basic form of this electrode is shown before and after sealing in Figure 8.

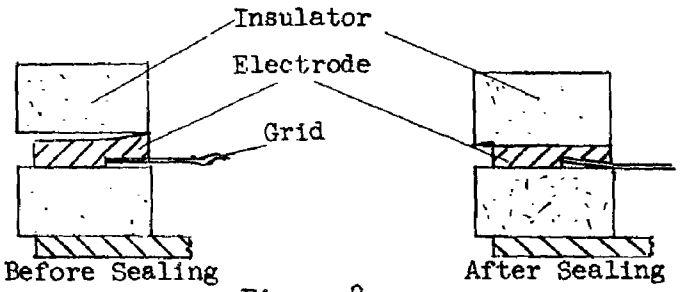

Figure 8

Grid Tensioning Electrode

This type grid tensioning electrode has been successful in holding flat a 0.001" titanium grid which heretofore had always buckled and touched either the anode or the cathode. Although some grid shorts are still occurring, it is believed that a refinement of this type grid tensioning technique will be completely successful in permitting the use of a thin, pure titanium grid in TIMM triodes.

Some problems encountered in the use of this electrode are as follows:

1. The strength of the grid ring at its thinnest cross-section, i.e., in the area between the sealing portion and the grid mounting portion, is critical. If it is too strong at sealing temperature, the grid portion will not deform and stretch the grid. It may hold the seal open or it may tilt the entire ring and cause an open or marginal seal. If it is too weak, the grid portion will deform at too low a temperature during

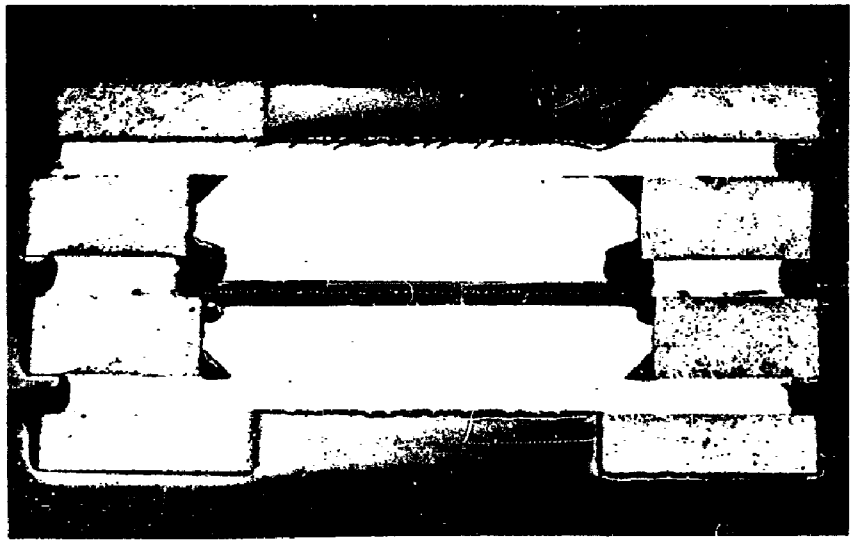

Cross Section of Triode With .003" Grid Electrode Recess and Machined Anode and Cathode Studs

Figure 7B

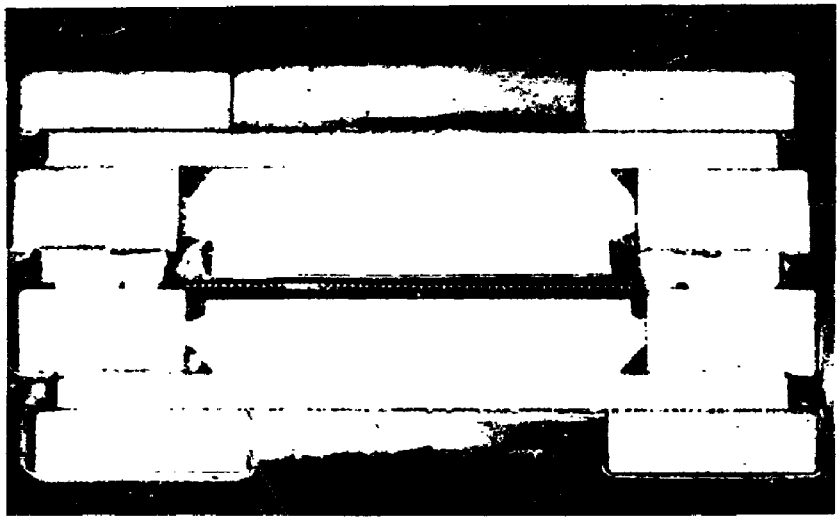

Cross Section of Triode With .0045" Grid Electrode Recess and Machined Anode and Cathode Studs

Figure 7C

the sealing cycle. This will allow the grid to again distort at sealing temperature.

2. The depth of the recess where the grid is fastened is fairly critical. Too much depth will cause too much grid stretching and consequently a damaged grid. Not enough depth will cause inadequate stretching resulting in a warped grid and possibly a seal held open by an extra thickness of metal around the inside of the ring. Too small a rise on the top side of the electrode will result in a poorly stretched grid which is not properly positioned in the tube.

3. The electrodes, formed by coining, distort during firing and alter the critical dimensions.

4. Grid electrode to insulator alignment is poor in some tubes causing the grid to be formed into the inside opening of the insulator and below its proper position. It may also cause insufficient deformation of the grid electrode thereby allowing the grid to distort.

In order to reduce the strength of the grid electrode in the area between its sealing and tensioning portions, it has been found necessary to provide some form of weakening groove between these sections. Three variations are shown in Figure 9.

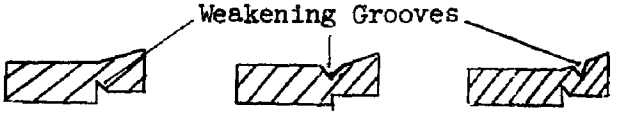

Figure 9
Cross Sections of Grid Tensioning
Electrode With Weakening Grooves

A further control for grid tensioning is the adjustment of the pressure which the sealing jig applies to the stack of tubes being sealed.

Experiments using different depths of the grid electrode recess were performed. Figures 7B and 7C show the results of two of these experiments. The grid electrode in 7B had a grid recess .003" deep while the electrode in 7C had a recess 0.0045" deep. Neither electrode had the weakening

grooves described above. It may be observed that although the electrode with the 0.003" recess held the grid generally flat, 7B, the tensioning by the other electrode was superior in that each grid wire was held parallel with the one adjacent to it (7C). Although the photographs do not display the seals to advantage, visual examination revealed that seals made to electrodes having no weakening groove were marginal.

Although the grids are generally being held flat, the present method of stretching requires further refinement to accurately locate the grid with respect to the cathode in every tube.

In order to control the distortion of the grid ring during the vacuum firing operation, it has been found necessary to change the order of fabrication and processing steps to the following:

1. Punch grid opening in blank electrode.
2. Degrease electrode and clean.
3. Vacuum fire electrode at high temperatures.
4. Form electrode by coining.
5. Tack weld grid mesh into place.
6. Vacuum fire electrode and grid at a lower temperature.
7. Weld grid and solder rings into place.

With this processing it has been found possible to hold the accurate electrode dimensions necessary until the electrode is placed in the tube. Two other advantages were also discovered with this revised processing schedule. The vacuum fired electrode was more easily coined making lower forming pressures and thus greater tool life possible. By tack welding the grid mesh in place in the electrode, it was more easily handled for vacuum firing with less chance of contamination pick-up from poor or improper handling.

It was found necessary to reduce the inside diameter of the ceramic insulator to provide better support when the grid electrode deforms to

tension the grid. Although the support is now much improved, additional effort is required to improve electrode to insulator alignment.

Further development of grid tensioning methods must include:

1. A grid electrode shape with fewer critical dimensions.
2. A grid tensioning method which will include an accurate reference plane to hold the electrode and grid in place.
3. A means to tension and position the grid that will always allow the seal to close and braze correctly.

Tube Processing

It has been noted in the past that tubes made from parts which were allowed to remain for an extended period of time in an oil diffusion pump-evacuated bell jar had very low or essentially zero emission. It was believed that if long periods of exposure to vapors from an oil diffusion pumped system could be so detrimental to tube characteristics, even a short exposure could be harmful.

When the ion pumped vacuum system was installed, comparison tests were performed to determine if this type vacuum system is superior to the oil diffusion type heretofore used. A sufficient number of parts for several lots of tubes were vacuum fired in either one or the other of two vacuum systems. Parts which were fired in each of these systems were separated into two groups and made into tubes, one group was sealed in the ion pumped system and the other in the oil diffusion pumped system. The tubes were then evaluated for emission and contact potential. Sample parts fired in each system were held for mass spectrometer evaluation.

The results of the tests are graphically displayed by emission distributions in Figure 10. These distributions clearly illustrate that tubes having parts processed or the sealing operation performed in an oil diffusion system are inferior to those completely processed in the ion system. Subsequent similar tests have not shown such a drastic

EMISSION DISTRIBUTION FOR OIL VERSUS ION PUMPING

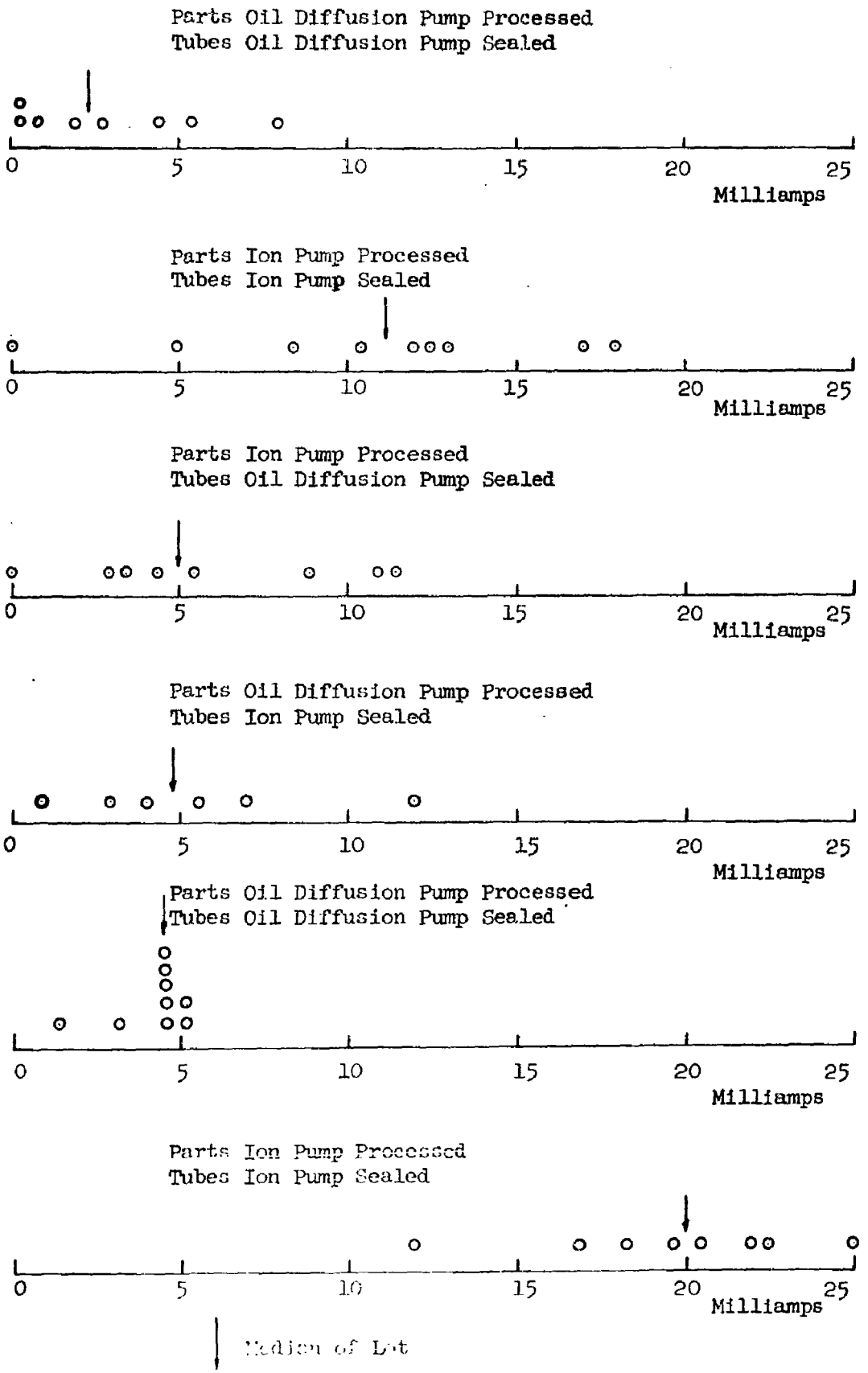

Figure 10

difference, but the accumulated data on tubes made in each system also indicate that the ion vacuum system is superior for parts and tube processing. Life test results of these tubes will be discussed in a later portion of this report.

When these data indicating superiority of the ion pumped vacuum system were obtained, the practice of firing all parts in this system was adopted. With the adoption of this practice another advantage of the ion pumped system was realized. Good practice dictates that parts being processed must not be left in an oil diffusion system any longer than is necessary because of the increase in oil back-streaming at low bell jar pressures. In the past, it has been found necessary to clean and vacuum fire parts immediately prior to their use. With these time limitations, all operations must be performed in one day, making it impossible to have parts fired and ready for tubes until late in the morning. Since parts can remain in the ion system for extended periods without being contaminated by oil back-streaming, it has been found advantageous to pre-process parts and place them in the evacuated bell jar over night. The parts are then ready for vacuum firing the next morning. In this way it has been found possible to save several hours a day. This extended bell jar evacuation time has also made it possible to fire at a much lower pressure than would otherwise be possible.

Figure 11 shows a double oven arrangement now being used in the bell jar of the ion pumped system. With two ovens permanently installed in the bell jar and an appropriate switching arrangement, it has been found possible to fire parts at two different schedules during one processing cycle. It is also possible to fire parts or to seal tubes without having to change ovens in the bell jar.

Figure 12 shows data obtained from mass spectrometer testing of parts which were vacuum fired in the two vacuum systems. Also shown are data

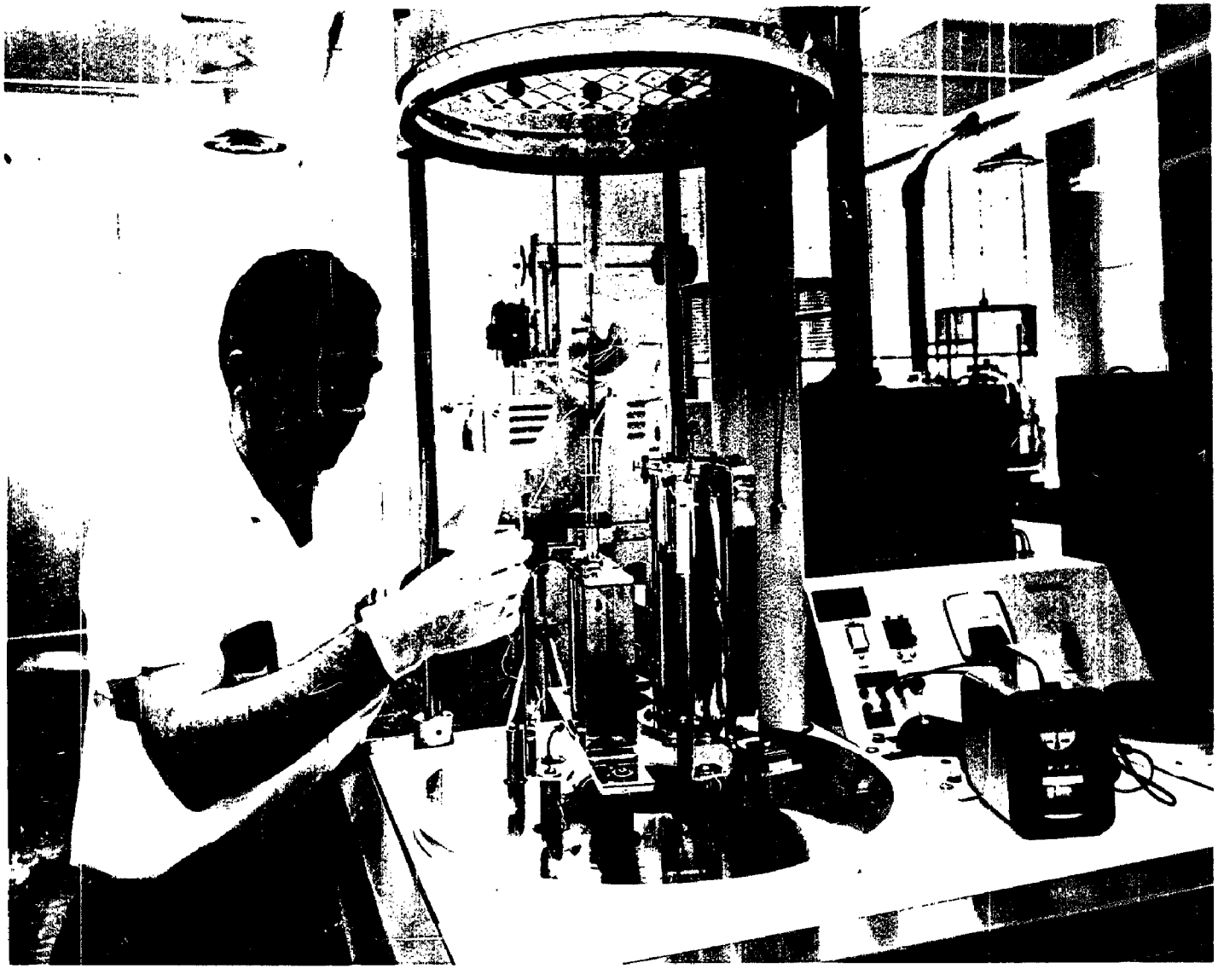

ION PUMP

Double Oven Arrangement

FIG. 11

GAS EVOLUTION & TEMPERATURE VS ELAPSED TIME OF TEST

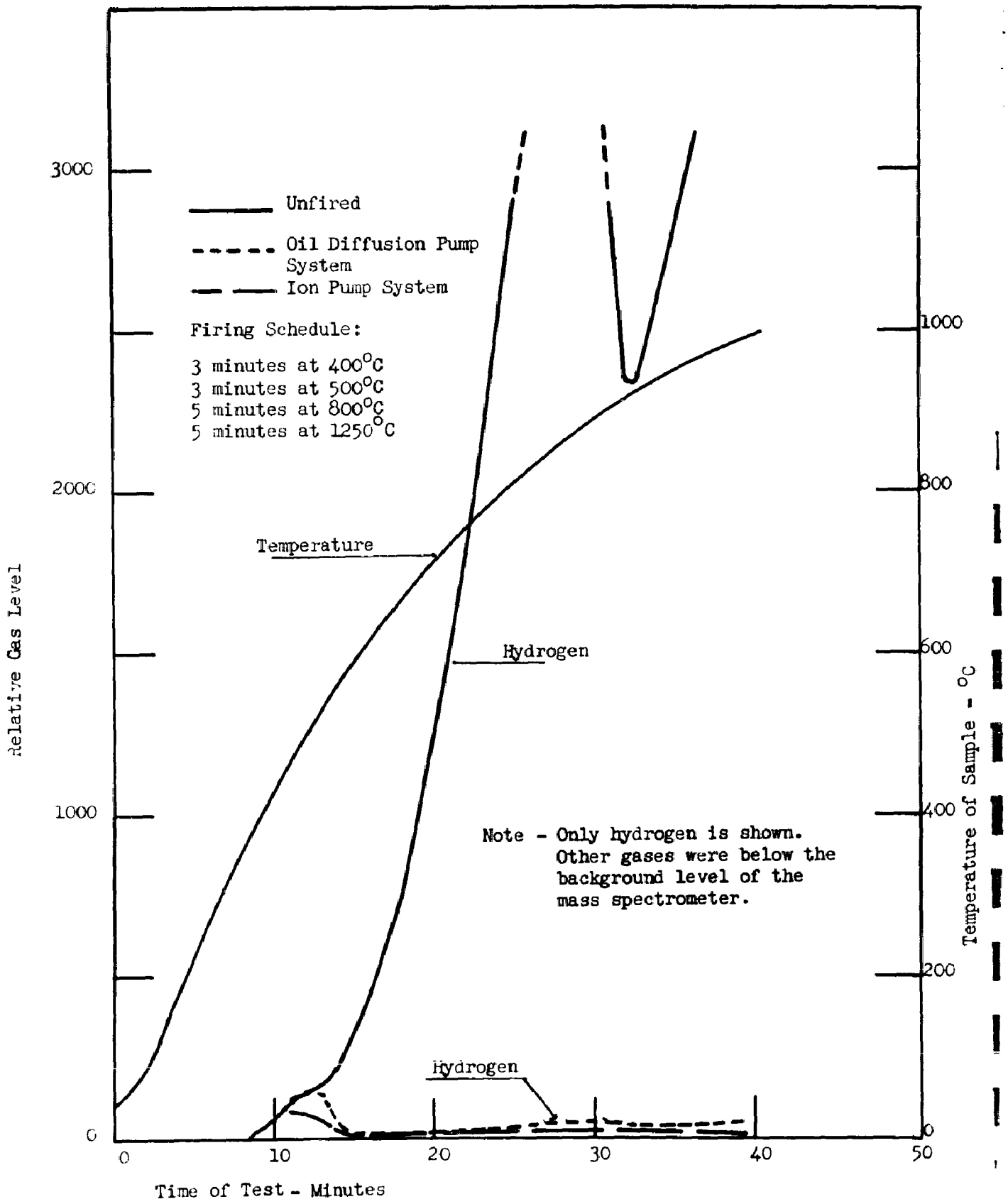

Figure 12

for unfired parts taken from the same group. The only gas detectable over the background level of the instrument was hydrogen. Although a very slight difference exists in the hydrogen level between the parts fired in the two systems, it is believed that oil molecules, not detectable by mass spectrometry methods, are responsible for the differences of behavior these parts have in the tubes.

It has been observed that the contact potential of a TIMM triode will occasionally increase during operation. Consequently, the effect of stabilizing schedules upon contact potential, both high and low, were studied. The results of one such test are shown in Figure 13. These data were obtained by choosing five tubes with a range of contact potentials and processing these tubes in the following manner:

Step 1 - The tube was heated to 750 C for one hour.

Step 2 - The tube was operated for two hours at 580 C, drawing 4 milliamperes of cathode current.

Step 3 - The tube was operated for 25 hours under the same conditions of Step 2.

Readings were taken at the end of each step. The data illustrate the same results which have been observed in the past; generally, the contact potential will drop slightly and the emission may rise temporarily. One tube increased in contact potential from one volt to almost two volts; however, this processing is not a reliable method for correcting all low contact potential tubes.

Data on tubes previously stabilized will be reported in the life test portion of this report.

Further stabilizing tests will be performed to study the effect that stabilizing has on life test results and to determine the effect on tube characteristics before and after module fabrication.

EFFECTS OF STABILIZING ON TIMM TRIODES

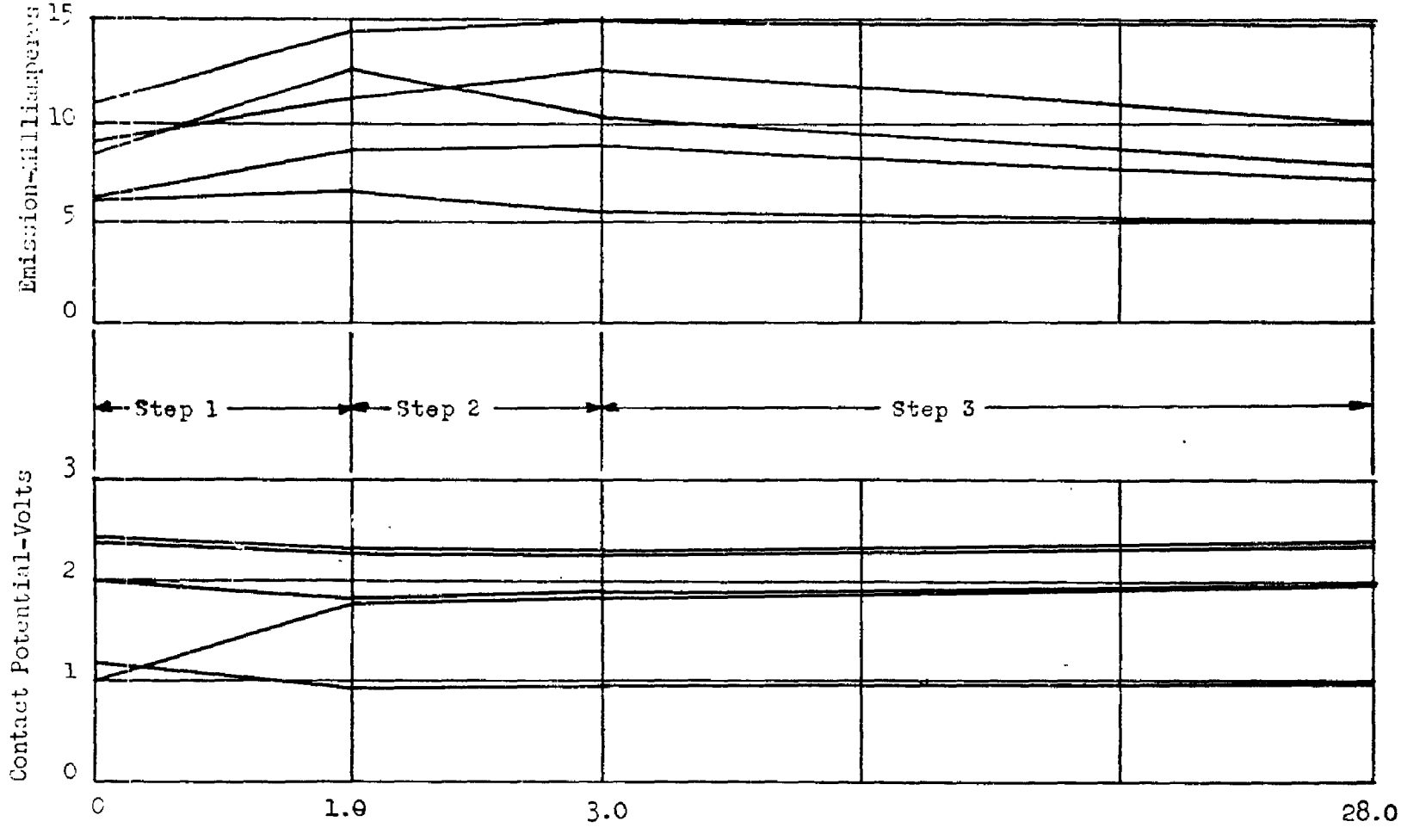

Stabilizing Schedule:

Step 1 - 60 Minutes at 750 C - No Cathode Current
Step 2 - 2 Hours at 500 C - 4.0 ma Cathode Current
Step 3 - 25 Hours at 580 C - 4.0 ma Cathode Current

Note - Samples were chosen for a range of Contact Potentials

Figure 13

Testing Methods

The usual method of measuring triode emission is unsatisfactory when used to measure emission of TIMM triodes. The emission is measured by connecting the grid to the plate and applying an appropriate voltage to these two electrodes. The total cathode current measured is comprised mainly of electrons being drawn to the grid. A thin titanium TIMM triode grid will dissipate but very little power without buckling, and permanently changing characteristics of the tube.

One way to avoid buckling the grid and permanently changing tube characteristics is to apply a significantly reduced voltage. This method, however, will not measure saturated emission.

The new method now in use involves connecting the grid through a current limiting resistor to anode and applying a higher voltage to the anode. In this way the grid current is restricted to a few milliamperes.

Test Results

Life Test

The diode life tests comparing electrode materials (Lots 222, 224 and 294) have operated beyond 4500 hours. These tubes are operating at 580 C with a cathode current of two milliamperes. Data for these tests are shown in Figures 14 and 15. At this time the tubes made from vacuum annealed material appear to have a superior emission level. There is no apparent difference in contact potential levels between the three lots of tubes.

Another group of diodes (Lot 237) with vacuum annealed titanium parts have been operating at 580 C while drawing saturated emission. These data are shown in Figure 16. Although the emission level is somewhat lower than the same kind of tubes operated at a lower cathode current, the emission level has remained essentially constant for the last three thousand hours.

DIODE EMISSION VS HOURS OF LIFE
FOR VARIOUS ELECTRODE MATERIALS

Life Test Conditions: Temperature = 580°C, Eb = 10v, RL = 3300 ohms

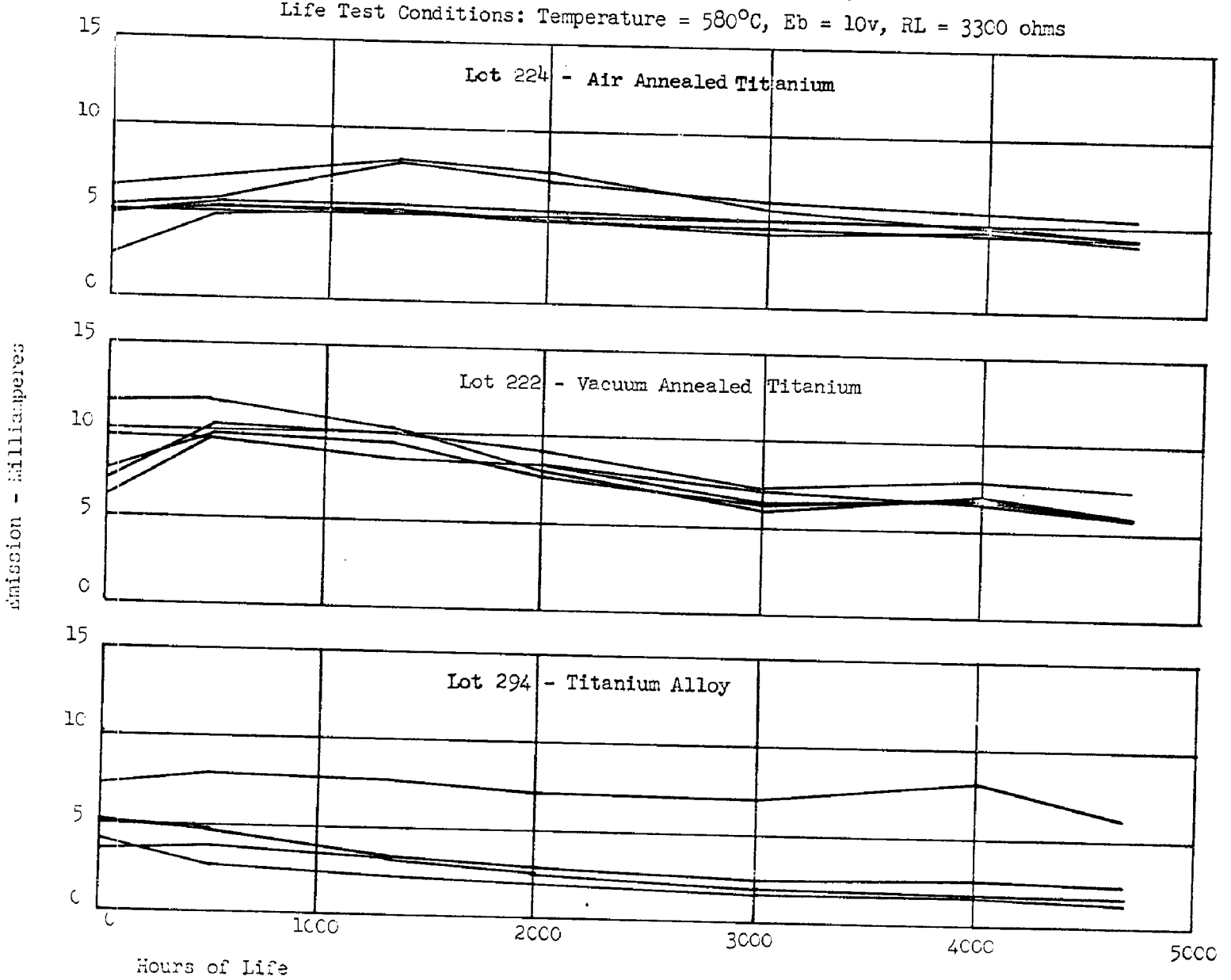

Figure 14

DIODE CONTACT POTENTIAL VS HOURS OF LIFE
FOR VARIOUS ELECTRODE MATERIALS

Life Test Conditions: Temperature = 580°C, Eb = 10v, RL = 3300 ohms

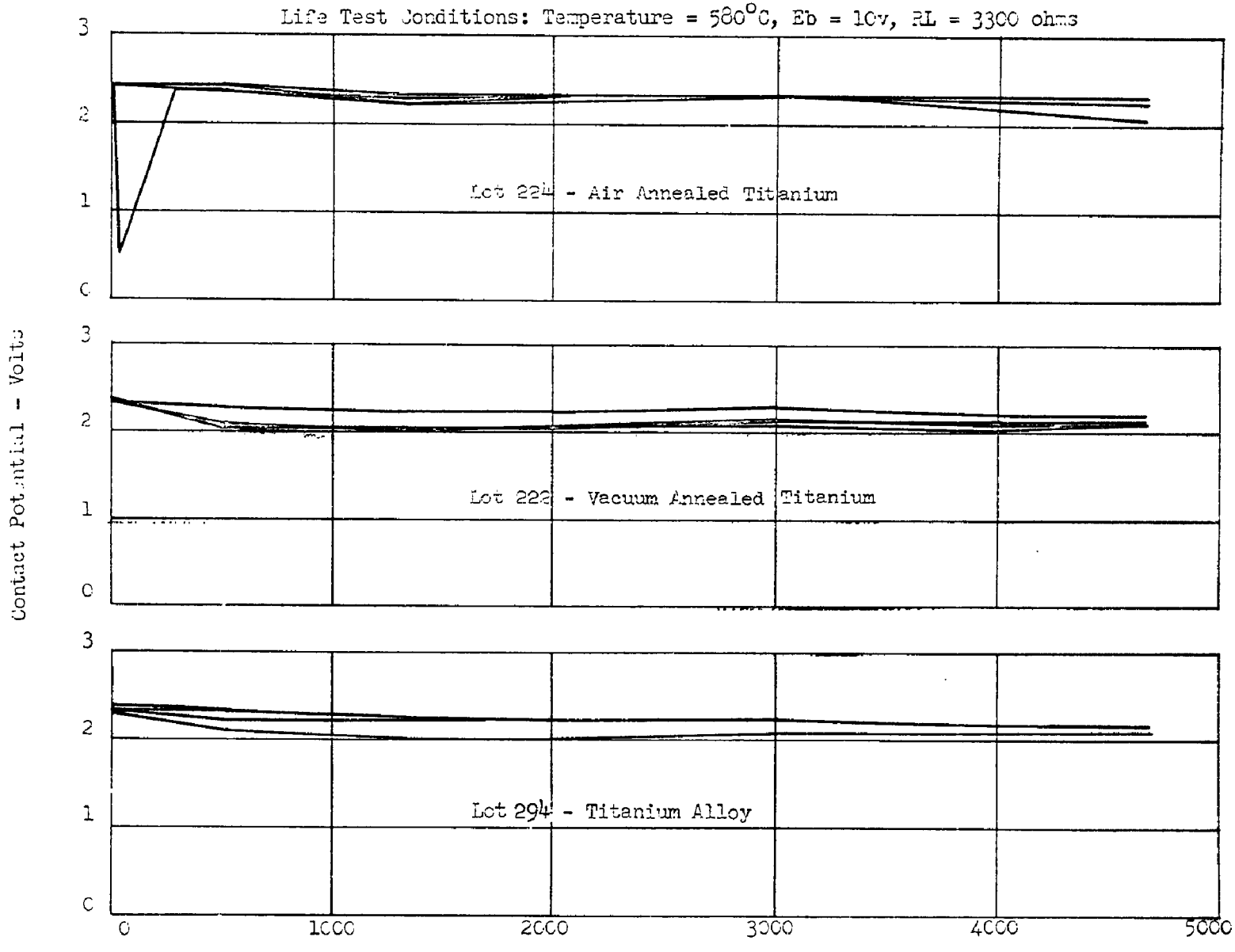

Figure 15

DIODE CONTACT POTENTIAL AND EMISSION WHEN OPERATED
AT SATURATED EMISSION VS HOURS OF LIFE

Lot #237 - Vacuum Annealed Titanium Electrodes

Life Test Conditions: Temperature 580°C, Eb = 10v, RL = 470 ohms

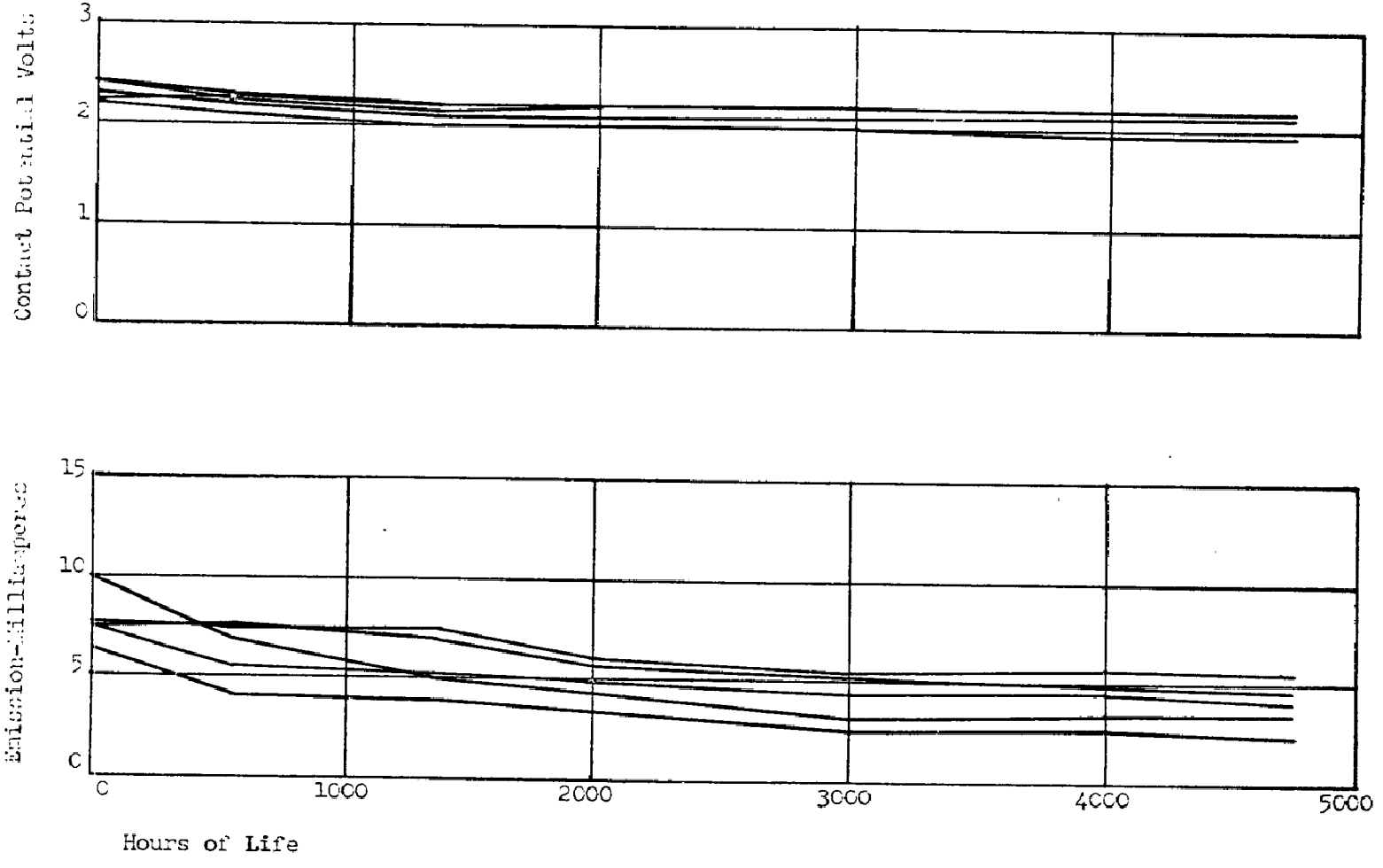

Figure 16

Data on diodes comparing the ion pumped vacuum system to the oil diffusion pumped system are shown in Figure 17. The operating temperature of the tubes on this life test is higher, 625 C, than the tests previously discussed. A higher temperature is used to accelerate the usual deterioration of the tube during its life so that a comparison could be obtained in a shorter period of time. Both lots were operated at saturated emission. It was found that the higher emission tubes processed in the ion pumped vacuum system operated at such a high level of cathode current at 625 C that the contact potential dropped almost to zero. (This effect has been observed on other tubes which were allowed to draw too much current at a high temperature.) The emission level of the tubes processed in the ion pumped vacuum system has remained at a higher level than those processed in the oil diffusion pumped system throughout the 1000 hours of operation.

It is believed that an accelerated life test such as this should be operated at a constant cathode current. To correlate results with those that might be obtained at 580 C, a control test at this temperature should also be performed.

Figures 18 and 19 show life test data on diodes which were made during the coating thickness tests discussed previously. These tests were also operated at the accelerated condition of 650 C. These data indicate that the emission level slumps rapidly when the cathode has a thicker coating. This may be due to a high resistance interface developing between the coating and the cathode base. The thicker coating appears to have a more uniform contact potential. This is contrary to what might be predicted from the original data showing dependence of contact potential on coating thickness.

DIODE EMISSION VS HOURS OF LIFE
FOR DIFFERENT VACUUM SYSTEMS

Life Test Conditions: Temperature 625°C, Eb = 10v, RL = 470 ohms

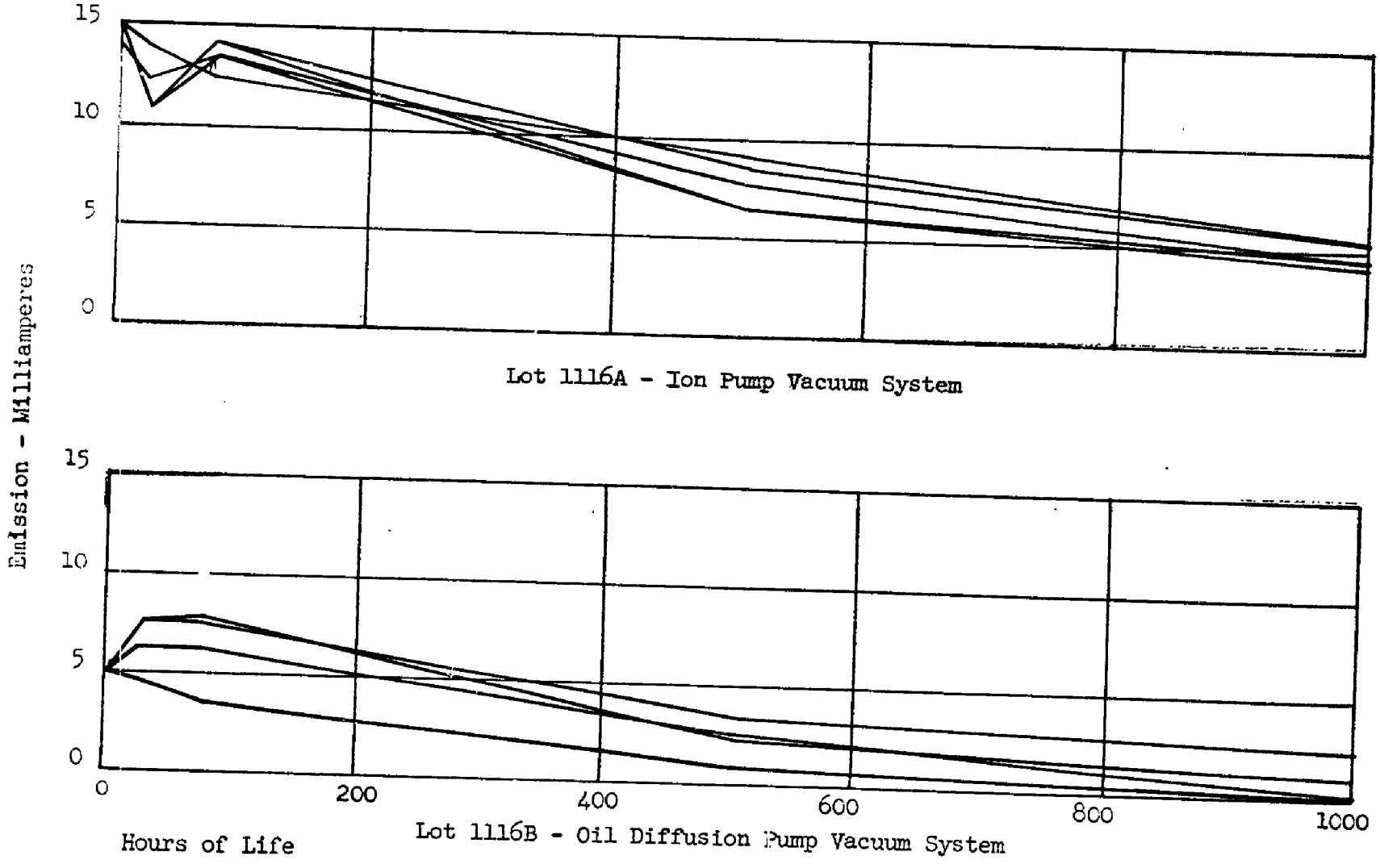

Figure 17

DIODE CONTACT POTENTIAL VS HOURS OF LIFE
FOR VARIOUS CATHODE COATING CONSISTANCIES

Life Test Conditions: Temperature = 625°C, Ep = 10v, R_L = 470 ohms

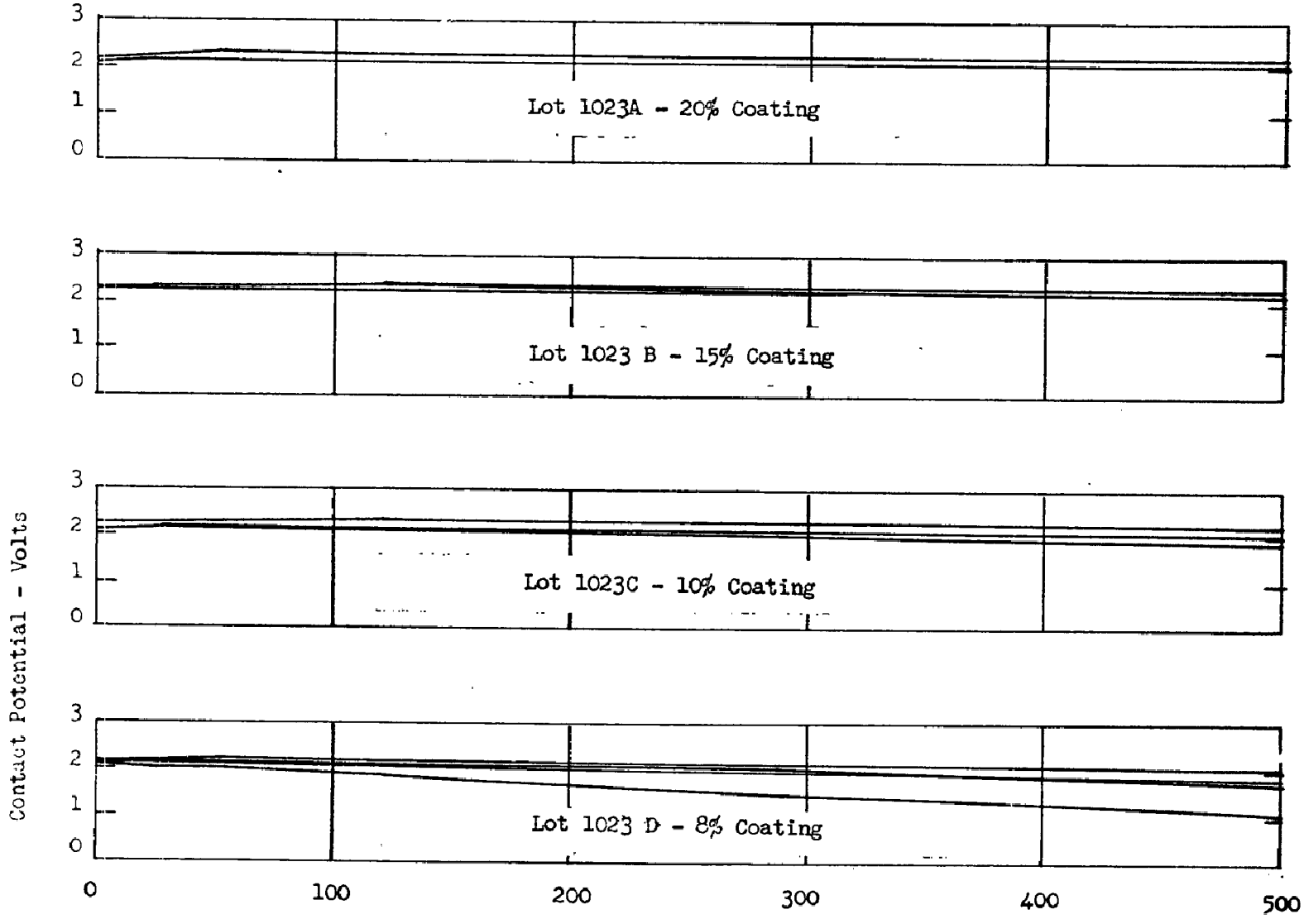

Note - % Coating is proportion of Strontium 70 / Barium 30 cathode coating (S. I. H1-1R-3) in reagent grade acetone

Figure 18

DIODE EMISSION VS HOURS OF LIFE
FOR VARIOUS CATHODE COATING CONSISTANCIES
Life Test Conditions & Temperature = 625°C, Ep = 10v, R_L = 470 ohms

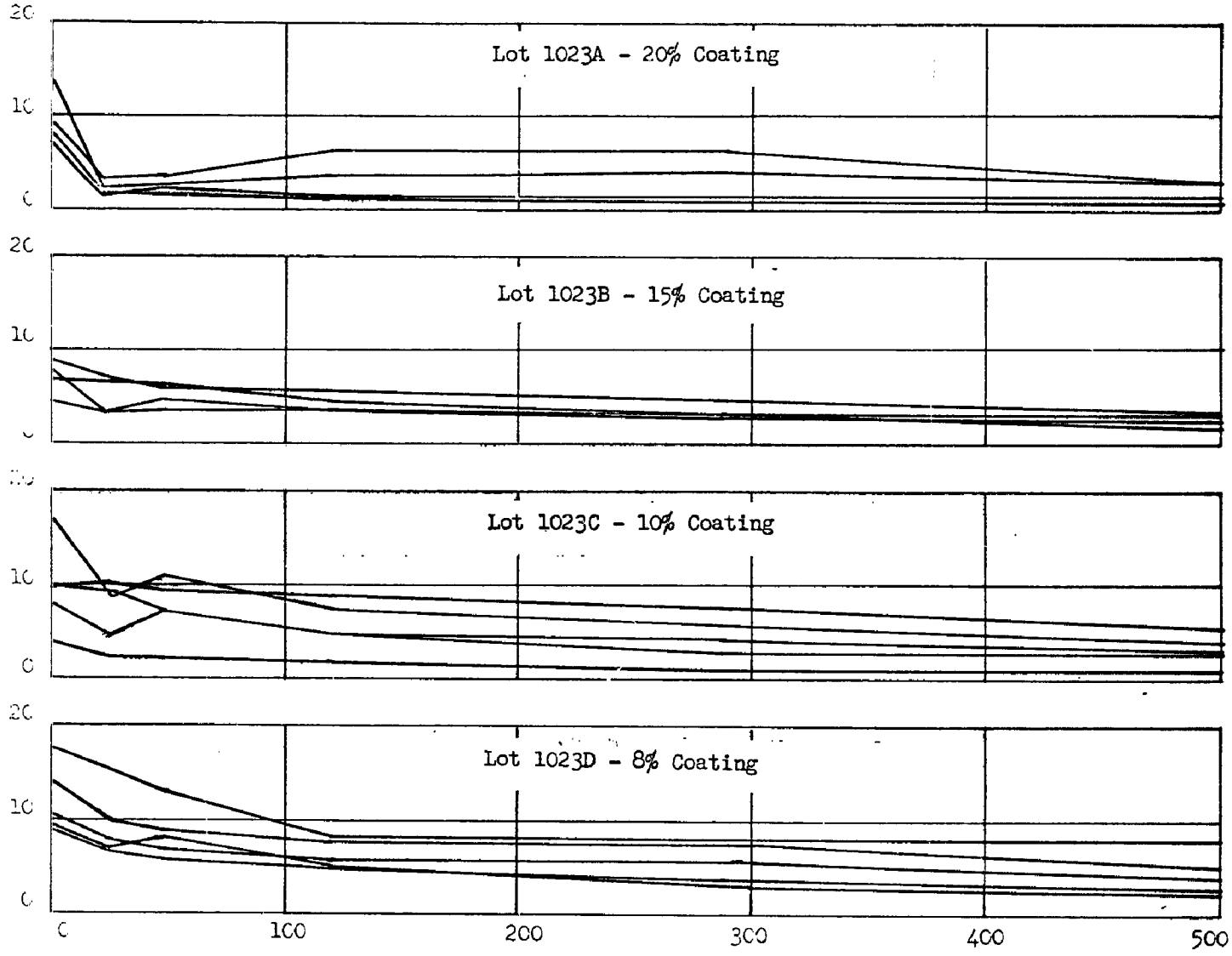

Note - % Coating is proportion of Strontium 70 / Barium 30 cathode coating (S. I. H1-1R-3) in reagent grade acetone

Figure 19

Additional life test data are shown in Figures 20, 21 and 22. These tests compare triode operation at E_p = 50 volts to operation at E_p = 10 volts. These tests also compare stabilized tubes with nonstabilized tubes. At the 2500 hour point, the differences between these lots are insignificant.

Triode data comparing the effects of processing in the two types of vacuum systems are shown in Figures 23 and 24. The tubes made in the oil diffusion pumped system have a lower contact potential and consequently are operating at a higher plate current. This causes transconductance to be higher on these tubes than on other groups when the applied test voltages are the same. The tubes processed in the ion pumped system appear to be slightly more stable. It is believed that a better comparison of these two groups of tubes could have been made if the transconductance had been measured at a constant plate current thereby eliminating the differences of operating points caused by the different values of contact potential.

Shock Test

Shock testing of TDMM triodes was continued this period. All tubes tested used the 0.007" x 0.007" mesh. All tubes were shocked five times at 675 G in each of three directions as shown in Figure 25A. The plate current was recorded before and after each blow, and upon the completion of the tests, d-c readings were taken for comparison against readings taken before the test. These before and after readings are shown in Table 6. Figure 25B displays the plate family trace before and after shock testing tube #4452.

It can be noted from these data that there were no instances of grid failure due to shock testing. The large decrease in measured contact potential (see recorded d-c readings) in some cases is misleading because

TRIODE EMISSION VS HOURS OF LIFE
For Stabilized and Unstabilized Tubes

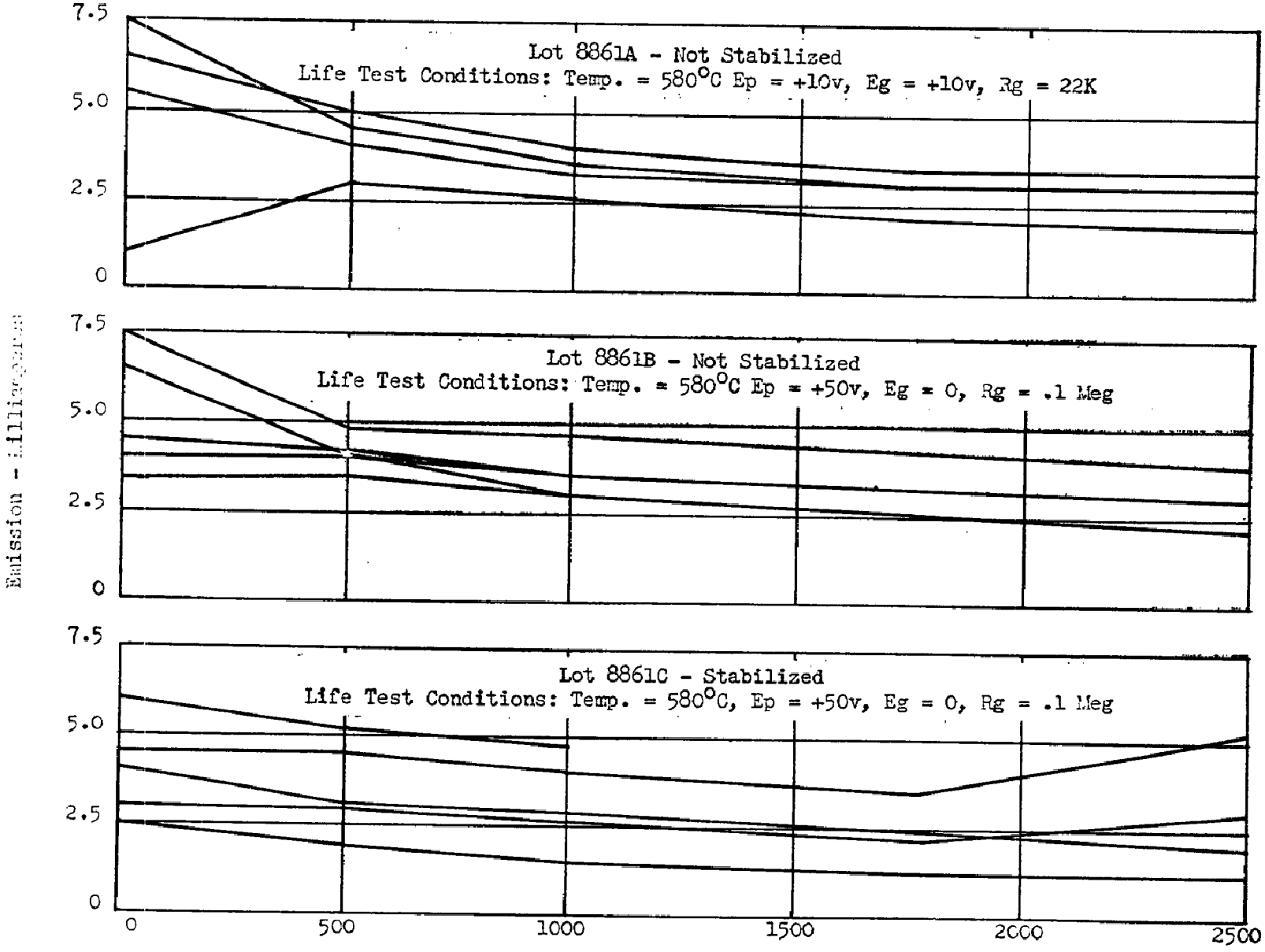

Figure 20

TRIODE GRID-CATHODE CONTACT POTENTIAL VS HOURS OF LIFE

For Stabilized and Unstabilized Tubes

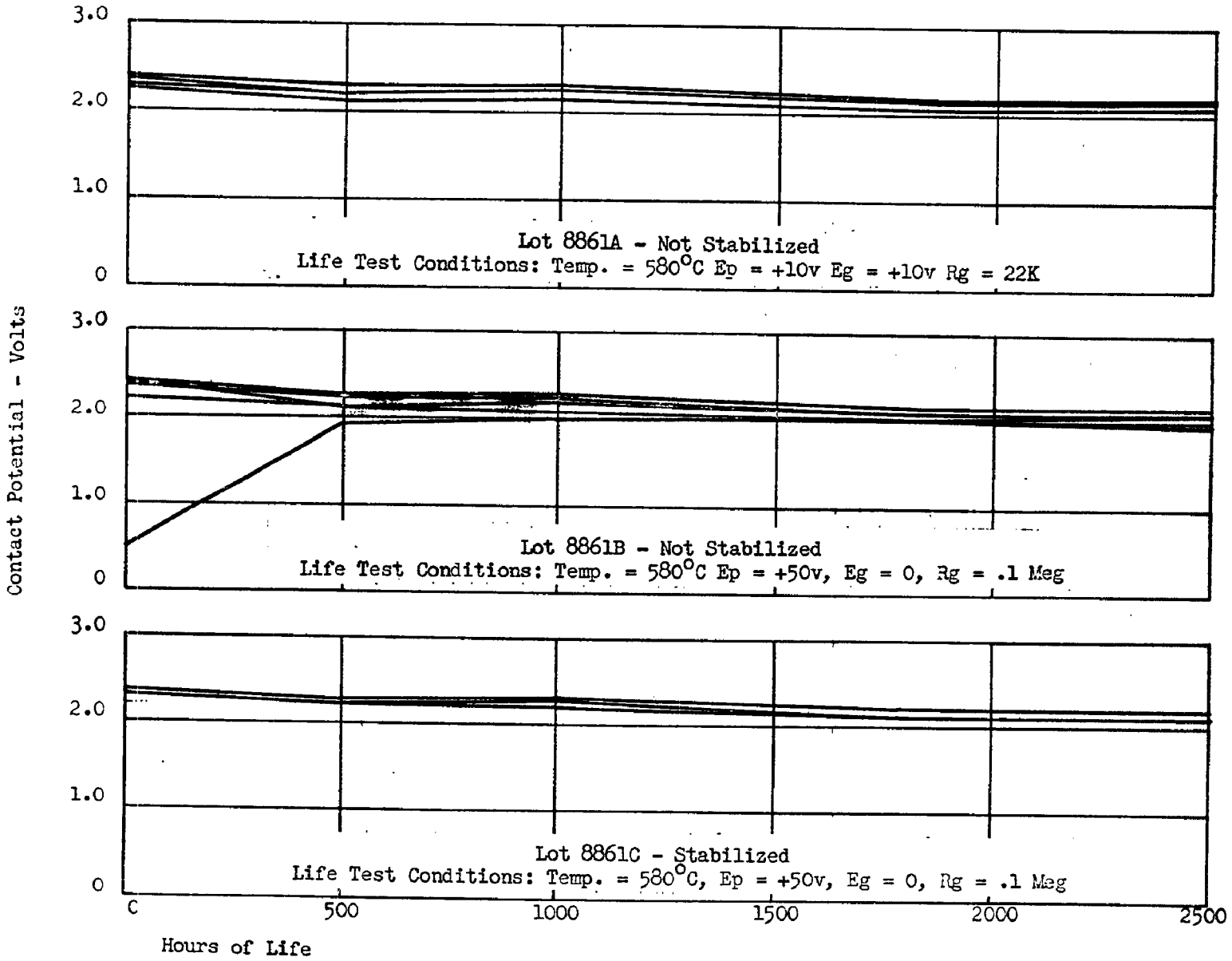

Figure 21

TRIODE TRANSCONDUCTANCE VS HOURS OF LIFE
For Stabilized and Unstabilized Tubes

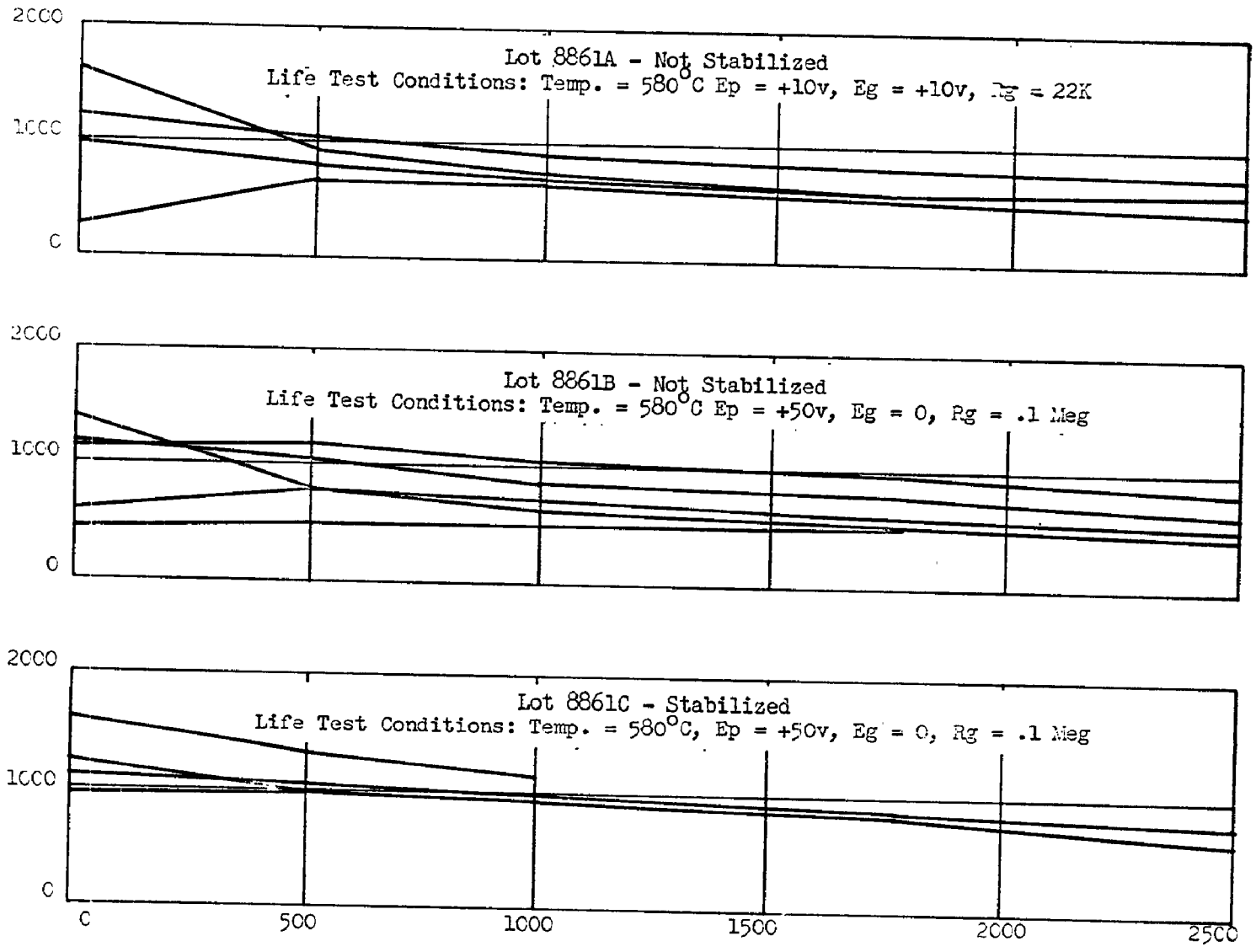

Figure 22

TRIODE GRID-CATHODE CONTACT POTENTIAL VS HOURS OF LIFE
FOR DIFFERENT VACUUM SYSTEMS

Life Test Conditions: Temperature = 580°C, Ep = 50 vg, Eg = +1.0v, Rg = 100K

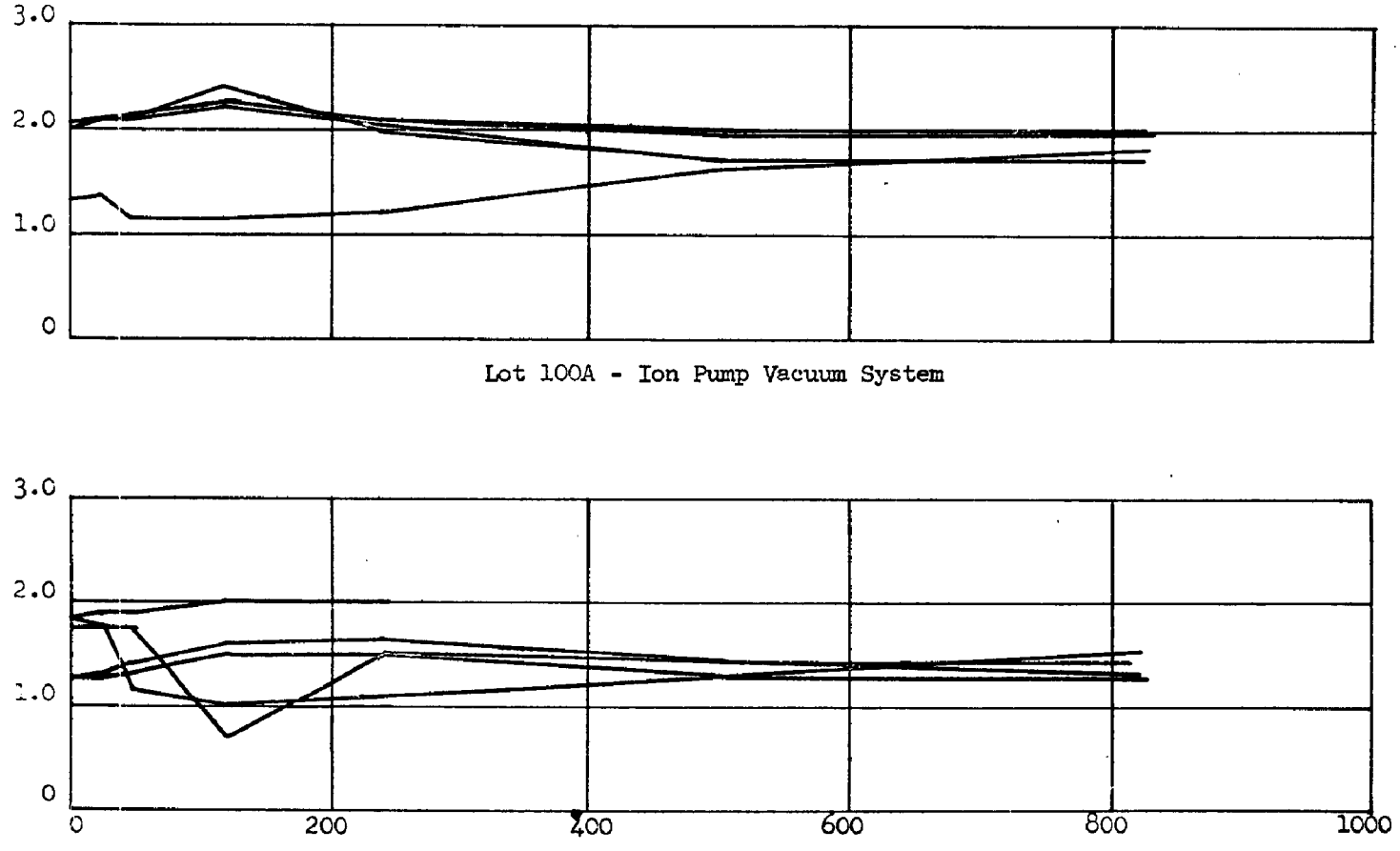

Figure 23

TRIODE TRANSCONDUCTANCE VS HOURS OF LIFE
FOR DIFFERENT VACUUM SYSTEMS

Life Test Conditions: Temperature = 580°C, Ep = 50v, Eg = +1v, Rg = 100K

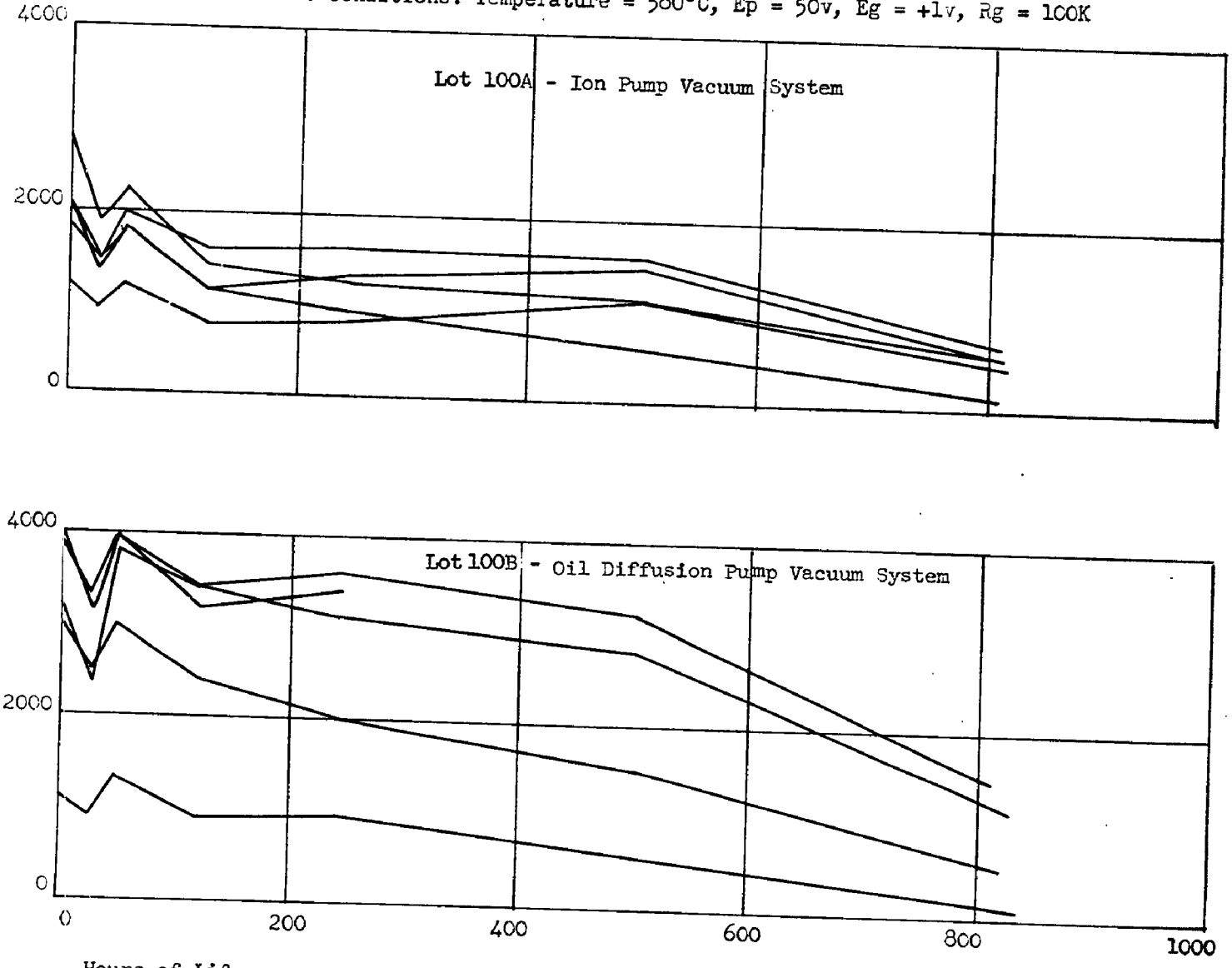

Figure 24

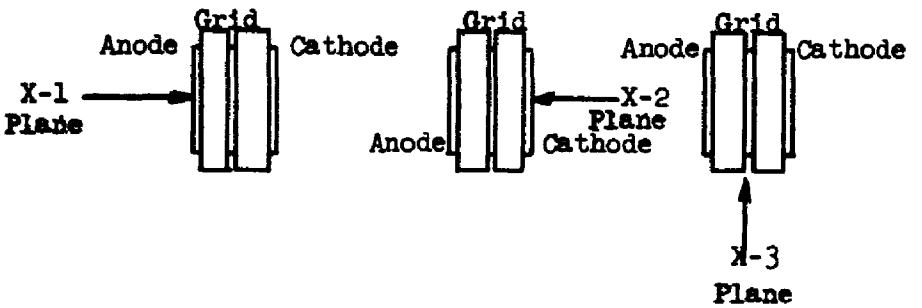

Direction of Shock Test Blows

Figure 25A

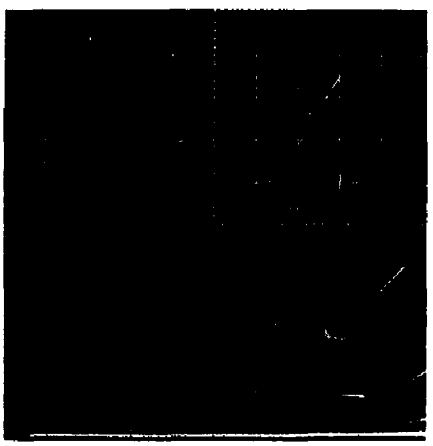

Before Shock Test

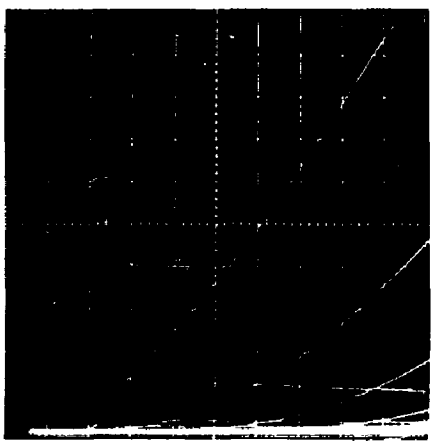

After Shock Test

Test Conditions

Horizontal Scale - 1 volt / Div. Vertical Scale - .2 ma / Div.

Grid Voltage - +2.5 volts max. - .5 volt / Step

Plate current is diagonal trace

Grid current is horizontal trace

The Plate Family of Tube #4452
Before and After Shock Test

Figure 25B

DC Readings Before and After Shock

Tube #	i_s (ma)	C.P.(V)	$I_{g_{1\mu a}}$	i_{p_1} (ma)	IR (meg)
4410					
Before Shock	8	.8	420	2.82	>3
After Shock	4.5	.84	370	2.50	>3
4610					
Before Shock	7	2.07	218	2.42	>3
After Shock	7	1.44	298	2.40	>3
4565					
Before Shock	4	2.20	170	1.05	2
After Shock	5	2.06	190	1.00	>3
4446					
Before Shock	3	1.05	380	1.28	>3
After Shock	WENT AIR AFTER COMPLETION OF TEST				
4452					
Before Shock	13	2.06	460	1.65	>3
After Shock	13	.92*	470	1.55	>3
4463					
Before Shock	16	2.00	800	2.17	>3 meg.
After Shock	13	.61*	860	2.10	>3

* Note explanation on Page 23.

Shock Test Conditions:
Grid Voltage +2.0 volts
Plate Voltage +10.0 volts
Shock Level 675 G/blow

Test Conditions
$I_s - E_p$ and E_g = 30v R_g = 15000 ohms
Contact Potential E_p = 0 I_g = 10 μa
I_g and $I_{p_1} - E_p$ = 7.0v E_g = + 2.5v
IR - E_g = -3.0v

Table 6

of measuring techniques. Contact potential is measured by determining the grid potential necessary for 10 μa of grid current. If a small piece of cathode coating should become dislodged from the cathode and adhere to the grid, the work function of this very small area would be reduced and the 10 μa current would be obtained at a very low voltage. Thus, the value of contact potential measured would be considerably lower than the average grid contact potential. This is clearly shown in the plate families of tube #4452 which suffered a large drop in measured contact potential while the plate families indicate very little change in characteristics.

The only shock test performed so far has been on the 0.007" x 0.007" grid which is 0.0015" thick. More shock tests will be performed on tubes with thinner grid materials.

Module Fabrication

The brazing of TIMM components into circuit modules is presently performed with aluminum as a brazing material because of previous difficulty with silver migration across some components which were brazed with Incusil 15. Some difficulty in obtaining consistently strong aluminum braze joints has been experienced. Modules have been brazed in both Argon and vacuum atmosphere using aluminum shims ranging from 0.0005" to 0.002" in thickness. The thicker material yields the stronger braze initially but deteriorates rapidly at operating temperature. This is believed to be due to relatively large voids in the braze joint where the metallic aluminum, remaining after the brazing operation, diffuses into the titanium. An investigation is now under way to determine the exact nature of this void problem and how best to solve it.

Summary of Tubes Made

A total of 936 triodes, 696 single section diodes and 93 triple section diodes were made as part of the research and development efforts. Of the total number of tubes made, 132 triodes, 378 diodes and 14 triple section diodes were considered to be acceptable*, usable components.

Again, as during the last reporting period, interelectrode shorts and low contact potential are still the major problems to be resolved. The problem of interelectrode shorts is aggravated by the close grid to cathode spacing used in triodes and the tendency for titanium grids to warp and bow at processing temperatures in excess of 1000 C and environmental temperatures of 580 C.

---

* An acceptable diode has no shorts, saturated emission > 4.0 ma, contact potential > 2.2 volts and R_p < 350 ohms.

* An acceptable triode has no shorts, insulation resistance over 1.0 megohm, saturated emission greater than 4.0 ma and contact potential over 2.2 volts.

RESISTOR DEVELOPMENT

Tungsten Film

Work was continued, during the first part of this reporting period, toward the development of tungsten film resistors. Efforts were devoted to the formation of metallic tungsten resistive elements by reducing WO_3 films which had been deposited on the ceramic substrate.

Two methods of deposition were utilized. In the first, the substrates were masked as usual for the evaporation process and positioned in the evaporation fixture A 0.030" diameter tungsten wire was used as the source of WO_3 by resistance heating at a pressure of approximately 10^{-1} torr. The temperature of the wire was increased until WO_3 vapor or "smoke" became visible in the bell jar, then held at this temperature for film build-up. In each test run, it was found that the WO_3 vapor had diffused between the mask and substrates and had deposited, to some degree, over the entire substrate surface. The deposited film was quite soft, fluffy and exhibited very poor bonding to the substrate. The weak bond was evidenced by stripping of the film during removal of the substrates from the masks.

Because of the undesirable film and bond properties and the problems involved in making suitable masks, this method of film application has not been pursued vigorously.

A spray technique was also employed whereby WO_3 powder was suspended in amylacetate. then sprayed onto the masked substrates using a conventional spray gun. Reasonably defined thin films were realized by this method: however. when thick films were attempted, the deposit tended to peel away from the substrate on removal from the mask.

After deposition of the WO_3 the substrates were dried. then fired in a molybdenum boat in a line hydrogen atmosphere to a temperature of 1250 C

for 10 minutes to accomplish reduction of the WO_3 to metallic tungsten. In no case was a conductive tungsten film achieved with a practical thickness of WO_3. With a heavy film (approximately 0.005"), continuity was achieved in those areas which did not peel during removal from the mask.

Because of the problem of line definition, the film thickness necessary for useable resistive values, poor bonding properties, and the anticipated problems of control associated with the reduction process, this approach to tungsten film resistors has been dropped from the present work plan.

Deposition of metallic tungsten resistive films on ceramic substrates by thermal decomposition of tungsten hexacarbonyl will be attempted during the next quarter.

Platinum and Rhodium Films

Efforts toward deposition of platinum and rhodium resistive elements were devoted to the evaporation method. Tungsten wire (0.020" diameter) was used as the heat source for both materials. For platinum deposition, a close wound helix of 0.005" platinum wire was formed on the tungsten wire heat source, while the rhodium source was prepared by plating this material over the tungsten wire.

Evaporation was accomplished by heating in vacuum at a pressure of less than 10^{-4} torr at a temperature slightly above the melting points of the respective materials.

The major problem encountered with these materials was one of depositing sufficient metal to produce resistors of useable values. As many as three sources were used on one batch of substrates; however, the lowest values produced in finished resistors were approximately 500K ohms at 580 C for platinum and two megohms at 580 C for rhodium. Values within each batch ranged from those stated above to infinity. The resistance change

with temperature was negative for both types and ranged from 50 to 75 per cent from room temperature to 580 C.

Sixteen platinum film units ranging from 500K to 800K ohms have been prepared for life test. Values for rhodium film resistors were so high and scattered that it was felt no practical data could be obtained from life testing.

Ground Surface Substrate Resistors

Several batches of evaporated carbon film resistors were made utilizing ground surface OW-102 substrates. This resistor is shown in Figure 26.

RESISTOR WITH GROUND SURFACE SUBSTRATE

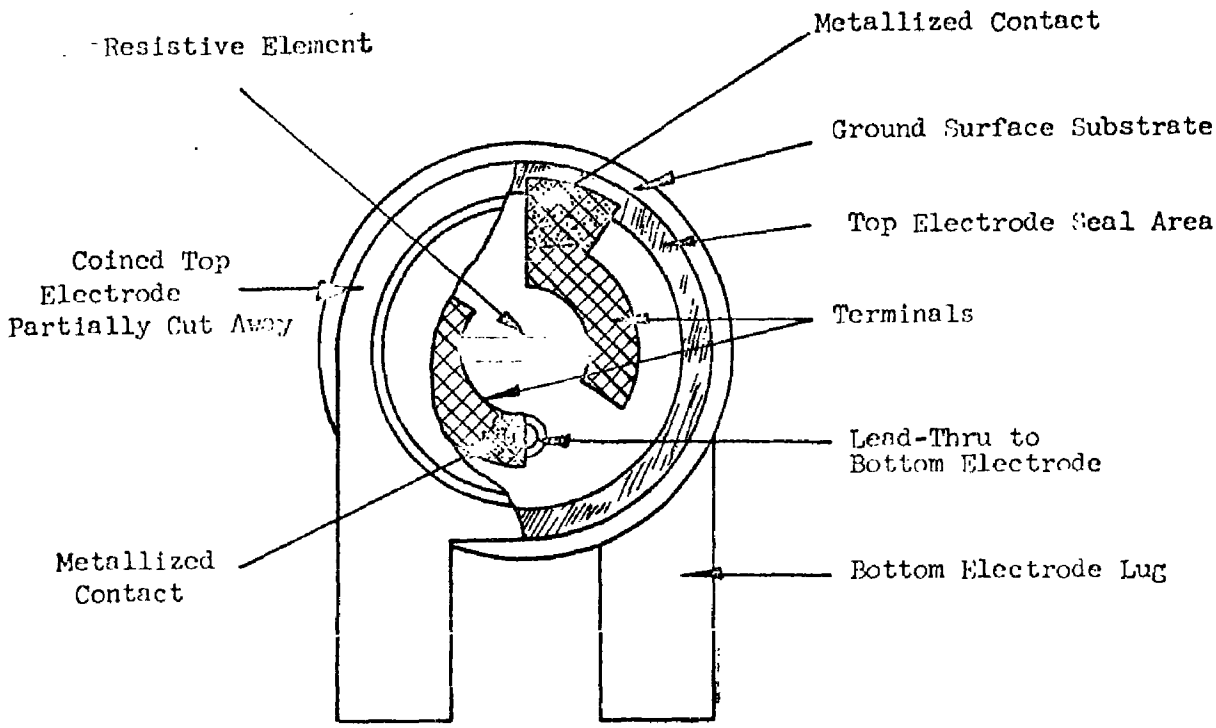

Figure 26

Here, the substrate surface on which the resistive element is deposited was ground flat using a 120 grit diamond wheel. Clearance between the film and top electrode was achieved by coining this electrode to form a recess of from 0.005" to 0.006". This coined electrode is shown in Figure 27b.

The purpose for making this type resistor was to determine if there were any advantages to be realized in depositing the resistive film on a relatively smooth surface. There were no initial differences evident. Forty units have been put on life test at 580 C ambient temperature. Sixteen of these are dissipating approximately 0.25 watts/unit with the remaining 24 dissipating approximately 0.1 watts/unit.

Low Capacitance Resistor

Approximately 75 evaporated carbon units have been made according to the design shown in Figure 27a. The top electrode is the coined type shown in Figure 27b, but with the lug removed. The bottom electrodes are shown in Figure 28. These units were designed and fabricated in an attempt to reduce the capacitance from that inherent in the standard design and which, in certain applications, is prohibitive.

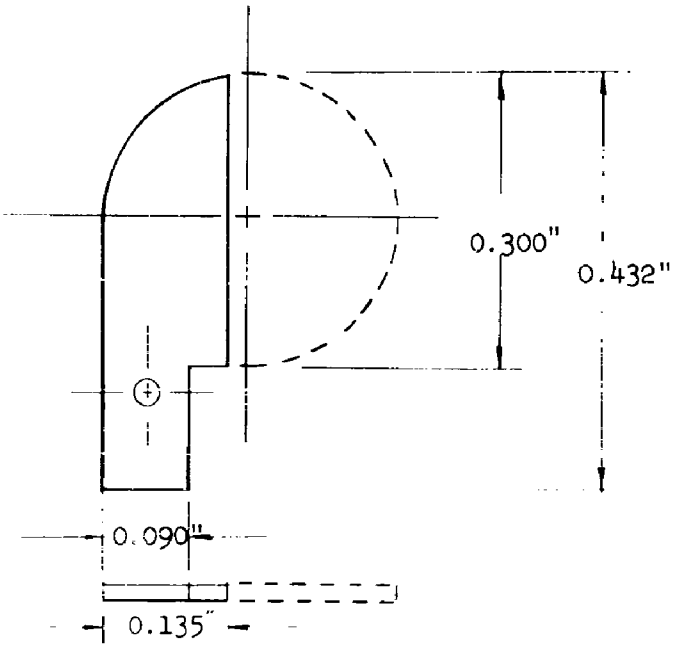

Figure 28

LOW CAPACITANCE RESISTOR

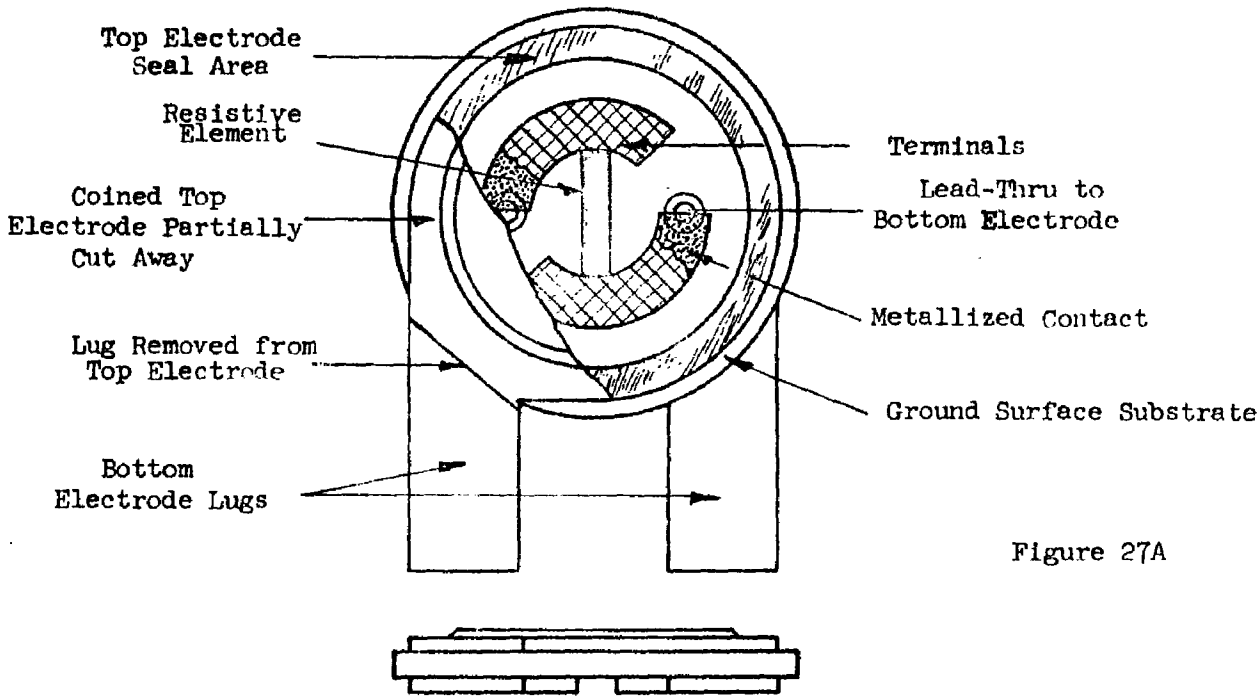

Figure 27A

COINED ELECTRODE

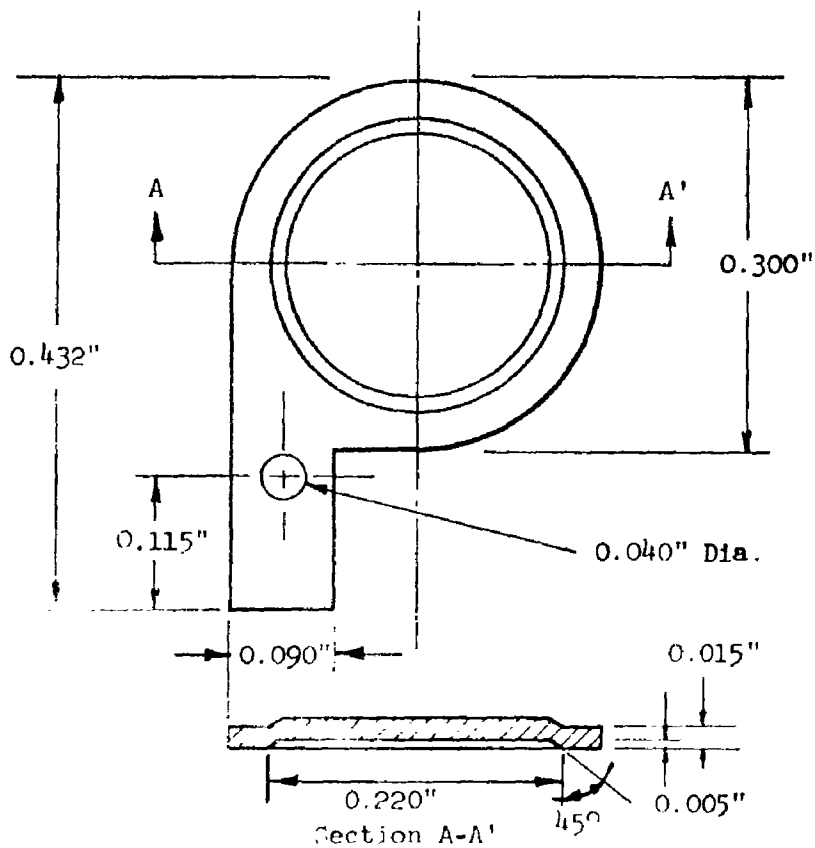

Figure 27B

The following table shows the results of measurements made on (1) low capacitance types, (2) regular pyrolytic carbon types, and (3) regular evaporated carbon types. Measurements were made on a Type 250-A Boonton RX Meter at room temperature.

TABLE 7

Capacitance at Various Frequencies for Resistors of Low Capacitance and Regular Design

Design	DC Resistance at 580 C	Capacitance (pf)			
		10 Mc	30 Mc	50 Mc	100 Mc
Low Capacitance	13.2K	1.9	1.8	1.9	2.1
Low Capacitance	19.8K	1.8	1.7	1.7	1.9
Regular Pyrolytic	3.1K	5.0	5.0	5.4	7.0
Regular Pyrolytic	22.3K	5.6	5.8	6.0	8.1
Regular [illegible]	3.3K	5.3	5.4	5.7	7.6
Regular Evaporated	22.2K	5.6	5.8	5.9	7.8

It is apparent from the above that the low capacitance design has decreased capacitance by approximately 65 - 70%.

Since materials, processing and element design remain unchanged, it is assumed that no new information would be derived from life testing; therefore, tests of this nature are not being considered.

Ceramic Body OW-129 as Substrate Material

Twenty-six evaporated carbon film resistors utilizing OW-129 as the substrate material have been made. This material is very similar to OW-102 with the exception that the oxide purity is considerably higher. The composition lies within limits covered in a patent application filed by R. H. Bristow of the Power Tube Department, General Electric Company, Schenectady, New York.

The added units were fabricated with OW-102 and OW-129 substrates in adjacent positions throughout the entire processing schedule. Sixteen resistors

from each substrate lot have been put on 580 C ambient life test. Life test data on these units is not available at this time. There were no noticeable differences detected in initial testing.

Shock and Vibration

Several pyrolytic and evaporated carbon resistors have been delivered to the Testing Laboratory for shock and vibration evaluation, as equipment becomes available. No rigid test specifications have been determined as yet; however, it is anticipated that the shock tests will be conducted from 450 - 600 G's and that the vibration test will be from 50 - 2000 cps at 10 - 15 G's.

High Value Resistors

A considerable amount of time during the latter part of this period was devoted to fabricating 470K ohm resistors to satisfy circuitry requirements for the dynamic word generator display unit being prepared for the contract review meeting at Wright Field January 16, 1962.

Carbon Film Life Test Results

Figure 29 shows life test results on pyrolytic and evaporated carbon film resistors for 5000 hours. The resistance values were chosen such that for the applied voltage the load dissipation ranges from 0.25 to 0.40 watts/unit. Degradation of both types is apparent. The total change in the pyrolytic type at the end of 5000 hours is nearly 14% or about twice that in the evaporated units. The rate of change, however, has been approximately the same for both types since 3000 hours.

Figure 30 shows life test results to 4500 hours for pyrolytic carbon film resistors operating over a load range of from 0.1 to 1.0 watt/unit. Figure 31 shows the same type of information for evaporated carbon resistors over a 3000-hour period. Although the evaporated units have been

LIFE TEST

CARBON FILM RESISTORS

Test Conditions:

Ambient Temperature - 580 C
Applied Voltage - 50v RMS
Power Dissipation - 0.25 - 0.4 watts/unit

Test Sample:

+ - 38 Units Evaporated Carbon
o - 47 Units Pyrolytic Carbon

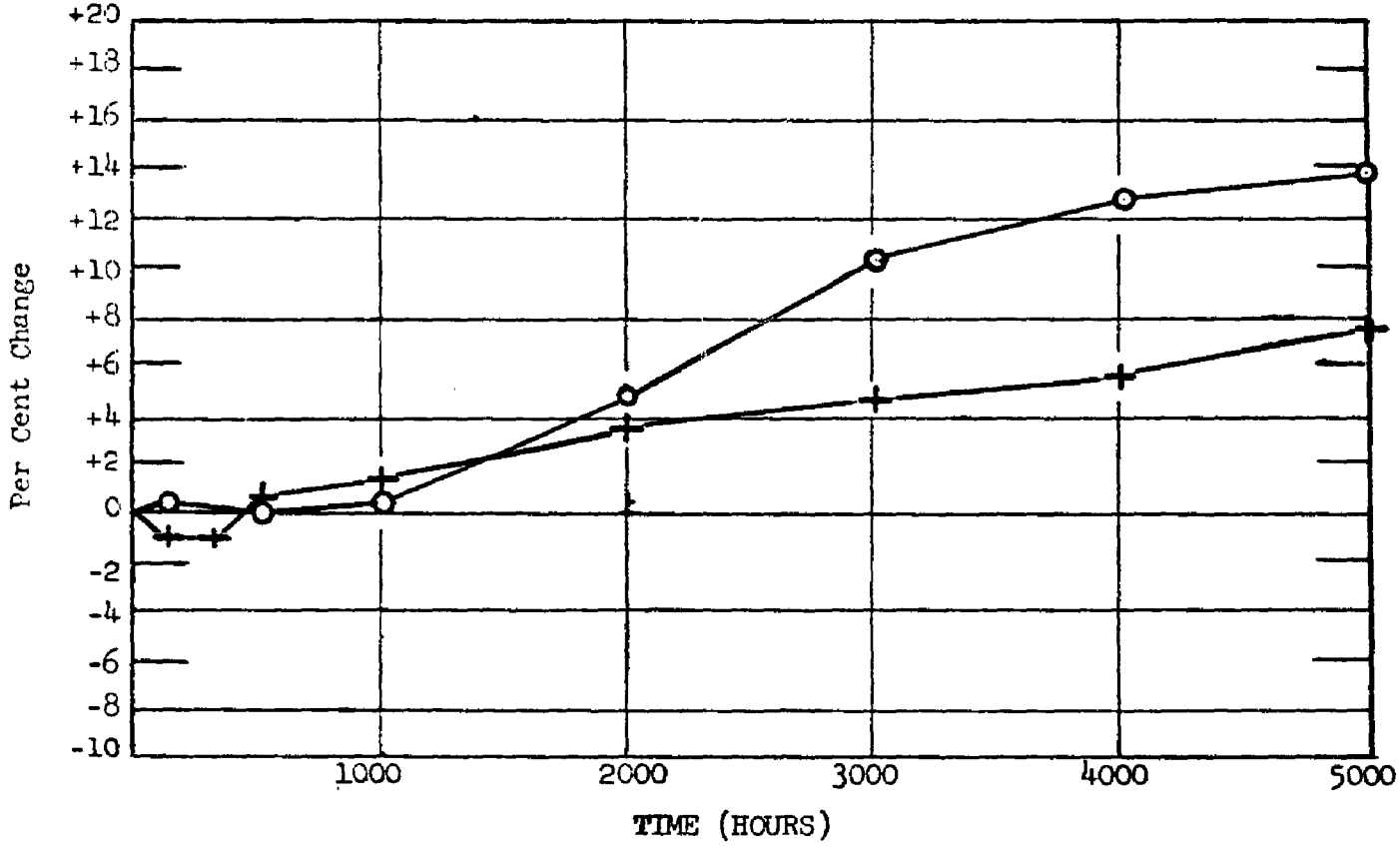

Figure 29

LIFE TEST
PYROLYTIC CARBON FILM RESISTORS
OPERATING OVER RANGE OF LOAD LEVELS

Test Conditions:

Ambient Temperature - 580 C
Power Dissipation - 0.1 - 1.0 watt

Test Sample:

8 Units at Each Load

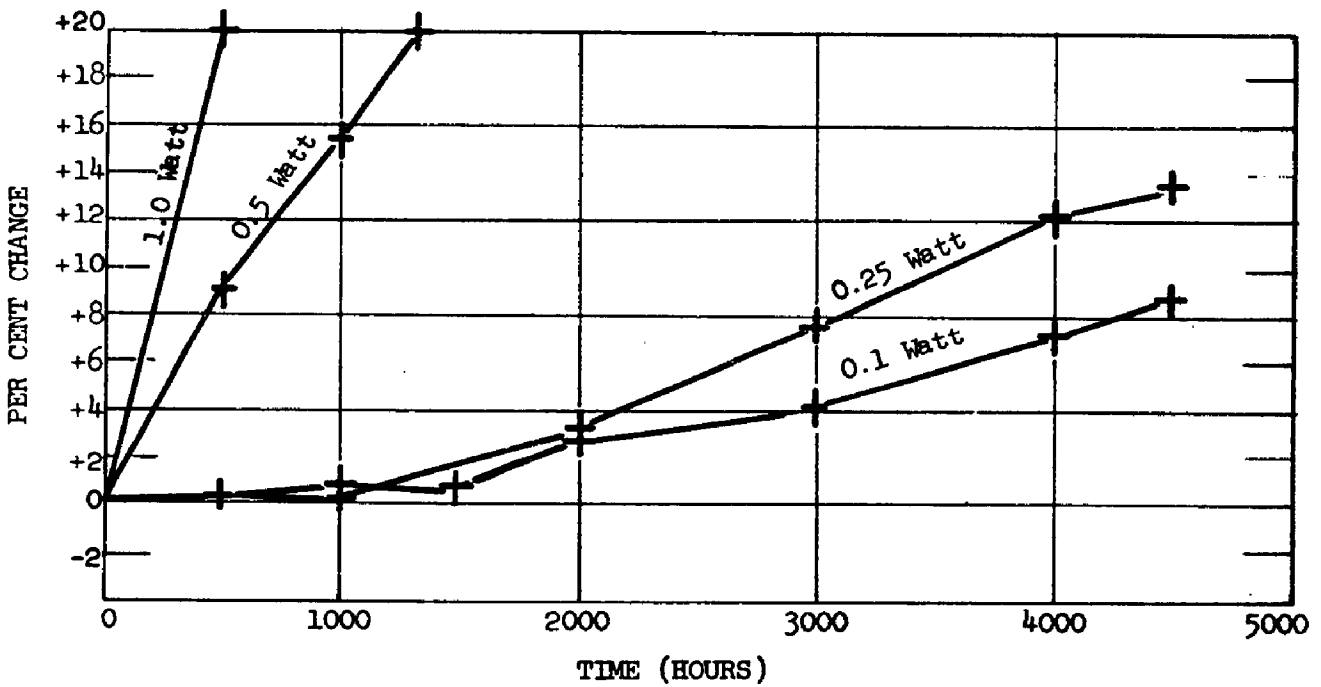

Figure 30

LIFE TEST
EVAPORATED CARBON RESISTORS
OPERATING OVER A RANGE OF LOAD LEVELS

Test Conditions:

Ambient Temperature - 580 C
Power Dissipation - 0.1 - 0.8 Watts/Unit

Test Sample:

8 Units at Each Load

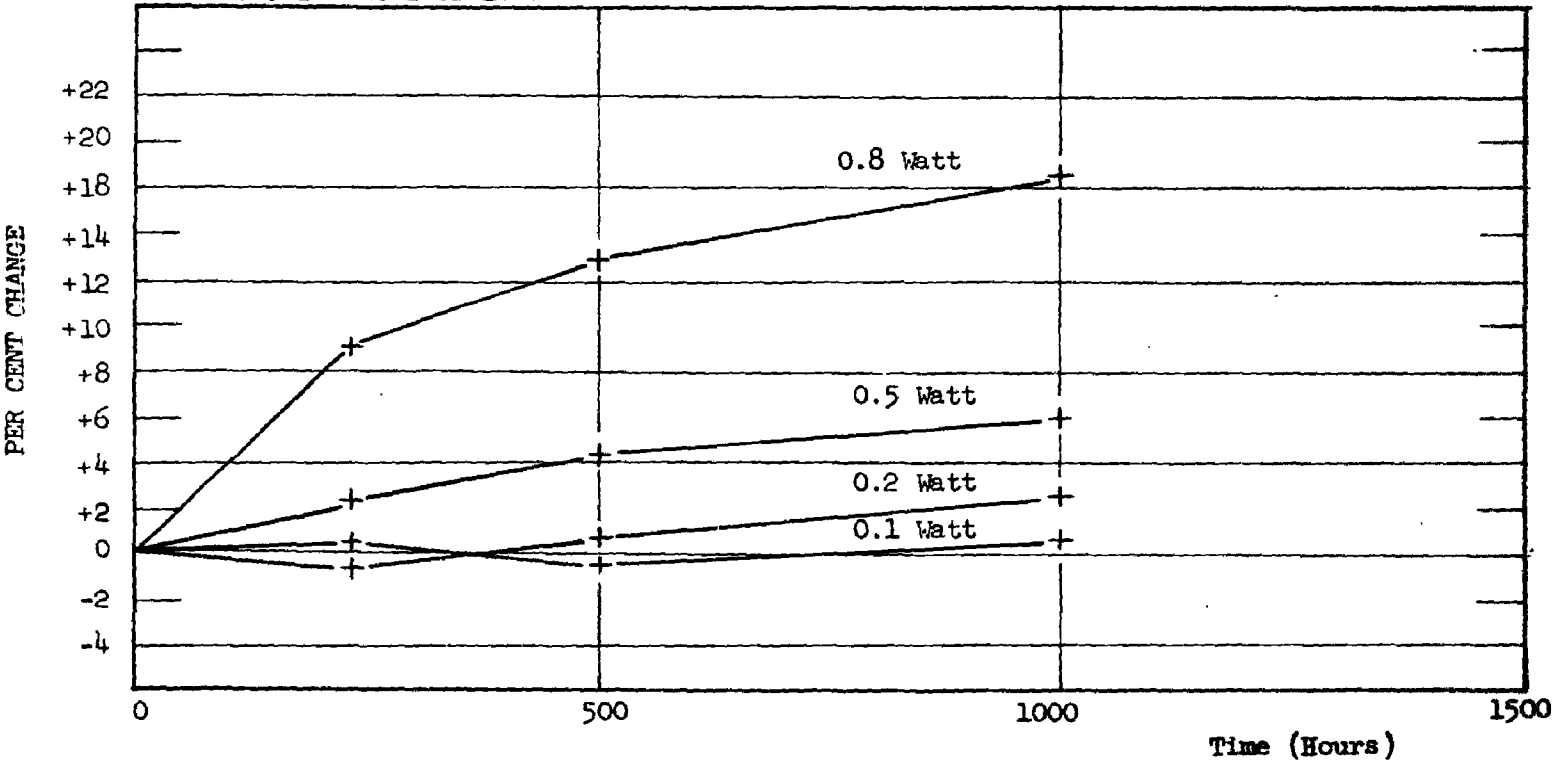

FIGURE 31

on test a shorter period of time, it is apparent from the data that the rate of resistance change with time increases with increasing applied load for both type resistors. It is further noted that the change in the units, operating at approximately half watt and one watt, is much more rapid for the pyrolytic film than the evaporated carbon film resistors. No large differences are apparent in units operating at 0.1 and 0.2 watts at the end of 1000 hours.

It is postulated that the increased resistance change with applied load may be due to the higher resistive element temperature in those units operating at higher loads. The ambient temperature is held constant at 580 C; however, the resistors in the life test stack will be at some temperature above this, depending upon the power dissipated in the stack.

Since the TIMM circuits will be operating at a module temperature of approximately 580 C, it now seems apparent that resistors should be life tested with the complete stack at this temperature. This would dictate that all units on life test in one oven be operating at the same load with the furnace temperature adjusted to give the proper stack temperature.

Another approach to cooler operation of the resistive element would be to increase the contact area between the element and the ceramic substrate. Masks have been designed and ordered for producing a 0.040" wide element which will double the contact area. However, with double the contact area for a given resistance value, the film will be only half as thick. Because of this reduction in film thickness, the sensitivity of the monitoring system will be similarly reduced. Another technique under consideration would make it possible to retain the same resistive film thickness by utilizing an increased path length

Metal Film Life Test Results

Figure 32 shows 580 C life test results on nichrome and molybdenum film resistors to the end of 1500 hours. Test samples consist of eight units of each type resistor operating at approximately 1/4 watt/unit.

The results shown for molybdenum resistive films were from units with values of approximately 2.4K ohms. One group of eight molybdenum film resistors, with values of approximately 5 - 6K ohms, were also put on life, however, all eight units failed (discontinuity of the resistive film) between zero and 500 hours. It appears this may be the same type problem encountered with nichrome resistors having values above a few hundred ohms, where electrical discontinuity developed at the juncture of the element and terminal.

LIFE TEST

METAL FILM RESISTORS

Test Conditions:

Ambient Temperature - 580 C
Power Dissipation - 0.25 watts/unit

Test Sample:

+ 8 Units Nichrome (100)
o 8 Units Molybdenum (2.4K)

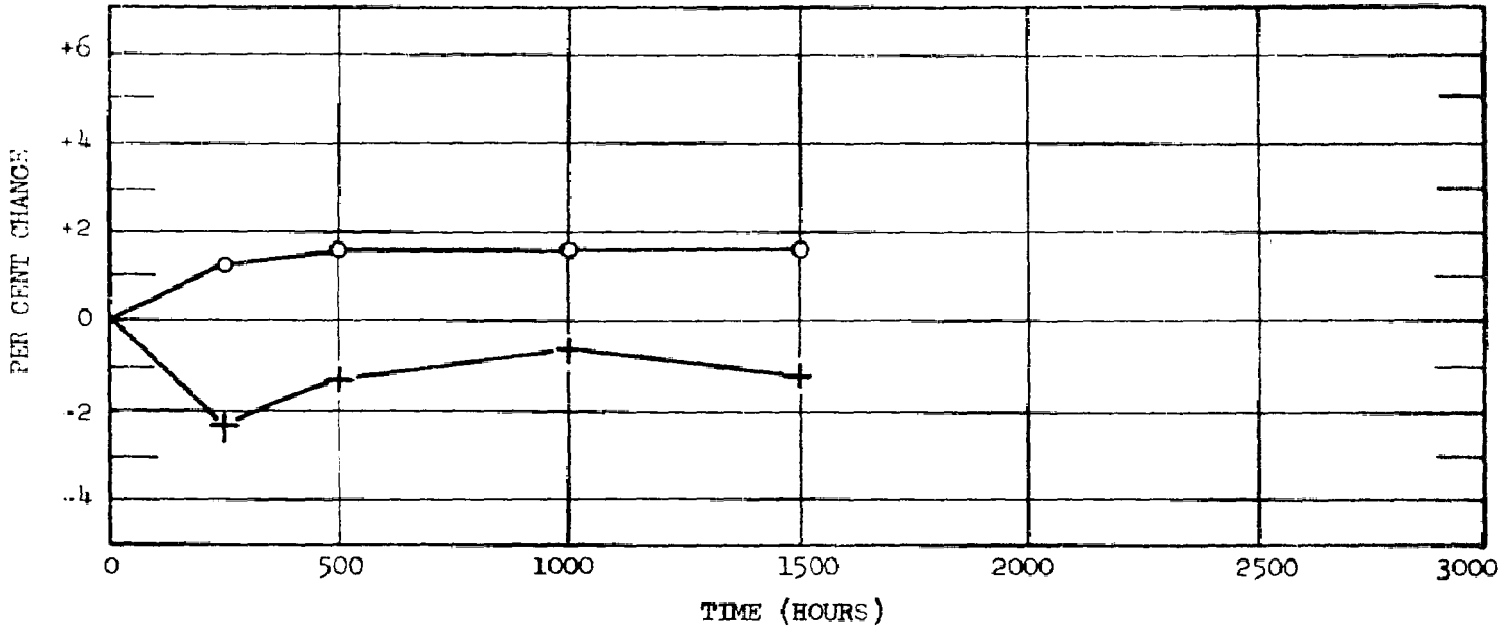

Figure 32

High Temperature Conductivity

Stacked ceramic capacitors (.005" thick OW-102 dielectric), operating at 580 C, have shown a marked increase in resistance during the application of the 200 volt d-c life test conditions. The change in resistance has been measured only in the guarded lead, which is the positive direction of the d-c applied. The increase in resistance is from a range of 10-30 megohms to 3000-5000 megohms. At the same time, resistance in the negative direction may be approximately the same as the original value or slightly lower. This appears to be a low frequency phenomenon related to the apparent very drastic change in dielectric constant below 10 kc.

In the pulse shaper network, a large stack capacitor (300 pf) was used at 10 kc. This was the first application where this phenomenon introduced losses which deformed the circuit characteristic. It was first thought that there was a low internal resistance in the capacitor, but later experiments point to a rectifier action or emf generation at the titanium-ceramic interface.

The temperature-resistivity characteristic was measured on 2.24 $in.^2$ sample discs of 0.050" thick OW-102 ceramic with platinized electrodes (Dupont Platinum Bright). The plot of conductivity (ρ) versus the reciprocal of absolute temperature (Figure 33) is nearly a straight line to the upper temperature limit of the test equipment. Examination of data accumulated on a number of stacked, sealed units shows a change in slope at 500- 600 C, and the change is dependent on the previously applied voltage. The change in slope indicates a change in activation energy and a different conduction mechanism predominating above 500 C.

CONDUCTIVITY-TEMPERATURE RELATIONSHIP

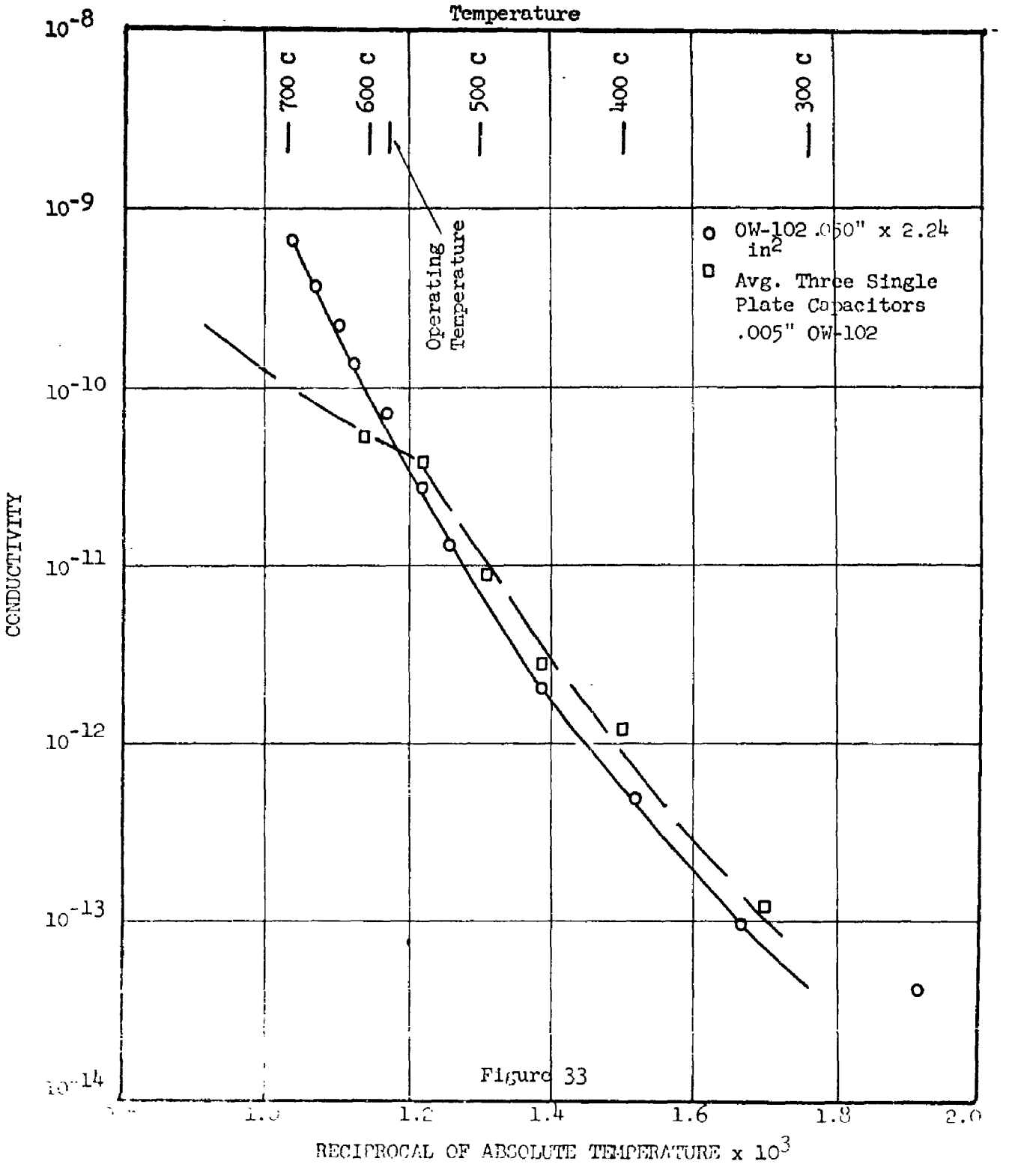

Figure 33

A series of tests were run on titanium sealed ceramic using a simple, single plate capacitor configuration (shown in Figure 34). Data are compiled in Table 8 and plotted as conductivity (ρ) versus reciprocal of absolute temperature ($1/K^{o} \times 10^{3}$) in Figures 35-38. For these tests, ceramic compositions OW-102, OW-116 and OW-126 were used. Composition OW-116 was sealed to 16 per cent chrome iron electrodes with a nickel-titanium eutectic. Ceramic OW-126 is the same body as OW-102 except for the addition of one per cent TiO_2 to the batch composition. Resistivity-temperature measurements were made at 50 and 100 volts d-c in both the forward and reverse direction. The data are plotted as conductivity in curves 35-38.

In addition, the effect of other materials in the seal, expecially copper, was studied. A definite increase in the leakage current level resulted in every case. The collection of these data are incomplete at this time but will be included in the next report.

The increase of temperature above 580 C, coupled with the application of voltage, causes polarization in very short periods of time. At 700 C and 300 volts d-c for 10 minutes, a marked change in resistance in the positive direction is noted. The difference in forward and reverse current, with voltage, is shown in Figure 39. On the same curve the forward and reverse current for a platinized disc is plotted. The data show that the resistance or leakage current approaches the value noted for the original material in one direction and diverges in the opposite.

It was observed that after the application of 300 volts, a voltage could be read out of the unit well beyond the normal time constant of the capacitor. In fact, the unit can be shorted or loaded for periods of [illegible] and [illegible], a partial reduction of the voltage is noted. Table 9 shows the magnitude of this voltage

CROSS SECTION

SINGLE PLATE CAPACITOR UNIT

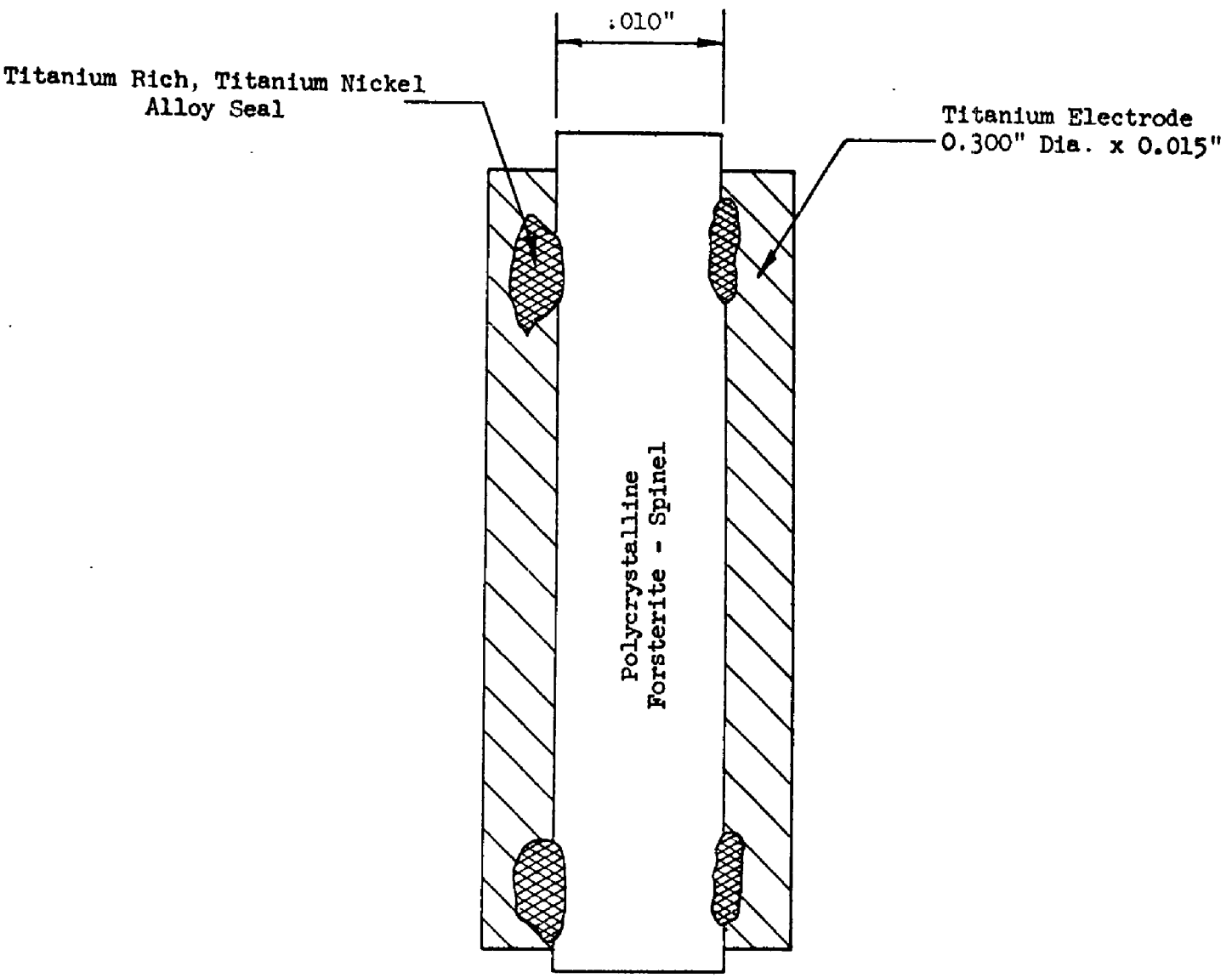

Figure 34

TABLE 8

OW-126 - Thickness 10 Mil (0.010") - Single Section

Temp. (°C)	Leakage Current +50V	Leakage Current -50V	Leakage Current +100V	Leakage Current -100V	Conductivity (Ohm-cm)$^{-1}$ +50V	Conductivity (Ohm-cm)$^{-1}$ -50V	Conductivity (Ohm-cm)$^{-1}$ +100V	Conductivity (Ohm-cm)$^{-1}$ -100V
300	1.18×10^{-9}	9.9×10^{-10}	2.42×10^{-9}	1.93×10^{-9}	1.32×10^{-12}	1.1×10^{-12}	1.32×10^{-12}	1.08×10^{-12}
350	4.8×10^{-9}	4.9×10^{-9}	1.03×10^{-8}	1.0×10^{-8}	5.55×10^{-12}	5.46×10^{-12}	5.55×10^{-12}	5.58×10^{-12}
400	3.0×10^{-8}	2.85×10^{-8}	6.1×10^{-8}	4.65×10^{-8}	3.33×10^{-11}	3.18×10^{-11}	3.4×10^{-11}	2.6×10^{-11}
435	6.3×10^{-8}	1.44×10^{-7}	1.13×10^{-7}	3.6×10^{-7}	7.0×10^{-11}	1.6×10^{-10}	6.3×10^{-11}	2.0×10^{-11}
470	9.5×10^{-8}	3.2×10^{-8}	1.71×10^{-7}	6.0×10^{-8}	1.06×10^{-10}	3.56×10^{-11}	9.5×10^{-11}	3.35×10^{-11}
500	2.22×10^{-7}	1.6×10^{-7}	2.82×10^{-7}	2.3×10^{-7}	2.47×10^{-10}	1.78×10^{-10}	1.57×10^{-10}	1.28×10^{-10}
550	2.1×10^{-7}	1.98×10^{-7}	4.15×10^{-7}	3.8×10^{-7}	2.34×10^{-10}	2.2×10^{-10}	2.32×10^{-10}	2.12×10^{-10}
600	3.85×10^{-7}	3.55×10^{-7}	7.85×10^{-7}	7.25×10^{-7}	4.3×10^{-10}	3.96×10^{-10}	4.4×10^{-10}	4.05×10^{-10}
700	1.45×10^{-6}	1.45×10^{-6}	2.63×10^{-6}	2.58×10^{-6}	1.61×10^{-9}	1.61×10^{-9}	1.47×10^{-9}	1.49×10^{-9}

OW-116 - Thickness 5 Mil (0.005") - Single Section

300	3.3×10^{-10}	3.3×10^{-10}	6.4×10^{-10}	6.35×10^{-10}	1.83×10^{-13}	1.83×10^{-13}	1.78×10^{-13}	1.78×10^{-13}
350	6.2×10^{-10}	6.2×10^{-10}	1.25×10^{-9}	1.27×10^{-9}	3.44×10^{-13}	3.44×10^{-13}	3.48×10^{-13}	3.48×10^{-13}
400	1.86×10^{-9}	1.9×10^{-9}	4.1×10^{-9}	4.25×10^{-9}	1.04×10^{-12}	1.06×10^{-12}	1.14×10^{-12}	1.18×10^{-12}
435	8.8×10^{-9}	8.15×10^{-9}	1.72×10^{-8}	1.64×10^{-8}	4.9×10^{-12}	4.55×10^{-12}	4.78×10^{-12}	4.57×10^{-12}
470	1.65×10^{-8}	1.48×10^{-8}	3.1×10^{-8}	2.98×10^{-8}	9.2×10^{-12}	8.33×10^{-12}	8.65×10^{-12}	8.3×10^{-12}
500	3.8×10^{-8}	5.8×10^{-8}	8.2×10^{-8}	8.0×10^{-8}	2.11×10^{-11}	3.23×10^{-11}	1.77×10^{-11}	2.33×10^{-11}
550	8.45×10^{-8}	8.2×10^{-8}	1.46×10^{-7}	1.48×10^{-7}	4.72×10^{-11}	4.56×10^{-11}	4.07×10^{-11}	4.12×10^{-11}
600	1.98×10^{-7}	2.18×10^{-7}	3.75×10^{-7}	4.1×10^{-7}	1.1×10^{-10}	1.21×10^{-10}	1.04×10^{-10}	1.14×10^{-10}
700	1.0×10^{-6}	1.08×10^{-6}	1.9×10^{-6}	2.0×10^{-6}	5.56×10^{-10}	6.0×10^{-10}	5.3×10^{-10}	5.57×10^{-10}

TABLE 8 (Cont'd)

OW-102 - (No Nickel) Thickness 5 Mil (0.005") - Single Section

Temp. (°C)	Leakage Current +50V	-50V	+100V	-100V	Conductivity $(Ohm\text{-}cm)^{-1}$ +50V	-50V	+100V	-100V
300	2.8×10^{-10}	2.75×10^{-10}	5.35×10^{-10}	5.3×10^{-10}	1.56×10^{-13}	1.53×10^{-13}	1.49×10^{-13}	1.48×10^{-13}
350	4.75×10^{-10}	5.75×10^{-10}	1.15×10^{-9}	1.1×10^{-9}	3.2×10^{-13}	3.2×10^{-13}	3.2×10^{-13}	3.06×10^{-13}
400	1.6×10^{-9}	1.54×10^{-9}	3.3×10^{-9}	2.9×10^{-9}	8.94×10^{-13}	8.6×10^{-13}	9.35×10^{-13}	8.1×10^{-13}
435	4.15×10^{-9}	3.4×10^{-9}	7.9×10^{-9}	5.7×10^{-9}	2.3×10^{-12}	1.9×10^{-12}	2.2×10^{-12}	1.59×10^{-12}
470	7.15×10^{-9}	5.1×10^{-9}	1.03×10^{-8}	8.2×10^{-9}	3.98×10^{-12}	2.84×10^{-12}	2.87×10^{-12}	2.29×10^{-12}
500	1.15×10^{-8}	9.4×10^{-9}	1.43×10^{-8}	1.25×10^{-8}	6.4×10^{-12}	5.24×10^{-12}	6.96×10^{-12}	3.48×10^{-12}
550	1.65×10^{-8}	2.45×10^{-8}	2.64×10^{-8}	3.15×10^{-8}	9.25×10^{-12}	1.37×10^{-11}	7.35×10^{-12}	8.8×10^{-12}
600	4.8×10^{-8}	5.25×10^{-8}	7.05×10^{-8}	8.0×10^{-8}	2.68×10^{-11}	2.92×10^{-11}	1.96×10^{-11}	2.23×10^{-11}
700	2.4×10^{-7}	3.0×10^{-7}	3.6×10^{-7}	4.35×10^{-7}	1.34×10^{-10}	1.67×10^{-10}	1.0×10^{-10}	1.22×10^{-10}

OW-102 - Thickness 5 Mil (0.005") - Single Section

300	2.21×10^{-9}	1.82×10^{-9}	4.7×10^{-9}	3.65×10^{-9}	1.23×10^{-12}	1.01×10^{-12}	1.31×10^{-12}	1.01×10^{-12}
350	5.45×10^{-9}	6.45×10^{-9}	1.21×10^{-8}	1.37×10^{-8}	3.03×10^{-12}	3.59×10^{-12}	3.37×10^{-12}	3.82×10^{-12}
400	1.6×10^{-8}	1.95×10^{-8}	4.1×10^{-8}	4.7×10^{-8}	9.07×10^{-12}	1.09×10^{-11}	1.14×10^{-11}	1.31×10^{-11}
435	9.65×10^{-8}	3.0×10^{-8}	1.9×10^{-7}	6.5×10^{-8}	5.38×10^{-11}	1.67×10^{-11}	5.3×10^{-11}	1.81×10^{-11}
470	1.33×10^{-7}	5.5×10^{-8}	2.86×10^{-7}	1.1×10^{-7}	7.4×10^{-11}	3.06×10^{-11}	7.96×10^{-11}	3.06×10^{-11}
500	1.93×10^{-7}	9.55×10^{-8}	4.2×10^{-7}	1.94×10^{-7}	1.09×10^{-10}	5.33×10^{-11}	1.07×10^{-10}	5.15×10^{-11}
550	3.2×10^{-7}	3.4×10^{-7}	6.25×10^{-7}	6.75×10^{-7}	1.75×10^{-10}	1.9×10^{-10}	1.74×10^{-10}	1.87×10^{-10}
600	6.4×10^{-7}	6.7×10^{-7}	1.27×10^{-6}	1.38×10^{-6}	3.57×10^{-10}	3.74×10^{-10}	3.55×10^{-10}	3.85×10^{-10}
700	2.7×10^{-6}	3.0×10^{-6}	4.8×10^{-6}	5.5×10^{-6}	1.5×10^{-9}	1.67×10^{-9}	1.34×10^{-9}	1.53×10^{-9}

CONDUCTIVITY-TEMPERATURE RELATIONSHIP

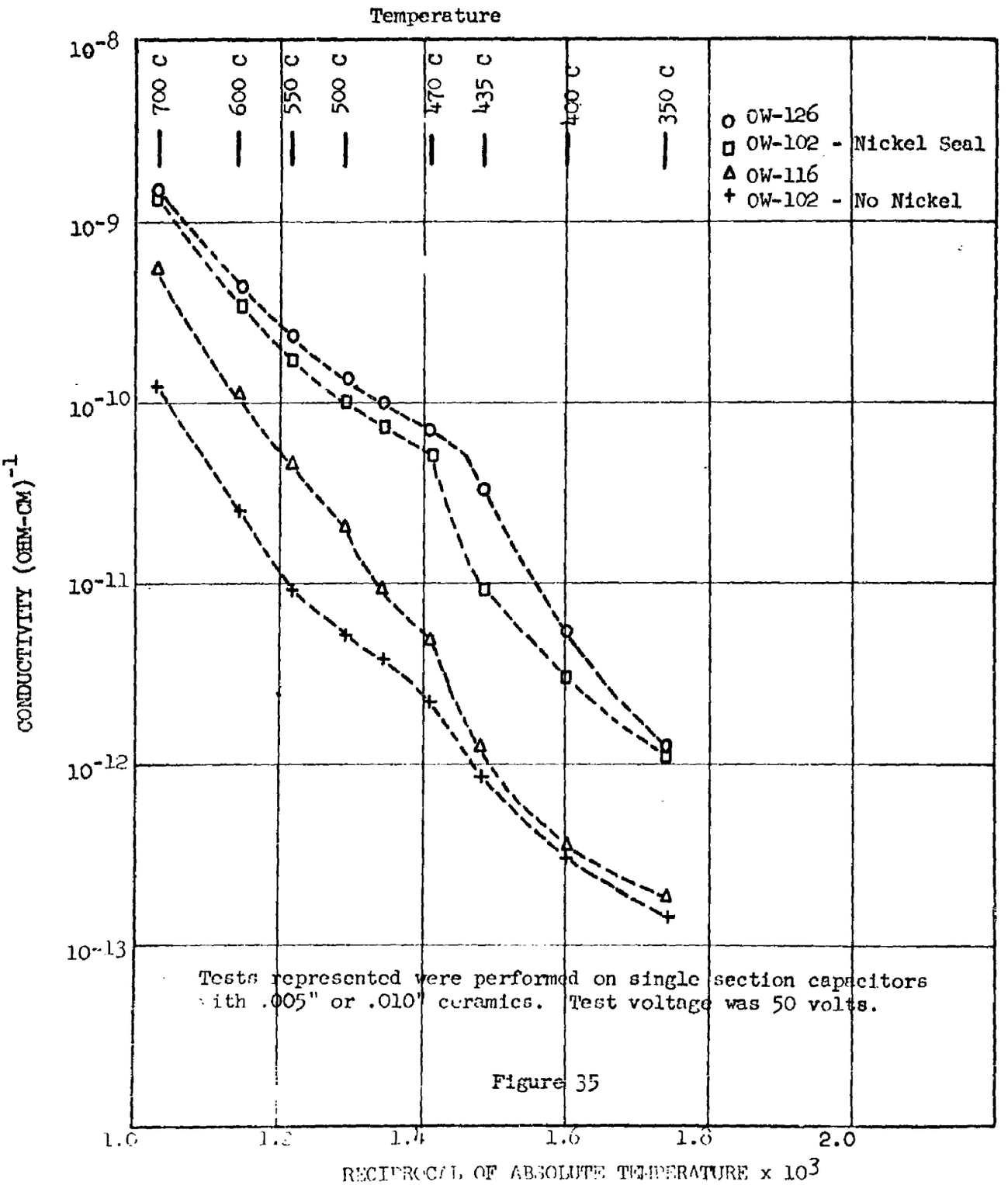

Tests represented were performed on single section capacitors with .005" or .010" ceramics. Test voltage was 50 volts.

Figure 35

CONDUCTIVITY-TEMPERATURE RELATIONSHIP

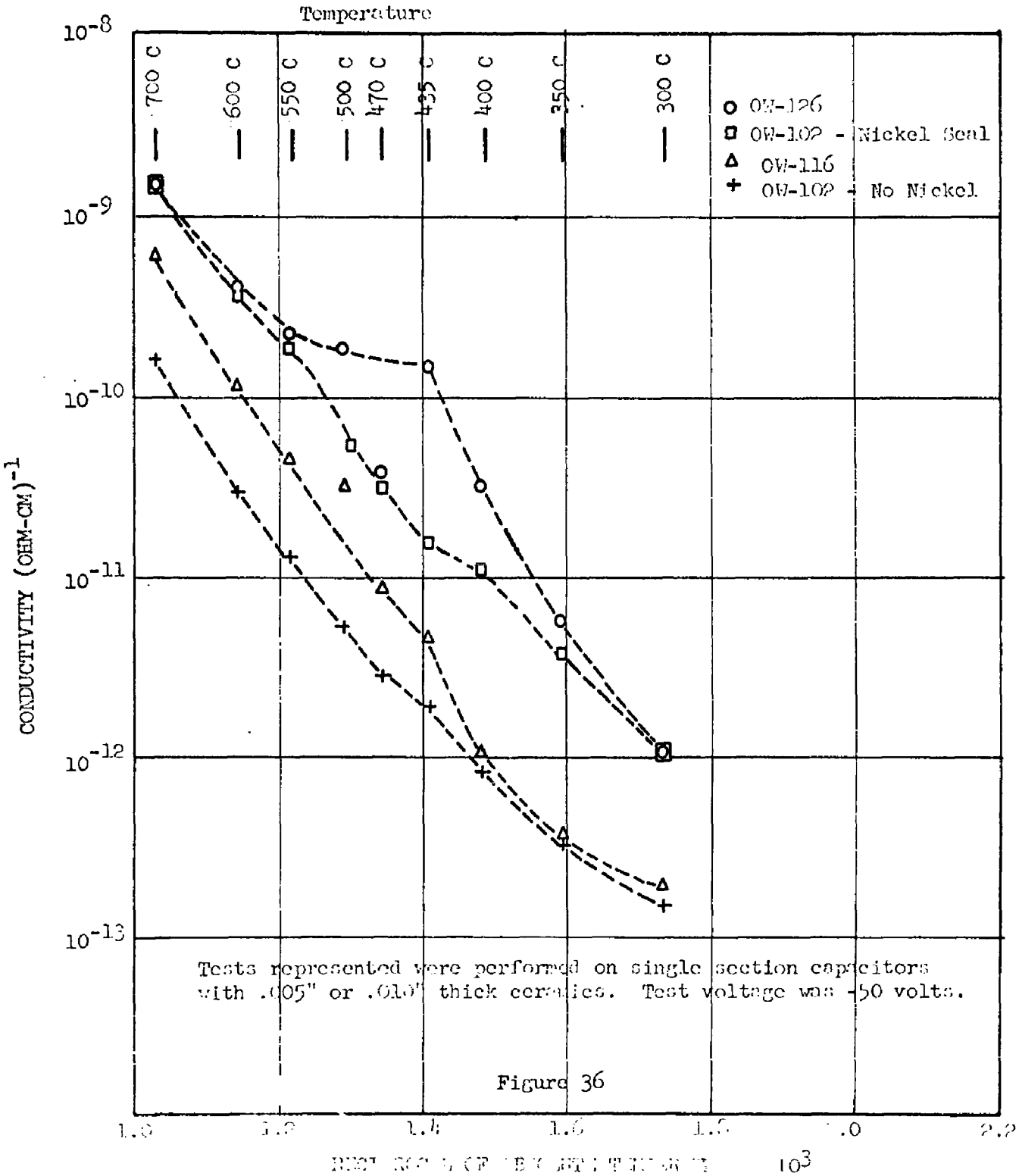

Tests represented were performed on single section capacitors with .005" or .010" thick ceramics. Test voltage was 50 volts.

Figure 36

CONDUCTIVITY-TEMPERATURE RELATIONSHIP

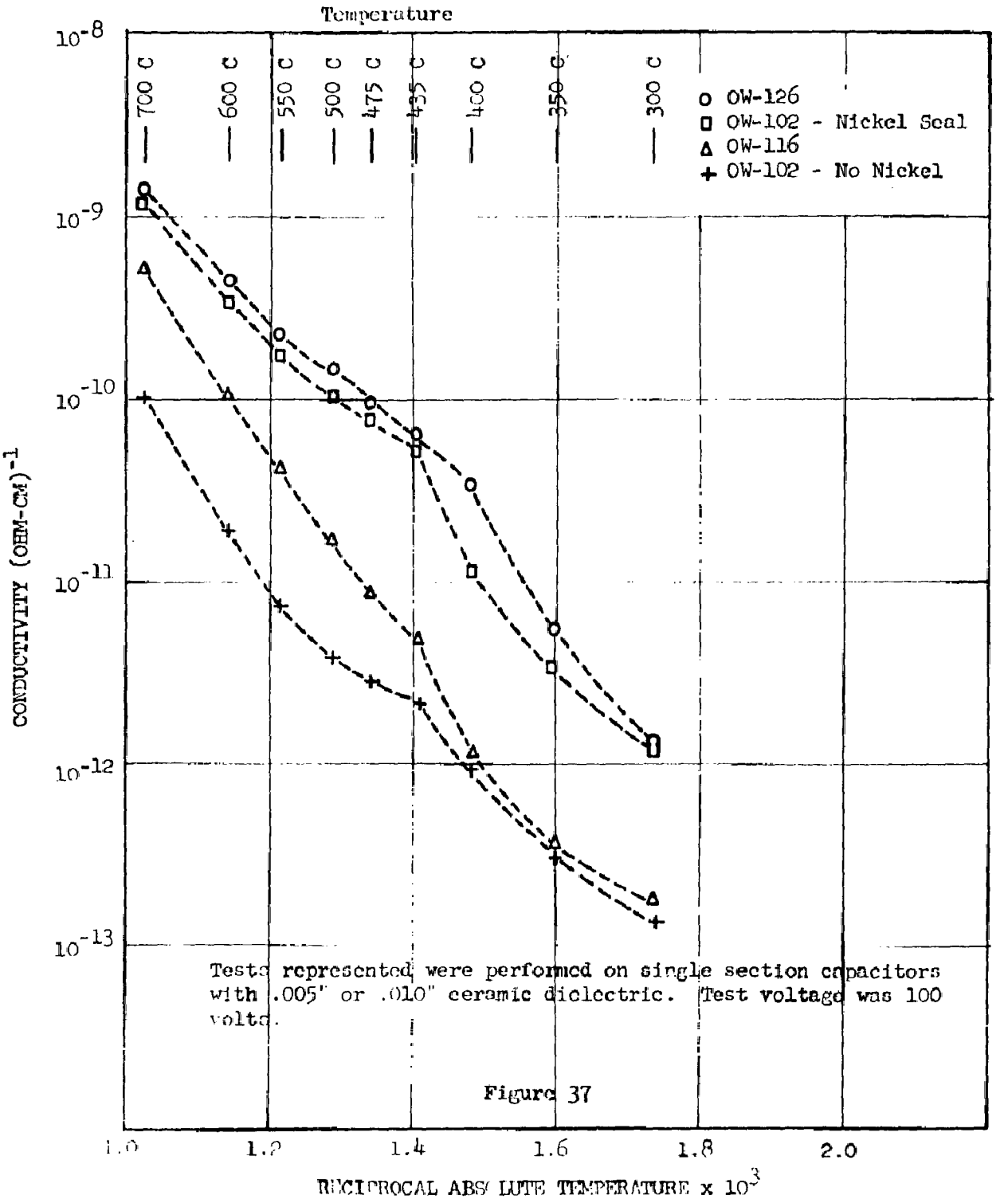

Tests represented were performed on single section capacitors with .005" or .010" ceramic dielectric. Test voltage was 100 volts.

Figure 37

CONDUCTIVITY-TEMPERATURE RELATIONSHIP

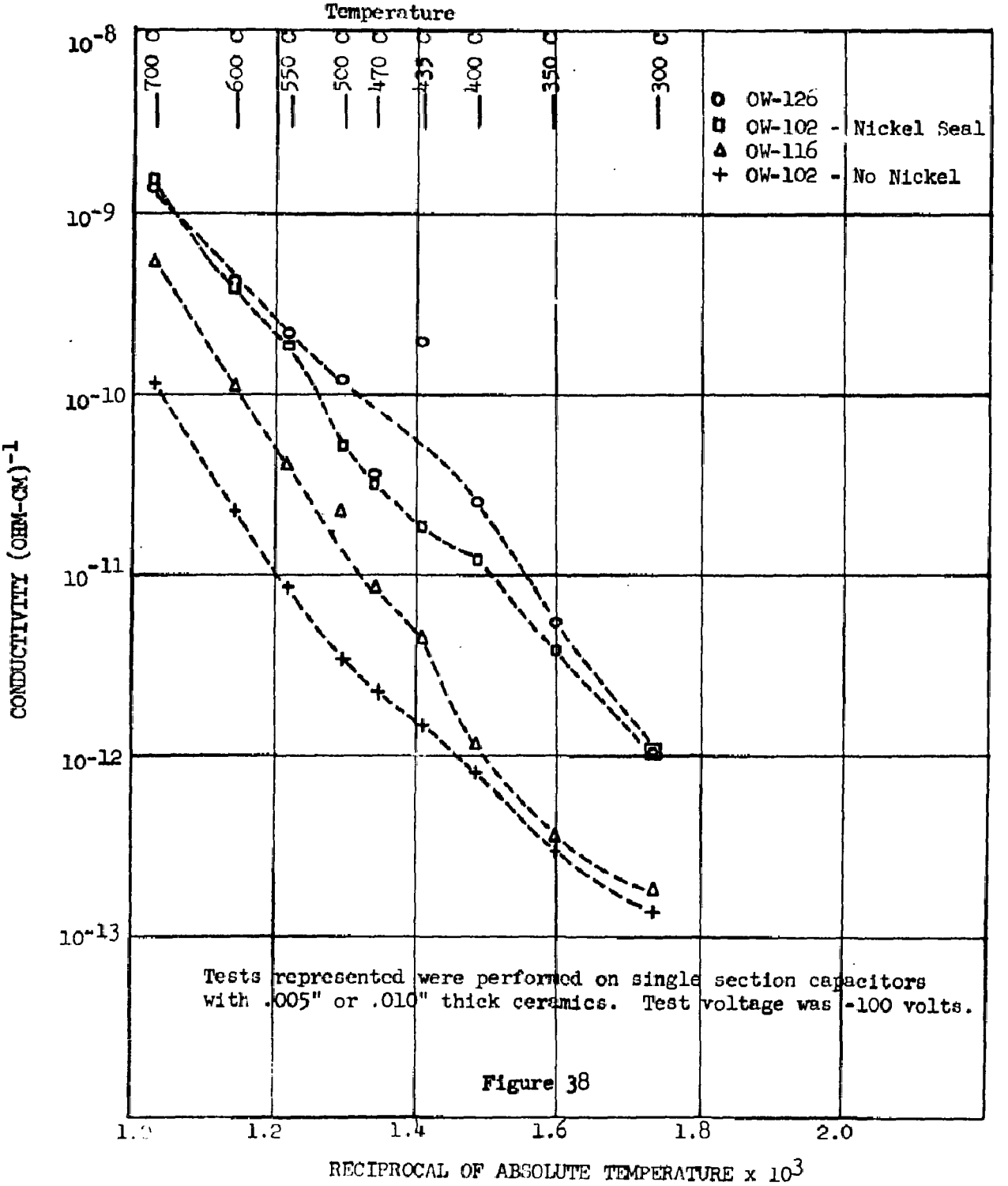

Tests represented were performed on single section capacitors with .005" or .010" thick ceramics. Test voltage was -100 volts.

Figure 38

CHANGE IN LEAKAGE CURRENT WITH POLARITY
AFTER APPLICATION OF DC VOLTAGE

OW-102 Pt ——————
OW-102 Ti — — —
300V DC - 10 Min.
700 C

Figure 39

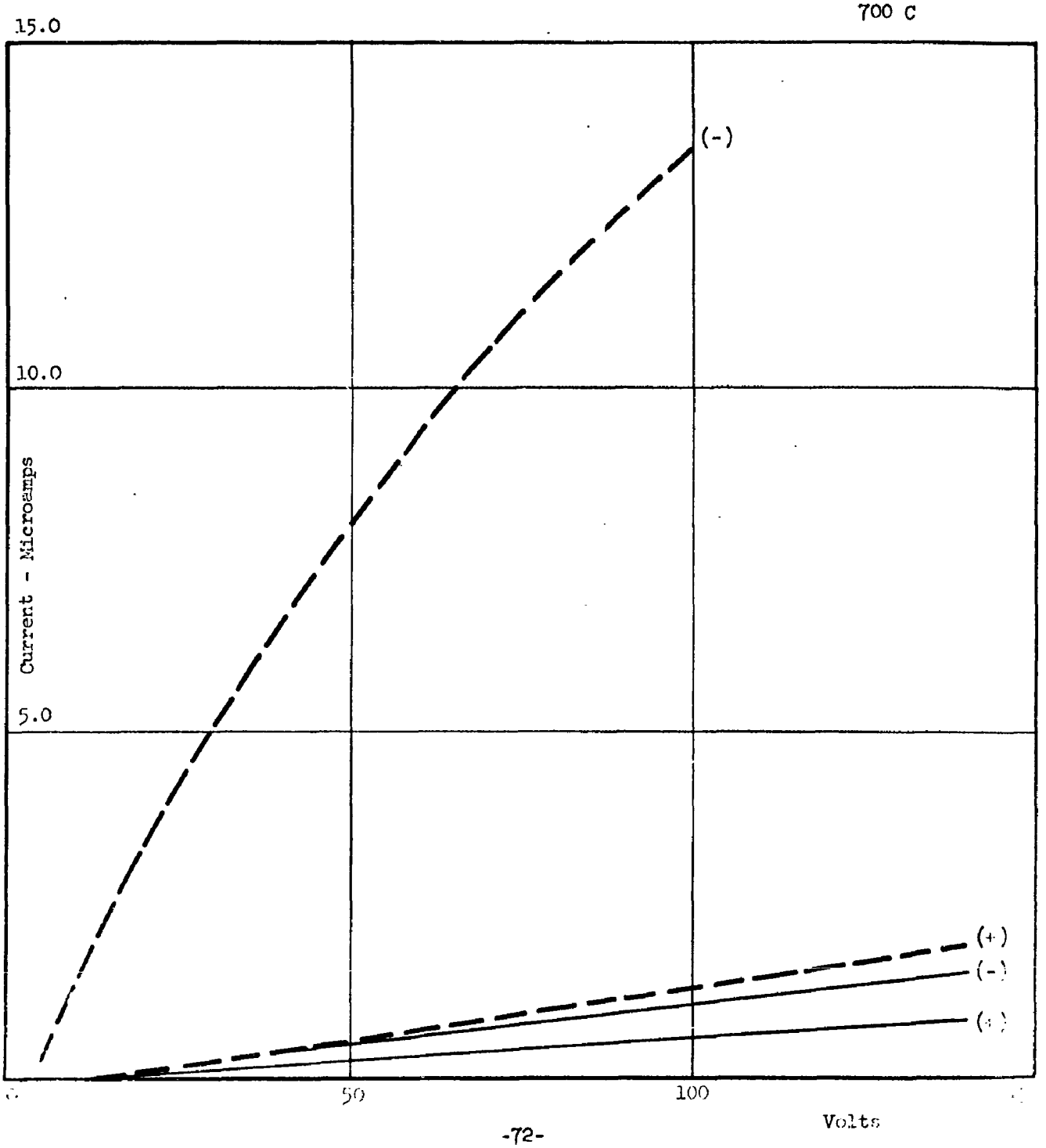

After 1 Minute	10 Megohms	1 Megohm	100 Kilohm
OW-116 - Cu-Ti	7 mv	0.7 mv	0.02 mv
OW-116 - Ni-Ti	10 mv	1.1 mv	0.09 mv
OW-102 - Ni+Cu	53 mv	5.9 mv	0.52 mv
OW-102 - Ni	11 mv	1.0 mv	0
OW-102 - No Ni	16 mv	1.4 mv	0.02 mv
After 70 Hours Not Recharged			
OW-116 - Cu-Ti	4.9 mv	0.5 mv	0
OW-116 - Ni-Ti	6.2 mv	0.63 mv	0.02 mv
OW-102 - Ni_Cu	34.0 mv	4.1 mv	0.4 mv
OW-102 - Ni	6.7 mv	0.6 mv	0.07 mv
OW-102 - No Ni	10.0 mv	1.0 mv	0.09 mv

TABLE 9

Thermally Induced Voltage-Time Relationship
for Capacitor Test Samples Under Varying Load

The 70 hour readings indicate that time effects generally do not eliminate the thermally induced voltages, however a reduction does occur. A comparison of insulation resistance versus the magnitude of this voltage is represented in Table 10.

Material	Insulation Resistance	Voltage Under 10 Megohm Load	Voltage Under 1 Megohm Load
OW-102 - Ni-Cu	63 Megohms	40.0 mv	5.6 mv
OW-102 - Mo-Cu	128 Megohms	22.0 mv	2.1 mv
OW-116 - Cu-Ti	361 Megohms	11.0 mv	1.4 mv
OW-102 - No Ni	365 Megohms	10.0 mv	1.0 mv
OW-102 - Ni	550 Megohms	6.7 mv	0.6 mv
OW-116 - Ni-Ti	557 Megohms	6.0 mv	0.8 mv

TABLE 10

Relationship Between Thermally Induced Voltage and Insulation Resistance for Capacitor Test Samples Under Load

The reversibility of the induced voltage was measured by several techniques. Figure 40 shows typical discharge curves for a unit which has been subjected to a 100 volt d-c charge. The unit was recharged to 10.0 volts positive and negative and the discharge voltage measured with time. The curves show that a negative voltage (approximately 50 millivolts)

TYPICAL DISCHARGE PHENOMENA

STACKED CERAMIC CAPACITOR AFTER DEPOLARIZATION

Figure 40

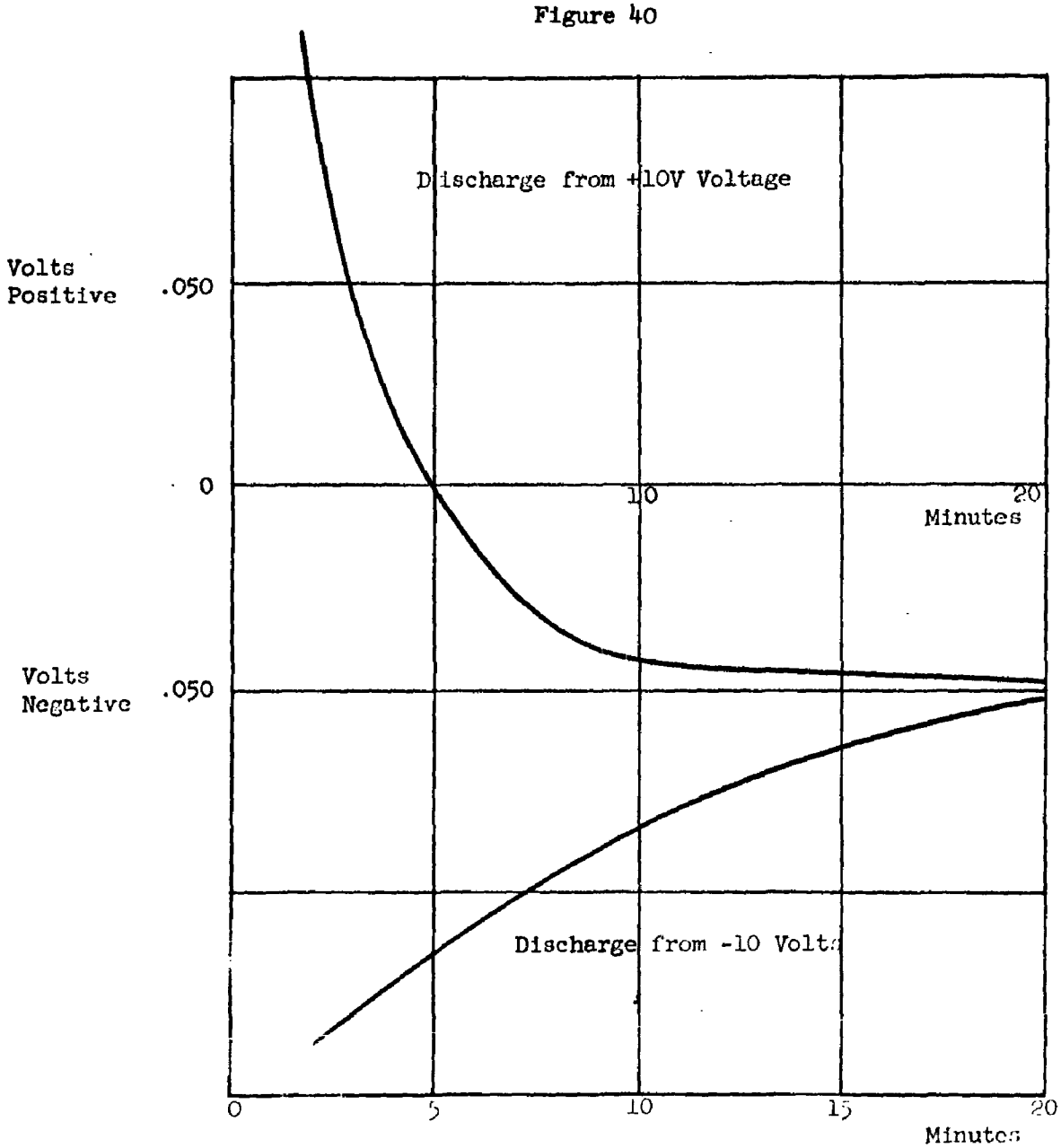

is the final discharge state. Further testing indicated this value could be reversed by polarizing the unit in the opposite direction for a period of time at a voltage level equivalent to the original polarizing voltage.

A number of tests were made to measure the temperature dependence reversibility. The results are shown in Figure 41. From this curve it is apparent that ceramic body OW-116 with chrome iron electrodes does not exhibit the same degree of voltage output as the titanium electroded materials OW 102, OW-126 and OW-125 (OW-102 with 1% Ta_2O_5).

Polarization

Each of the ceramic bodies used in this program has exhibited a polarization phenomenon. The application of a voltage for a short time period results in the reflection of this voltage from the device after the applied potential has been removed. In addition, reapplying the voltage with the polarity reversed is usually sufficient to reverse the direction of the polarization. This polarization is not apparent below 300 C. Several of the materials have been found to spontaneously polarize from an untested, unpolarized state to a low field state by raising the temperature of the sample above 400 C.

Attempts have been made to obtain visual indications of an open hysteresis loop using oscillographic methods. So far the methods have not been too reliable. Open loops have been obtained but a saturation effect was not observed. This was possible due to inadequate output power from the signal source.

Point by point representation of data taken over longer time periods provided the curves represented in Figure 42. The technique used was that of reading an output current from the device one minute after the charging

POTENTIAL DEVELOPED AT TEMPERATURE
FOR DIFFERENT POLARIZATION LEVELS

Figure 41

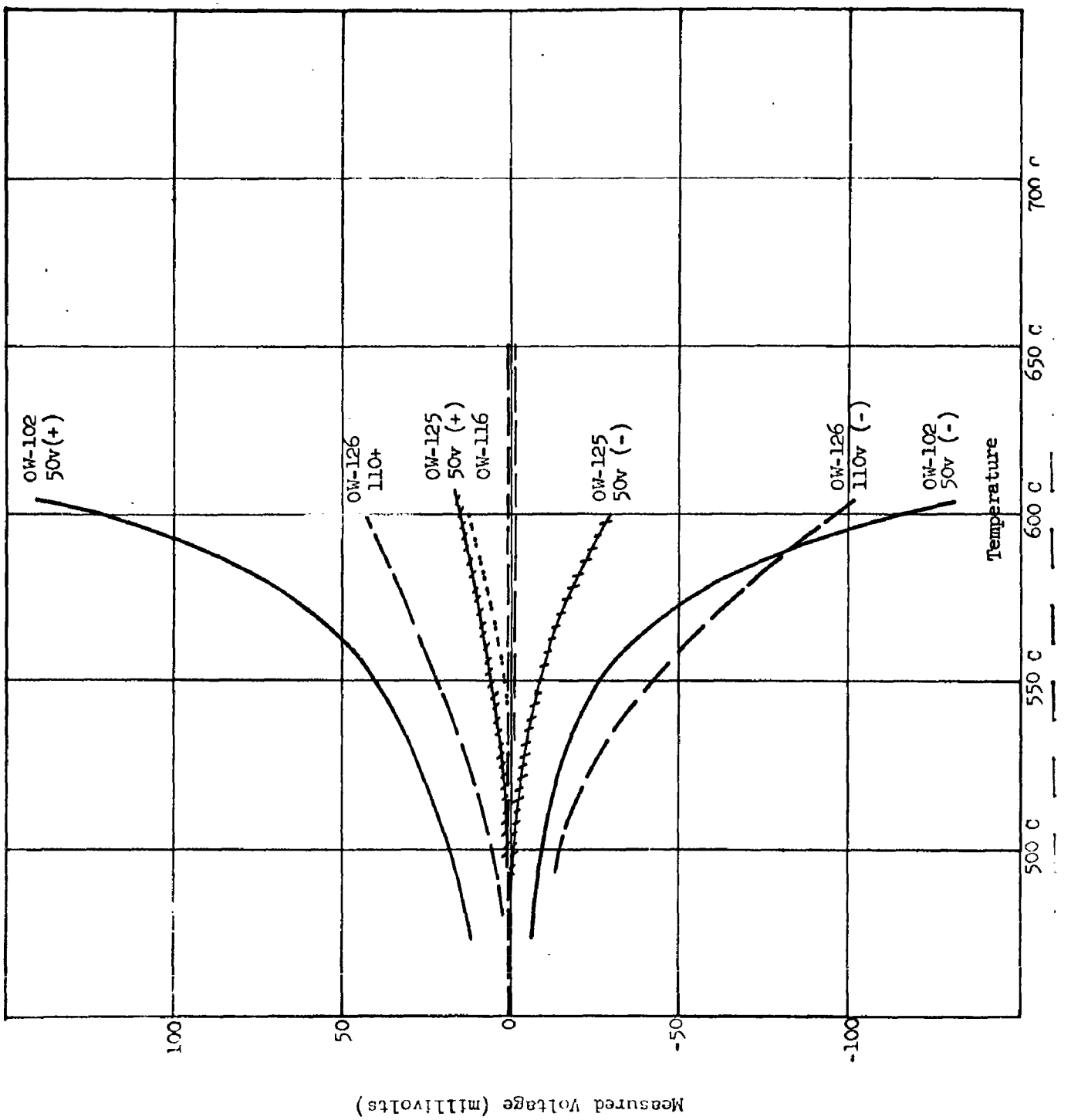

- RESIDUAL CURRENT VS. APPLIED VOLTAGE -

AN EFFECTIVE POLARIZATION HYSTERESIS LOOP
OF LONG-TIME MEASUREMENTS

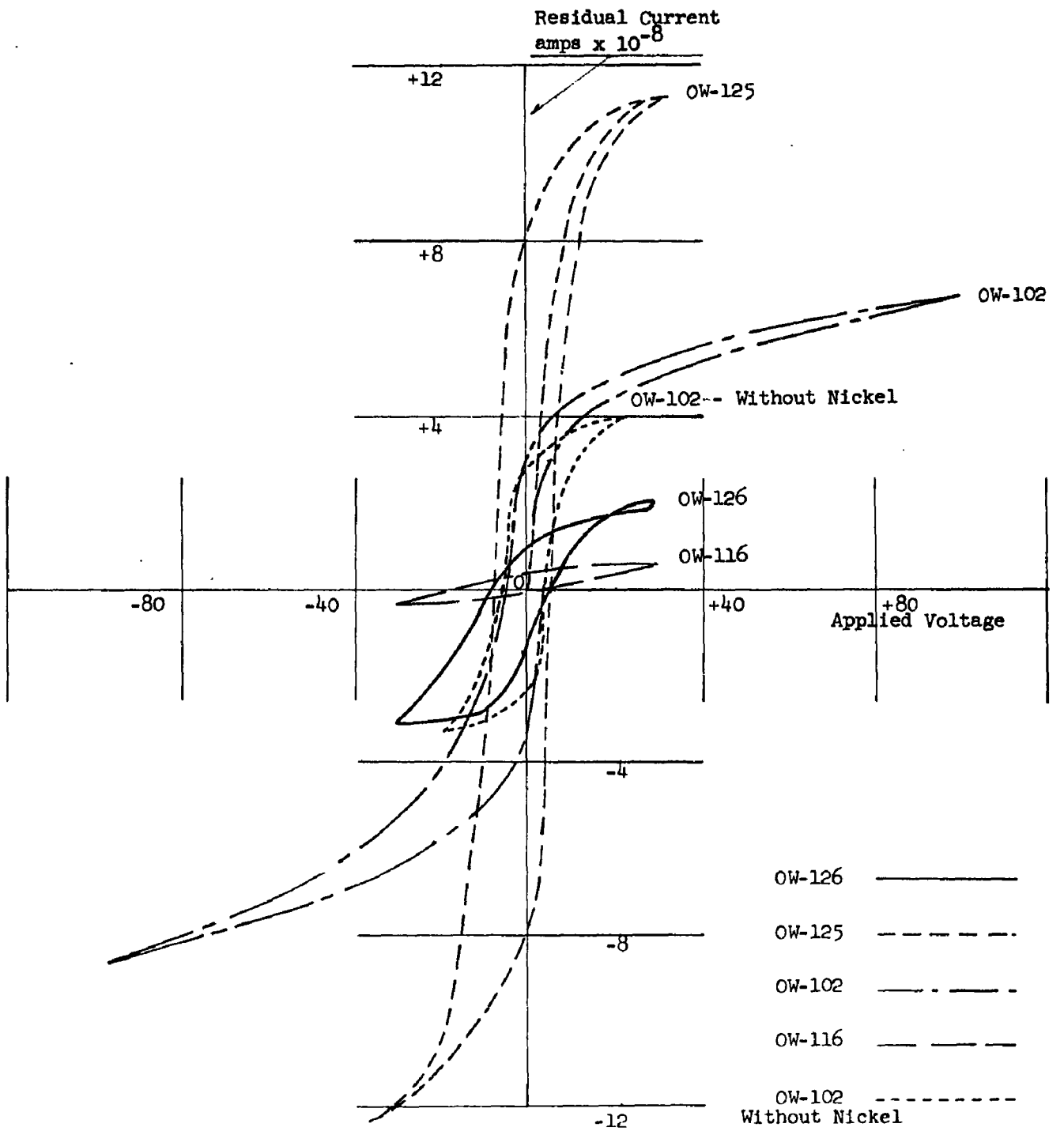

Figure 42

voltage had been removed. The circuit was essentially as represented below:

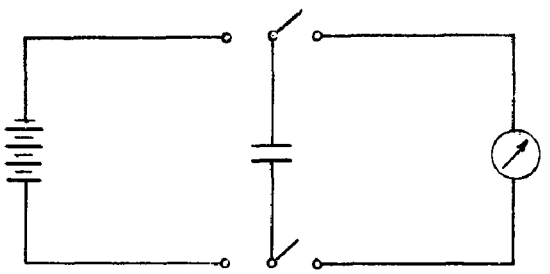

The test capacitor was charged for one minute, then removed from the voltage source and connected to the Keithley Model 410 micromicroammeter where the current was read after one minute of discharge. A value of residual voltage can be calculated from this using the value of the input impedance of the test instrument. Since changing the ranges also changes the value of the input impedance, this method also introduces some slight error. This test is to be continued using a high impedance voltmeter.

Table 11 below lists the test units which were made during this period for study of insulation properties.

Ceramic Body	Thickness	Number Sections	Type of Seal	Type of Electrodes	Amount Made	Amount Tested
OW-102	.005"	1	Nickle	Ti	10	2
	.005"	1	Heat & Pressure	Ti	13	5
	.005"	1	Cu-Ti	Ni	4	4
	.005"	1	Ti	Ni	4	4
	.010"	1	Ni	Ti	1	1
	.010"	1	Mo-Cu	Ti	6	6
OW-116	.005"	1	Ni-Ti	430 Stainless	9	3
	.005"	1	Cu-Ti	"	9	1
OW-125	.010"	1	Ni	Ti	9	4
(1% Ta_2O_5)	.010"	1	Ni+Cu	Ti	2	2
OW-102	.005	5	Ni	Ti	0	2 (from stock)
OW-126	.005	1	Ni	Ti	5	3
(1% TiO_2)	.010"	1	Ni	Ti	6	4
	.010"	1	Ni+Cu	Ti	1	1

TABLE 11

Description of Amount and Types of Capacitor Samples Made and Tested for Study of Insulation Properties

Dielectric Constant

As previously reported, there is a rapid change in measured capacity as the test frequency is reduced below 20 kc. The readings vary only slightly (3-5%) between 1 mc and 20 kc. The readings taken on five units currently on life test revealed the following changes when tested at 1.0 kc:

Dielectric Material	Capacity in pf at 1 Mc	Capacity in pf at 1 Kc
OW-116	64	104
OW-120	151	246
OW-125	151	277
OW-126	25	80
Mica	825	1100

The wide variation of capacity for OW-126 was not unexpected. This ceramic body has been doped with 1% titania (TiO_2). The increase noted for the other ceramic bodies is also explainable, but the increase in capacitance of the mica insulated sample was an unexpected result. Effort is being directed toward discovering an explanation for this phenomenon.

New Variable Capacitor Design

Another variable capacitor design has been completed and units have been made and tested. Figure 43A shows the construction details. Four of these units have been constructed to date. The two initial samples were not completely successful due to the fluidity of the active seal materials which produced larger effective electrode areas and a resulting reduction in capacitance variability. The last two were constructed with more care and with slightly lower sealing temperatures. These exhibited a capacitance range of from 3.6 pf to 17 pf. This can be extended by including additional sections. Effort is now being directed toward a clamping device which will render the stack immovable at a desired setting, yet which can be readily released for necessary adjustments. Two designs have been proposed but have not been tested.

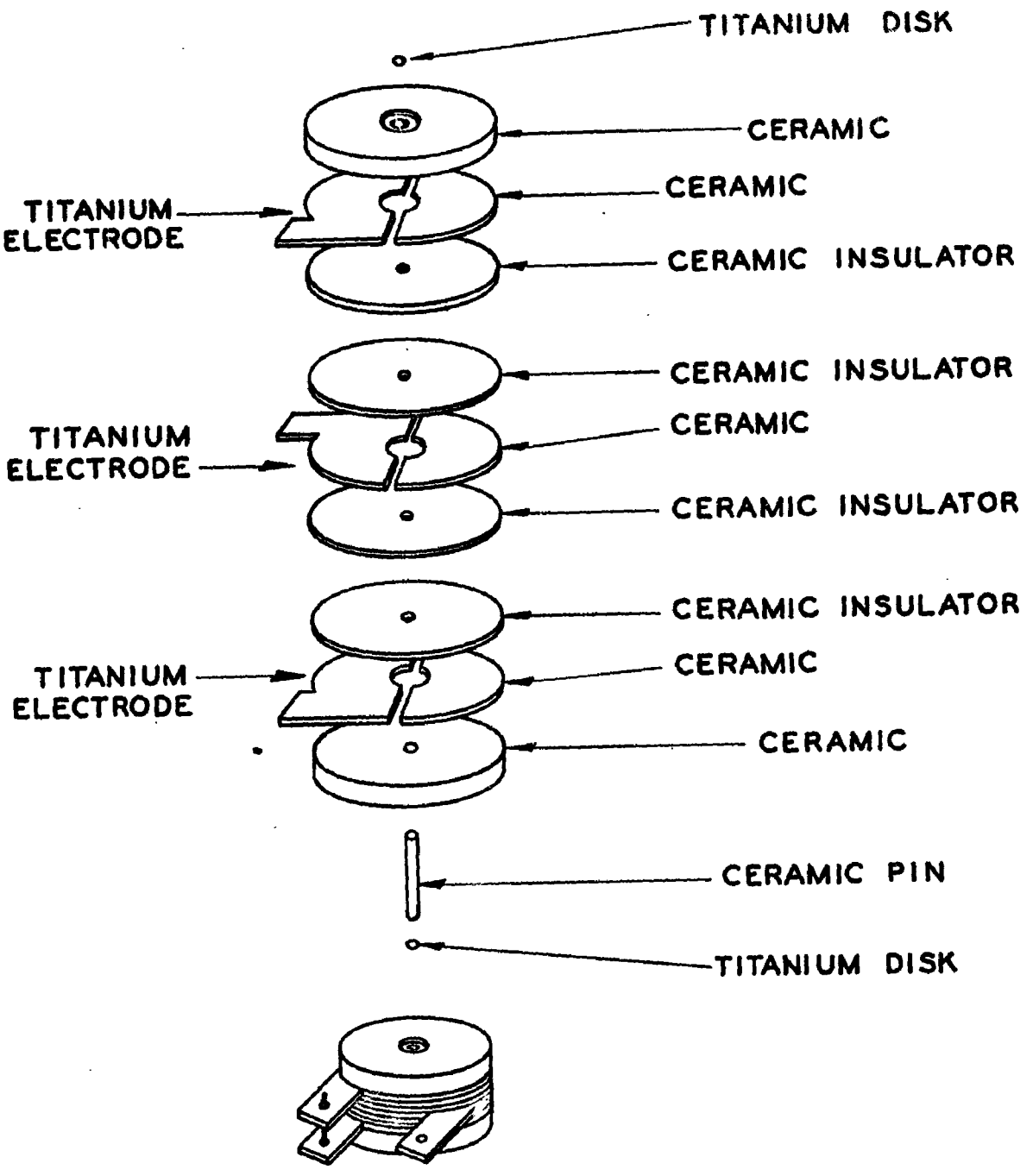

Figure 43

TIMM VARIABLE CAPACITOR

New Stacked Capacitor Design

During materials investigations, the number of electrode materials which could be evaluated was limited by the necessity of a matching coefficient of thermal expansion of metal and dielectric. A new design was proposed and four samples were made. This design is represented in Figure 43B. Two of these units shorted during sealing due to fluidity of seal materials, and one cracked open due to a sealing temperature which was too low. Greater care is required to construct and handle this model since the physical strength of a large stack is less than the original design. The reduction in metallic cross-section may prove to be an advantage at a later date. Fabrication of this type unit will continue only for evaluation of materials.

Conclusions

1. TiO_2 may prove to be the cause of changes in capacitor characteristics and the source of emf in stacked capacitors at 580 C. The use of the new capacitor design to eliminate titanium in all forms is one approach, neutralization of the concentration cell is another.

2. Conductivity data has provided strong support for the OW-116 ceramic body as being comparable to OW-102 in insulation resistance and conductivity. It has a further advantage in improved dissipation factor. The dielectric constant however is lower than OW-102.

3. The new variable capacitor design is more easily constructed and may show advantages in dielectric strength and versatility.

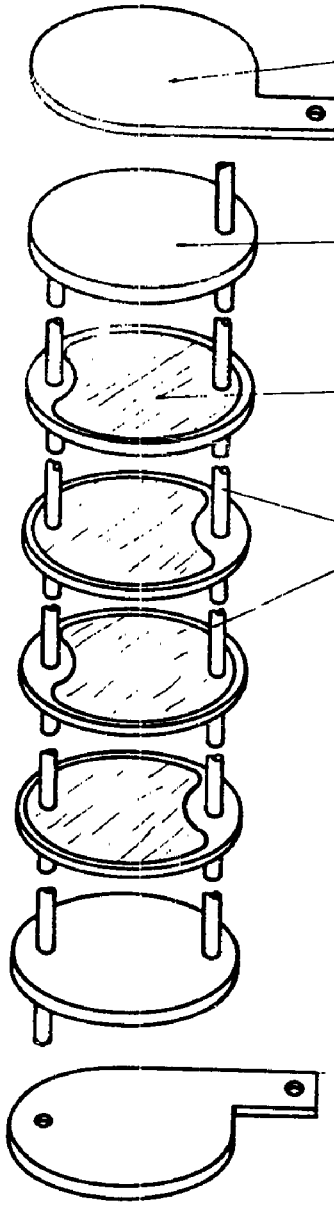

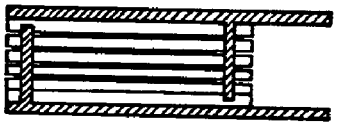

Stack Cross Section

TIMM Stack Capacitor

Proposed design incorporating thin cross section electrodes

Figure 43B

INDUCTOR DEVELOPMENT

A test unit has been designed for investigating various types of conductor winding wire and winding wire insulation. The unit consists of a ceramic spool around which a simple solenoid inductor may be wound. Preliminary units were fabricated using available dies to form the ceramic spool; and, since elaborate wire winding equipment was not available, the solenoids were wound by hand. The spool configuration is shown in Figure 44.

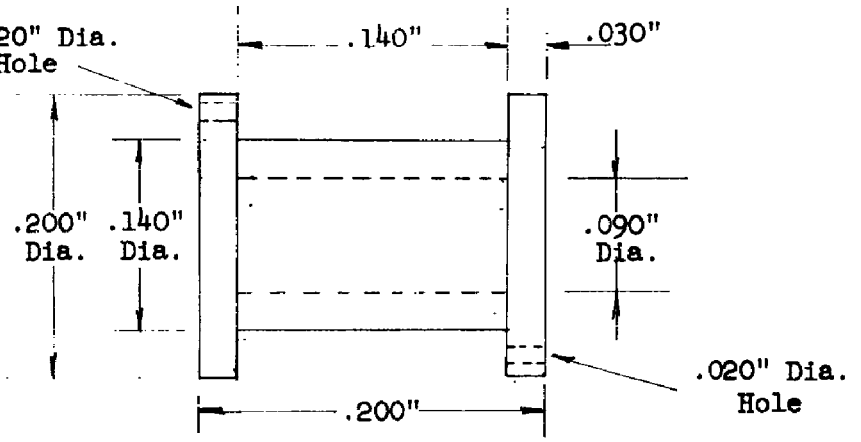

Inductor - Ceramic Spool Coil Form

Figure 44

Copper wire, 0.010" and 0.013" diameter, insulated with varnish insulation (Formex) was used as conductor wire material to aid in determining optimum dimensions for the spool. Room temperature test data, shown in Figure 45, was taken on these preliminary units at a frequency of 30 megacycles.

Spool and Coil Assembly

Materials used for fabricating units for the TIMM environment were OW-6 ceramic composition for the spool configuration and commercial copper magnet wire, having an unfired ceramic, resin-bonded insulation (Secon wire-Secon D) for the conductor winding wire. The process of fabricating test units was as follows:

1. Fire ceramic spool at 1100 C for approximately 10 minutes to burn off organic materials.

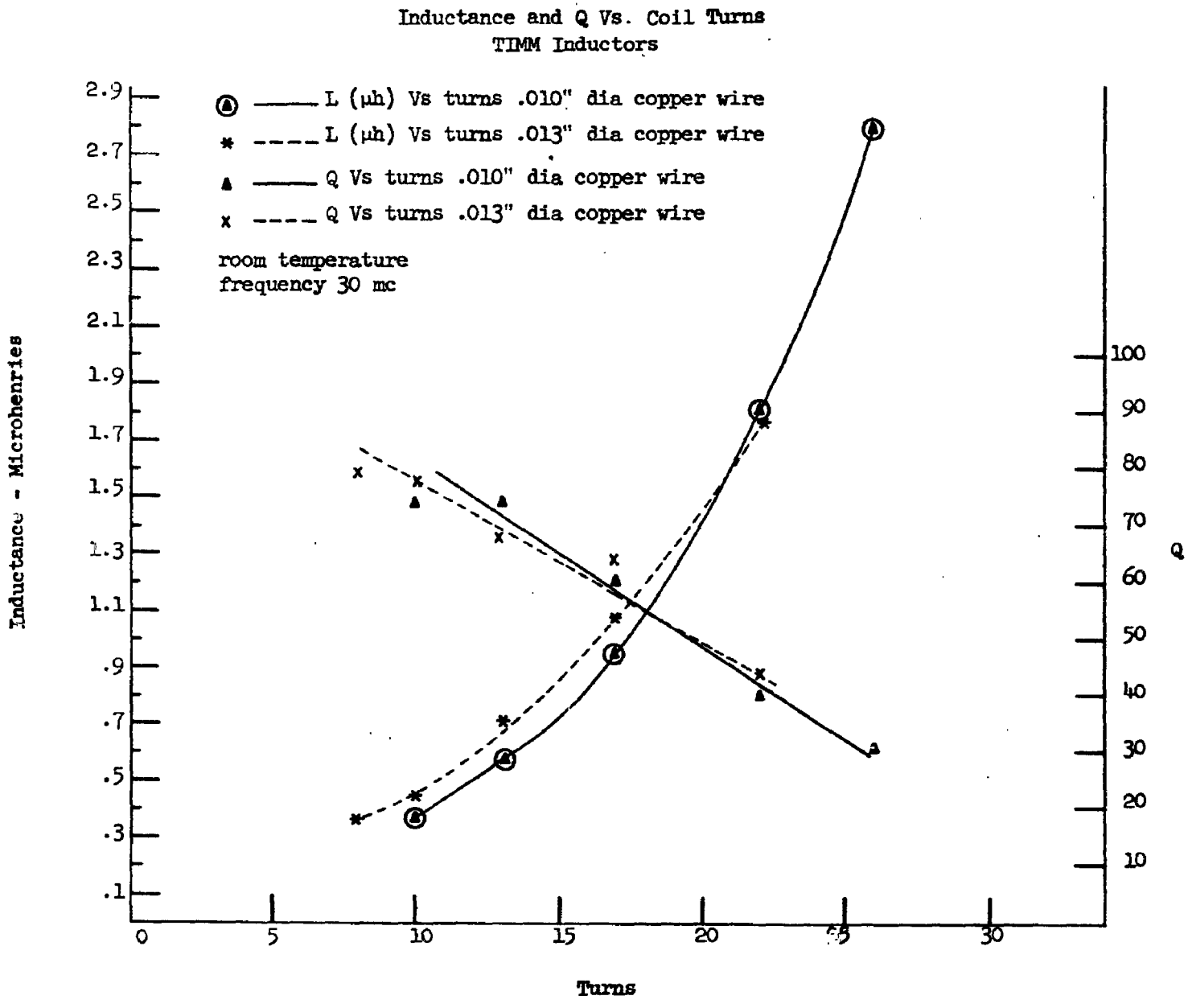
Inductance and Q Vs. Coil Turns
TIMM Inductors
L (μh) Vs turns .010" dia copper wire
L (μh) Vs turns .013" dia copper wire
Q Vs turns .010" dia copper wire
Q Vs turns .013" dia copper wire
room temperature
frequency 30 mc
Inductance - Microhenries
2.9
2.7
2.5
2.3
2.1
1.9
1.7
1.5
1.3
1.1
.9
.7
.5
.3
.1
100
90
80
70
60
50
40
30
20
10
Q
0
5
10
15
20
25
30
Turns

Figure 45

2. Wind copper magnet wire, with Secon D insulation, to the desired number of turns by hand.

3. Mature Secon D insulation at approximately 800 C, in air, for 10 minutes. This sets the insulation and burns away the Teflon overlay.

A number of units were fabricated according to the above procedure and tested for inductance and Q over a temperature range from room temperature to 580 C, and a frequency of 30.0 megacycles. Data shown in Figure 46 is for 0.010" diameter wire wound to 10, 14 and 20 turns.

Encapsulation

First attempts to enclose the ceramic spool and conductor wire assembly utilized an OW-6 ceramic cylinder into which the assembly would be placed and subsequently sealed with a titanium electrode and nickel-eutectic seal. Due to the lower eutectic temperature of the copper-titanium, the ends of the conductor wire, where connection is made to the titanium electrode, melted away during the higher temperatures involved with effecting the nickel-titanium seal.

To eliminate this problem, a ceramic composition OW-116 cylinder was used having ends metallized by a molybdate metallizing process. Telemet material, 0.020" thick with a 0.0025" copper cladding on each side, was used for the end electrodes. The thermal expansion of copper-clad telemet matches the thermal expansion of OW-116 ceramic. Sealing of the unit was achieved by using a nickel-copper-gold (Nicoro #80) brazing alloy having a liquidus temperature at 925 C. The seal is vacuum tight but appears to be weaker than the nickel-titanium seal.

The processing schedule for metallizing and sealing was as follows:

1. Fire ceramic at 1100 C for 10 minutes to burn off organic materials.

2. Dip ceramic cylinder (ends only) into the metallizing material, allow to dry under heat lamp.

Inductance & Q Vs Temperature for Different No. Turns
TIMMS Inductors

● — Q Vs temperature - 10 turns
◉ — Q Vs temperature - 14 turns
* — Q Vs temperature - 20 turns
▲ — L (μh) Vs temperature - 10 turns
◮ — L (μh) Vs temperature - 14 turns
▫ — L (μh) Vs temperature - 20 turns

Copper wire .010" dia with Secon "D" insulation

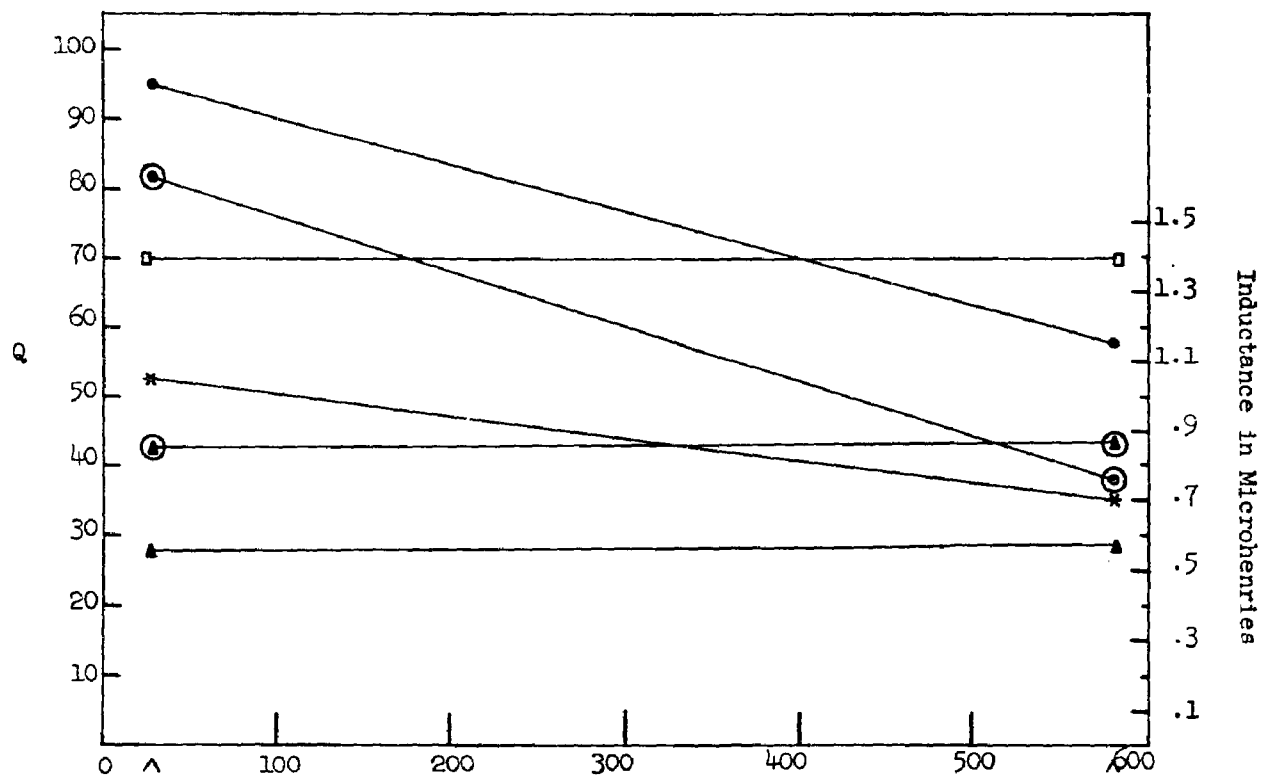

Figure 46

3. Place ceramic cylinder into moly boat and fire in hydrogen furnace at elevated temperature for 10 minutes.

4. Copper plate moly-coated cylinder ends for 5 minutes at 2.0 amps.

5. Hydrogen fire again at elevated temperature.

Electrode & Shim Material

1. Degrease in trichloroethylene - dry.

2. Degrease in methanol - dry.

3. Fire electrodes in vacuum - 5 minutes.

4. Fire shims in hydrogen - 600 C for 5 minutes.

5. Weld shims to electrodes using moly.

Alignment & Sealing

The alignment and sealing fixtures used for resistors, described in Interim Engineering Report #1 and shown in Figure 34 of that report, are also used for stacking and aligning inductor units. Sequential steps are as follows:

1. Stack component parts into sealing jig using ceramic spacers between complete units.

2. Place loaded jig into oven in vacuum system and pump to $< 1 \times 10^{-4}$ torr.

3. Seal at 925 C for 2.0 minutes.

Testing

The testing of encapsulated coils presents the problem of affixing test leads to extend into the furnace. In preparing coils for test, the following procedures were used:

1. Copper test leads (4 3/8" long) were brazed to each electrode. Leads were brazed rather than welded to prevent any high resistance at 30 megacycles.

2. The test leads were threaded through a piece of two-hole ceramic tubing for separation and to keep characteristics of leads the same from test coil to test coil.

The equipment used for evaluating the coils was a Boonton Radio Corporation meter and a small helical wound furnace that can be placed over the coil to be checked.

Data showing characteristics of the coils before and after encapsulation are included in Figure 47. It is difficult at this time, using the test procedure described above, to determine accuracy and validity of the data taken on the coils. A study is currently being made to determine optimum test and measuring conditions for evaluating inductance and Q of these units.

Ceramic Circuit Board Fabrication

A die has been designed to fabricate ceramic circuit boards for the 10-bit shift register circuitry. At the present time the boards have a finished-fired dimension of 3.145" x 3.145" x 0.060" thick. The ceramic composition, OW-102, is pressed at maximum pressure using the 15-ton Denison press. The board size shown above is the maximum recommended at this time, using available equipment, since shrinkage on the fired part is running 22.5 per cent. If a larger die were used, shrinkage would increase, making dimensions on the finished fired board difficult to hold within reasonable tolerances.

To provide versatility for circuit design work, the board is pressed, partially fired, and then geometrically disciplined holes are drilled to accommodate the desired components. This board configuration is shown in Figure 48.

Inductance & Q Vs Temperature
TRW Inductors Before and After Encapsulation

.010" Dia Copper Wire 14 Turns

o — Q Vs temp before encapsulation □ — After encapsulation

◎ — L (μh) before encapsulation ⊡ — After encapsulation

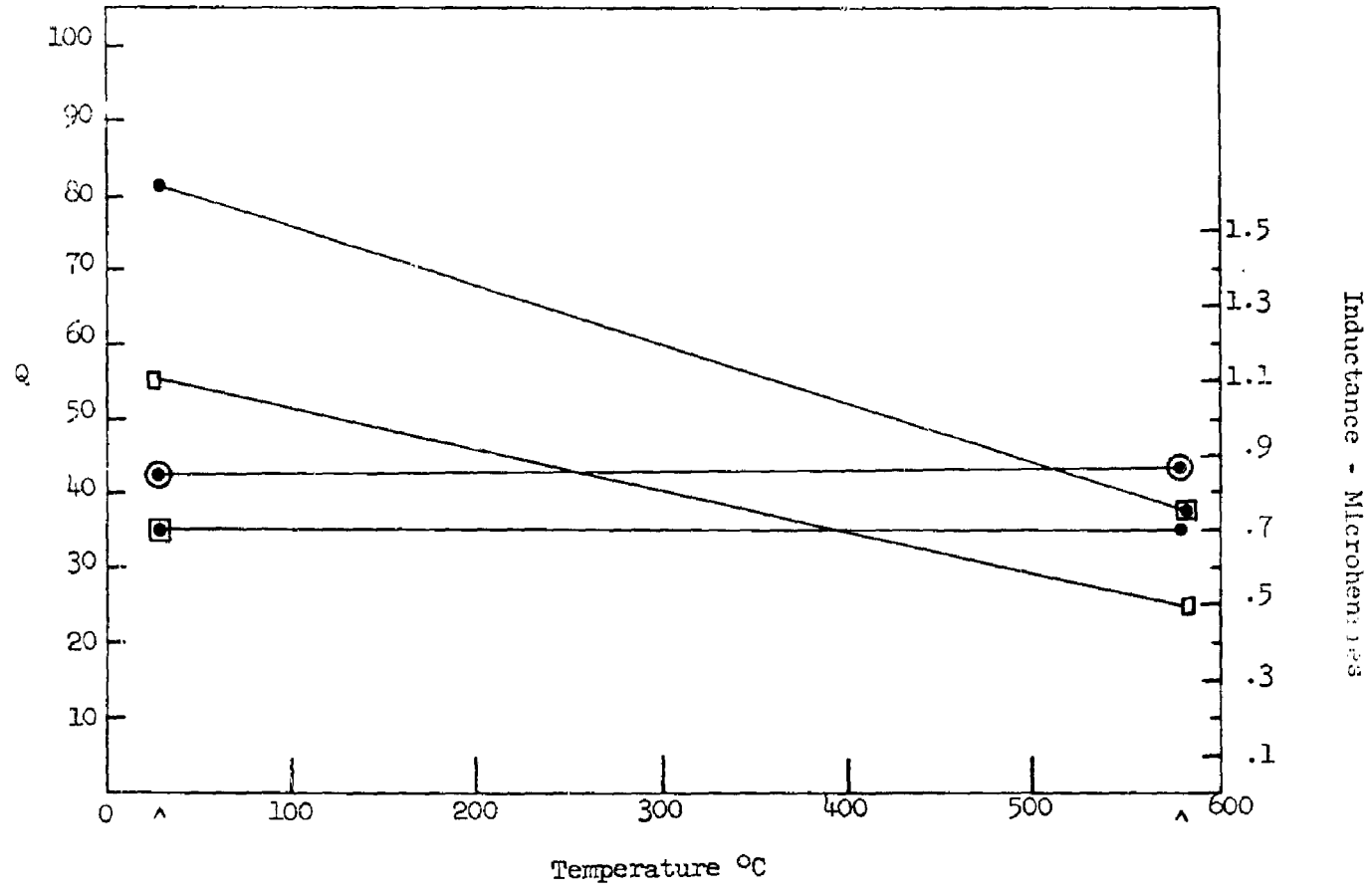

Figure 47

Ceramic Circuit Board

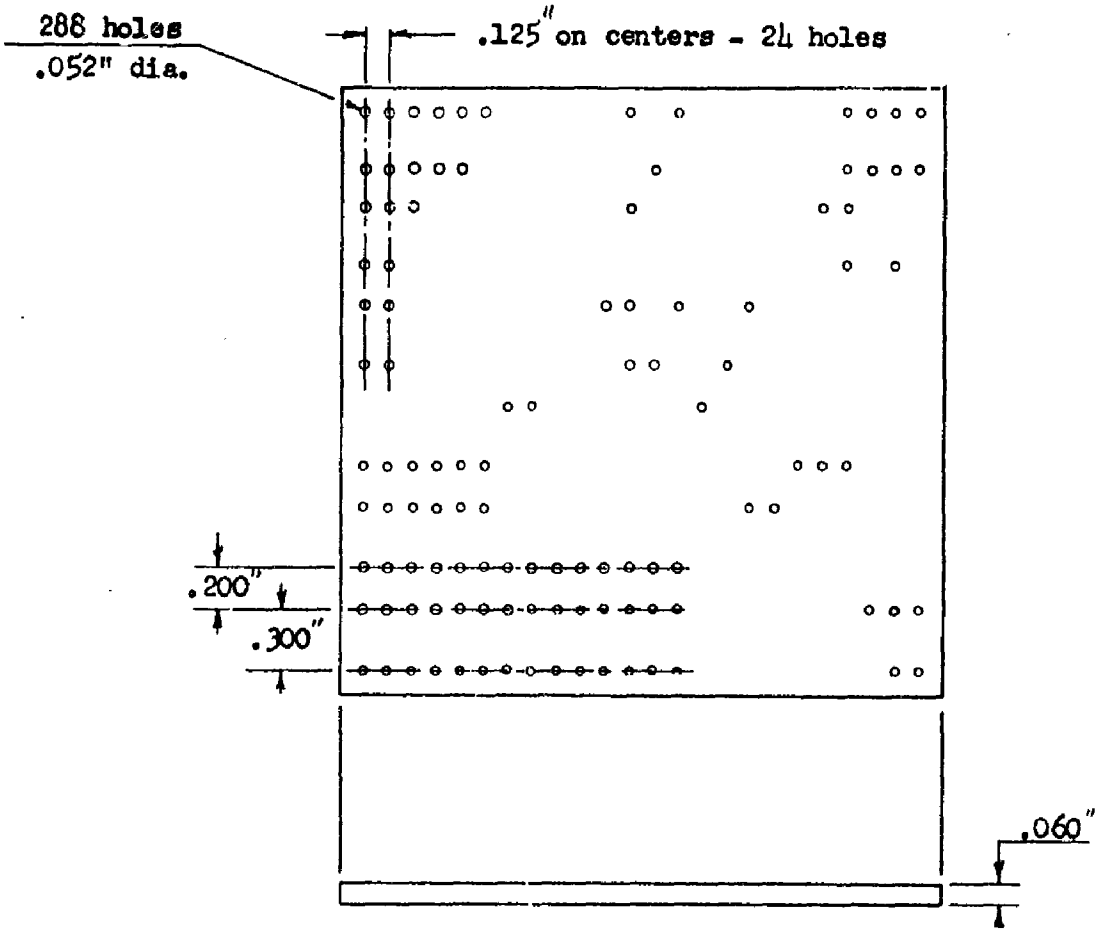

Figure 48

Half Adder

During the final design stage of the initially selected half adder circuitry, a simplified logic diagram, utilizing fewer components and circuits, was evaluated and found to perform satisfactorily. This resulted in a decrease in physical module size and an increase in circuit performange. The new logic is shown below in Figure 49.

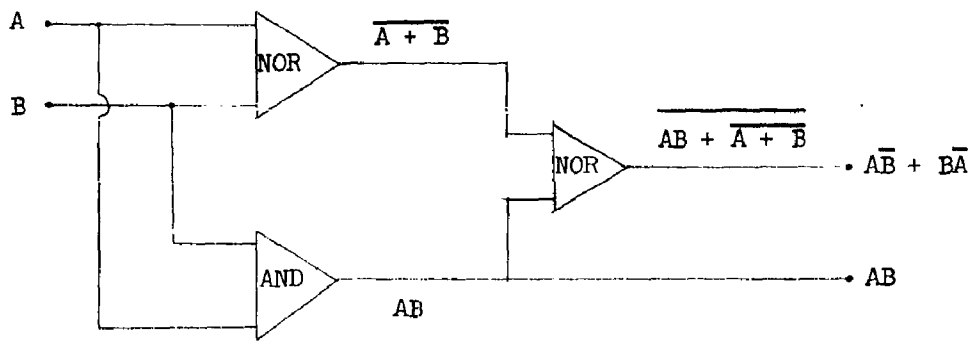

Logic

A	B	AB	$A\bar{B} + B\bar{A}$
1	0	0	1
0	1	0	1
1	1	1	0
0	0	0	0

Half Adder Circuit Logic Diagram

Figure 49

Since this logic diagram employs essentially the same type circuits used previously, the same design procedures apply. The two Nor circuits will be those designed previously; the And circuit resistors will have to be altered slightly as the circuit now operates into a slightly different load. The entire circuit was designed, breadboarded, and optimized. During the process, it was found that by making the grid resistors of the two Nor circuits 10K ohms, the rise times of the output pulses improved; also by adding a speedup capacitor across the output diodes of the driving Nor circuit, the rise times again improved. To make the two output circuits compatible, both the output Nor and And circuits were designed to work into a 5K ohm load. The circuit is shown below in Figure 50.

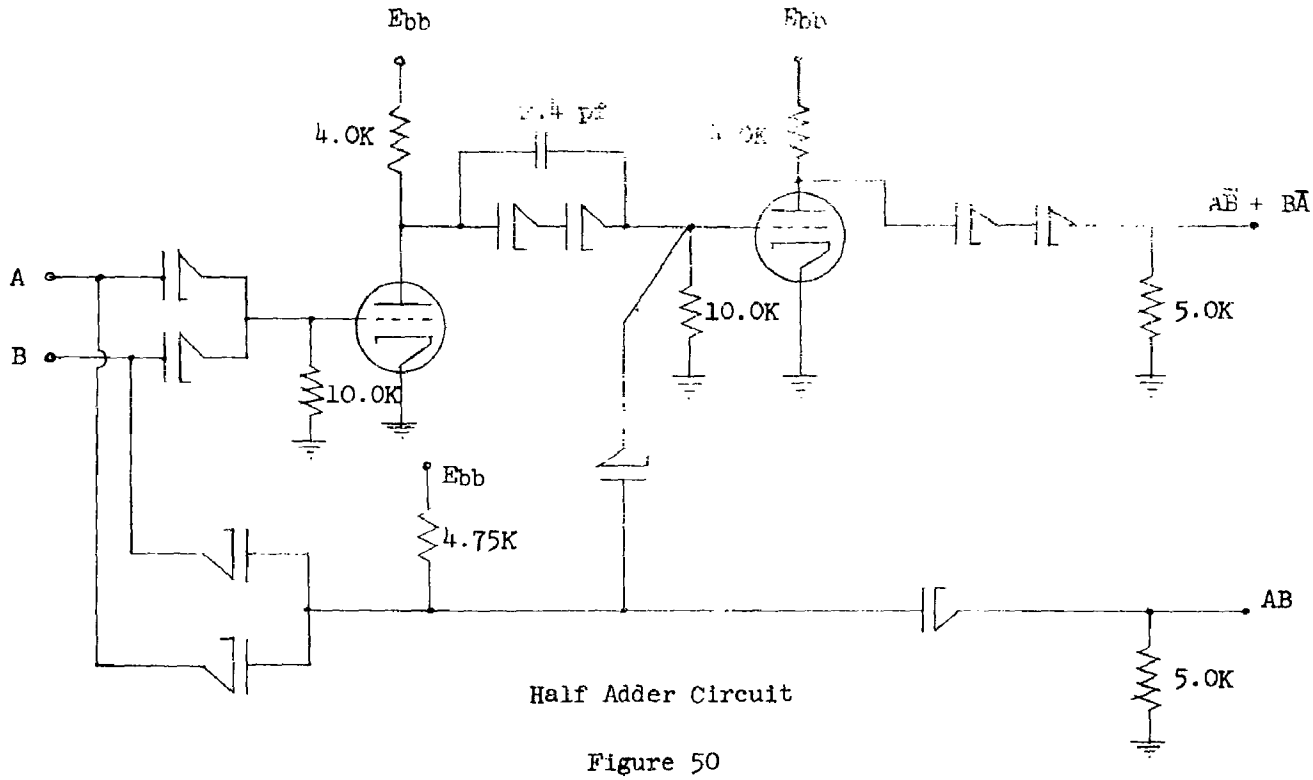

Half Adder Circuit

Figure 50

Rise times of the pulses out of the Sum portion of the circuit were between 0.2 and 0.3 microseconds while the rise times of the pulses out of the Carry portion approached 0.025 microseconds. Maximum pulse amplitudes occurred when the plate voltage was 11.4 volts; the total circuit current at this time was 4.4 milliamps. The results are shown in the photographs of Figure 51.

The design work for positioning components and properly placing component lugs for interconnecting the entire half adder circuit was completed during the period. Initially components having all tangential lugs were planned. Further studies, conducted toward the end of the report period, [illegible] tangential plus radial lug configurations to be more advantageous [illegible] point of integrating the circuit with a ceramic board. The layout for component placement and lug positioning will be reworked in the [illegible] to incorporate both type lug configurations.

portion of a sine wave was utilized; since it was assumed that the pulse was already amplified, a pulse of sufficient amplitude was chosen.

A minimum amount of circuitry being desirable, a Schmitt Trigger, shown below in Figure 52, was chosen to perform this reshaping operation.

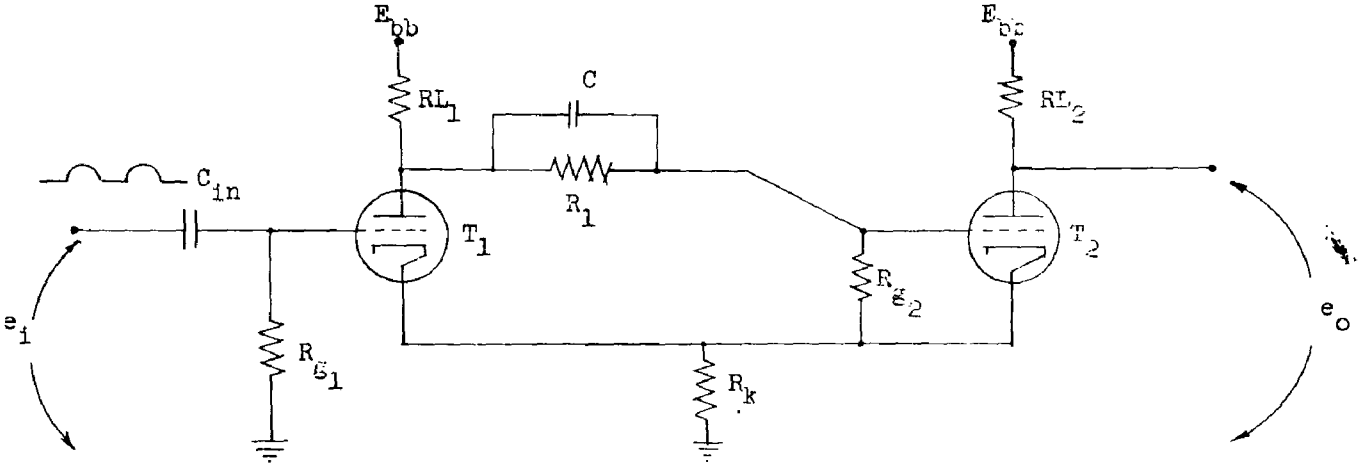

Schmitt Trigger Circuit

Figure 52

This circuit functions in the following manner. Assume that T2 is conducting and a bias voltage has been developed across Rk of sufficient magnitude that T1 is cut off. As a result, e_o is at a minimum. Now suppose the distorted pulse enters the grid of T1. As the pulse rises, a point will be reached where the bias on T1 is overcome and T1 will begin to conduct. When this happens, the grid of T2 will become less positive and T2 will draw less plate current; immediately the bias across the common cathode resistor Rk will decrease causing T1 to conduct more vigorously and the whole process to continue until T2 is cut off. As the pulse begins to decrease in amplitude, another point will be reached where the pulse will cut off T1 and cause T2 to conduct. If the output (e_o) of T2 is noted, it can be seen that e_o will rise sharply to some level, while T2 is initially cut off and remain at this level until T1 is cut off. At this time, e_o will decrease sharply to the original level. As a result, a square pulse is obtained at the plate of T2 as e_o. The duration of this pulse will be very

close to the duration between the two points on the distorted pulse that caused T1 to conduct and then cut off.

In order to obtain good rise and fall times on the output pulse (e_o), tubes having large current changes for small changes in bias voltage must be utilized. As a result, most of the Schmitt Trigger circuits using tubes will use pentodes.

The Schmitt Trigger circuit was attempted using low voltage triodes in order to conform to the low plate supply voltage required for other TIMM computer circuitry. Square output pulses were obtained; however, the rise and fall times could not be classified as good. The pulses could be improved with additional circuitry. The possibility of utilizing this approach is being considered.

R.F. Amplifier

Preliminary circuit work at 30 megacycles was initiated on the r-f amplifier circuit. At this frequency, circuit components, such as conductors and capacitors, can have fairly small values. Since this frequency was selected, an amplifier circuit of the grounded grid variety was chosen to eliminate the need of neutralization. The circuit is shown in Figure 53.

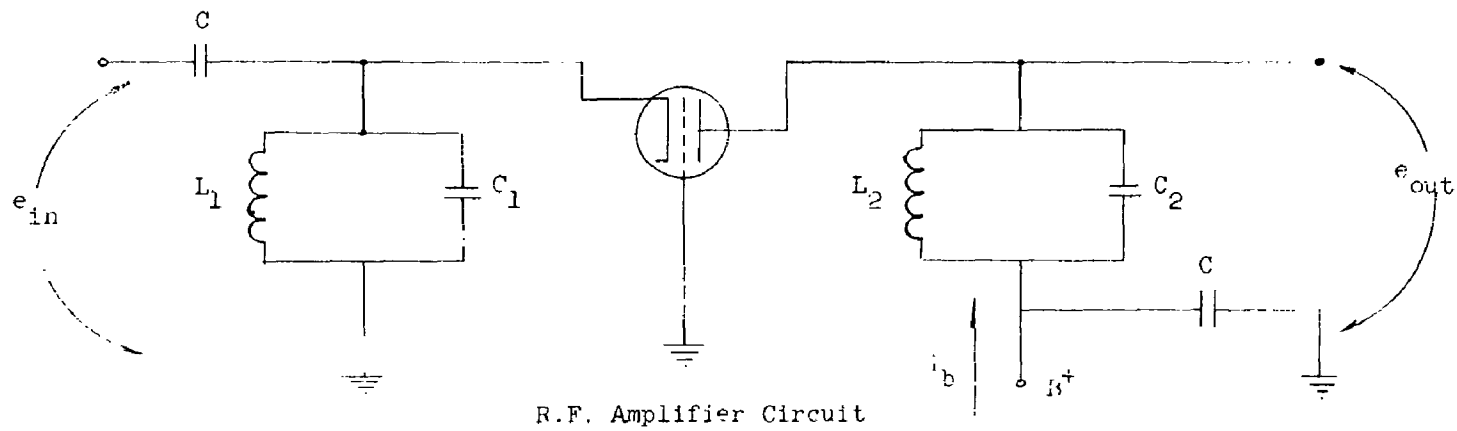

R.F. Amplifier Circuit

Figure 53

In order to determine the values of inductors and capacitors needed in the input and output resonant tank circuits, the interelectrode capacitances

of TIMM triodes must be known since these capacitances are in parallel with the tank circuit capacities. Twelve TIMM triodes were obtained; six were of the type that utilized 0.003" and 0.050" grid mesh, the other six triodes employed 0.007" x 0.007" grid mesh. For each of the two groups of triodes, two low mu, two medium mu, and two high mu types were chosen. The inter-electrode capacitances of the triodes were measured using the Wayne Kerr Model 501 R.F. Bridge, the General Radio 1330A oscillator, and the Hewlett Packard Model 400 C voltmeter. The procedure used is described on page 76 of the First Quarterly Report under Capacitor Electrical Measurements; all measurements were made at one megacycle with the triodes at 580 C unless otherwise specified. Data from these measurements are shown in Table 12.

Group A - 0.007" x 0.007" Grid Mesh Triodes

Triode Number	Mu (μ)	gm (micromhos)		Capacitances (gk) grid to cathode	(gp) grid to plate	(pf) plate to cathode (pk)
4334	4.0	1030		6.2	4.6	0.40
4202	5.4	1250		5.3	5.2	-
4256	7.0	1460		5.5	5.3	-
4269	7.7	1620		5.1	4.7	-
			25°C	4.5	4.1	-
4393	9.0	1390		5.2	4.9	-
4246	10.0	1810		4.7	4.4	-

Group B - 0.003" x 0.050" Grid Mesh Triodes

5079	20	2440	6.3	5.3	-
5080	24	2500	7.3	6.5	0.31
5054	27	3000	6.3	5.9	-
4818	28	3600	5.8	5.7	-
4887	36	3960	7.0	5.8	-
4819	43	3050	6.0	5.7	-

TABLE 12

From the preceding data, it can be seen that only one measurement of plate to cathode capacitance was made in each group. This measurement is only an

approximate value due to limitations of the test equipment. To measure capacitance of such small magnitude, a more elaborate setup will have to be utilized; this will be done in the near future.

Inductors are required for each of the tank circuits in the amplifier. Since these inductors will be utilized at 580 C, it is reasonable to assume that the unloaded Q's of the conductors will be lower at this elevated temperature than at 25 C. The resistance of a good conductive wire will increase as temperature increases and Q will vary inversely as the resistance of the wire. Anticipating TIMM inductors to have unloaded Q's of approximately 50, copper inductors were wound simulating these values. These units will be used external to the TIMM environment for preliminary circuit work.

On the schematic diagram of the grounded-grid amplifier, Figure 53, there are two capacitors labeled C. These capacitors need only be large enough to offer a small reactance to the operating frequency; one capacitor is the input, the other a by-pass capacitor. Triode (T1) is a higher voltage triode than used in all previous circuit work and can be utilized with plate voltages greater than 100 volts. The input signal (ei), approximately 30 megacycles, will have an RMS voltage of 1.4 volts. The following data were recorded for various inductance-capacitance combinations on the input and output tank circuits. All circuitry was external to the 580 C environment except the triode.

E_{bb} (v)	i_b (ma)	L1 (μh)	C1 (pf)	L2 (μh)	C2 (pf)	e_o (RMS volts)	Gain (db)
75.0	3.0	0.55	47	0.55	47	7.5	14.0
70.0	4.0	0.55	67	0.38	47	15.0	20.0
90.0	2.5	0.48	67	0.38	33	15.0	20.0

At 30 megacycles, the reactance of the above inductors is small. As a result, low impedances are presented to the triode. If larger impedances could be presented to the triode, the gain should increase since the gain of an

amplifier varies directly as the plate load impedance within reasonable limits. Slightly larger impedance value inductors are being obtained.

To increase knowledge of TIMM triode circuit performance, it was decided to conduct a frequency response test. A standard RC amplifier was built using TIMM triode #5009 in conjunction with standard components to function outside the TIMM environment. The circuit schematic diagram, triode characteristic and circuit data are shown below in Figure 54 and Table 13. A constant input voltage (ei) of 1.5 volts RMS was maintained over the recorded frequency range. With a plate voltage of 80.0 volts applied, the triode current was 1.5 milliamperes.

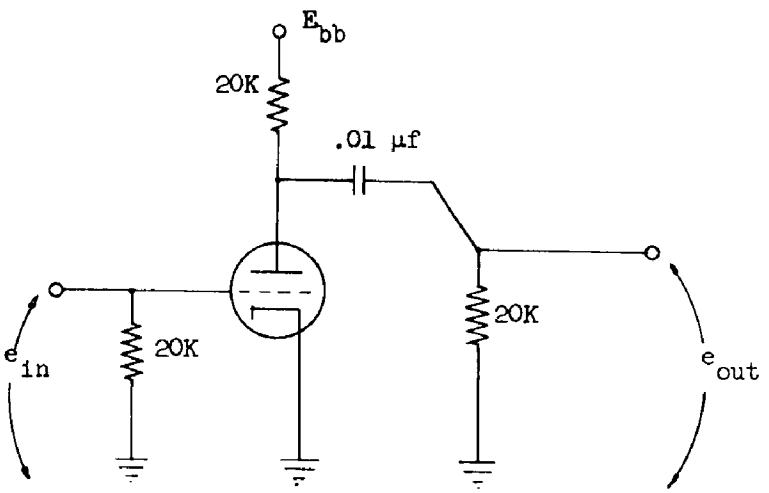

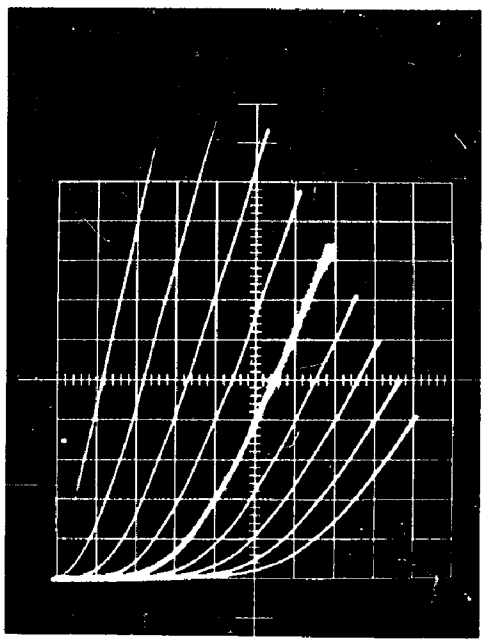

Figure 54
R.C. Amplifier Schematic
and Triode Plate Family

Frequency (cycles)	e_o (RMS Volts)	Gain (db)	
0.14 kc	4.1	8.7	
0.25 kc	6.3	12.5	
0.50 kc	9.1	15.7	
1.00 kc	11.0	17.4	
5.00 kc	11.0	17.4	
10.00 kc	11.0	17.4	R.C. Amplifier Circuit Data
50.00 kc	10.7	17.1	
0.10 Mc	10.6	17.0	
0.50 Mc	10.2	16.7	
1.0 Mc	10.1	16.5	
1.5 Mc	9.5	16.0	
2.0 Mc	8.9	15.5	
5.0 Mc	5.2	10.8	
10.0 Mc	2.9	5.7	

TABLE 13

A graph of the recorded data is shown in Figure 55.

Oscillator

As with the RF amplifier, a frequency of 30.0 megacycles was chosen for preliminary oscillator circuit work. A Colpitts oscillator circuit was chosen to eliminate tapping the circuit inductor. The schematic diagram for the Colpitts oscillator circuit is shown in Figure 56.

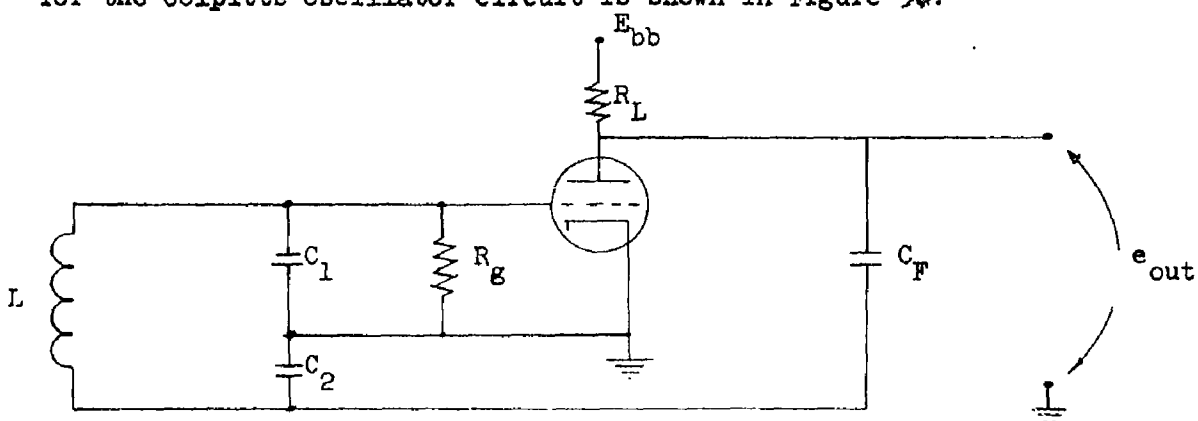

Colpitts Oscillator Circuit

Figure 56

As in other preliminary circuit work, the only TIMM component that will be utilized will be the triode; all other circuitry will be external to the TIMM environment. As in the case of the amplifier, the conductor (L) will be simulated to represent an approximate TIMM inductor. Capacitors C1 and

Frequency Response Curve

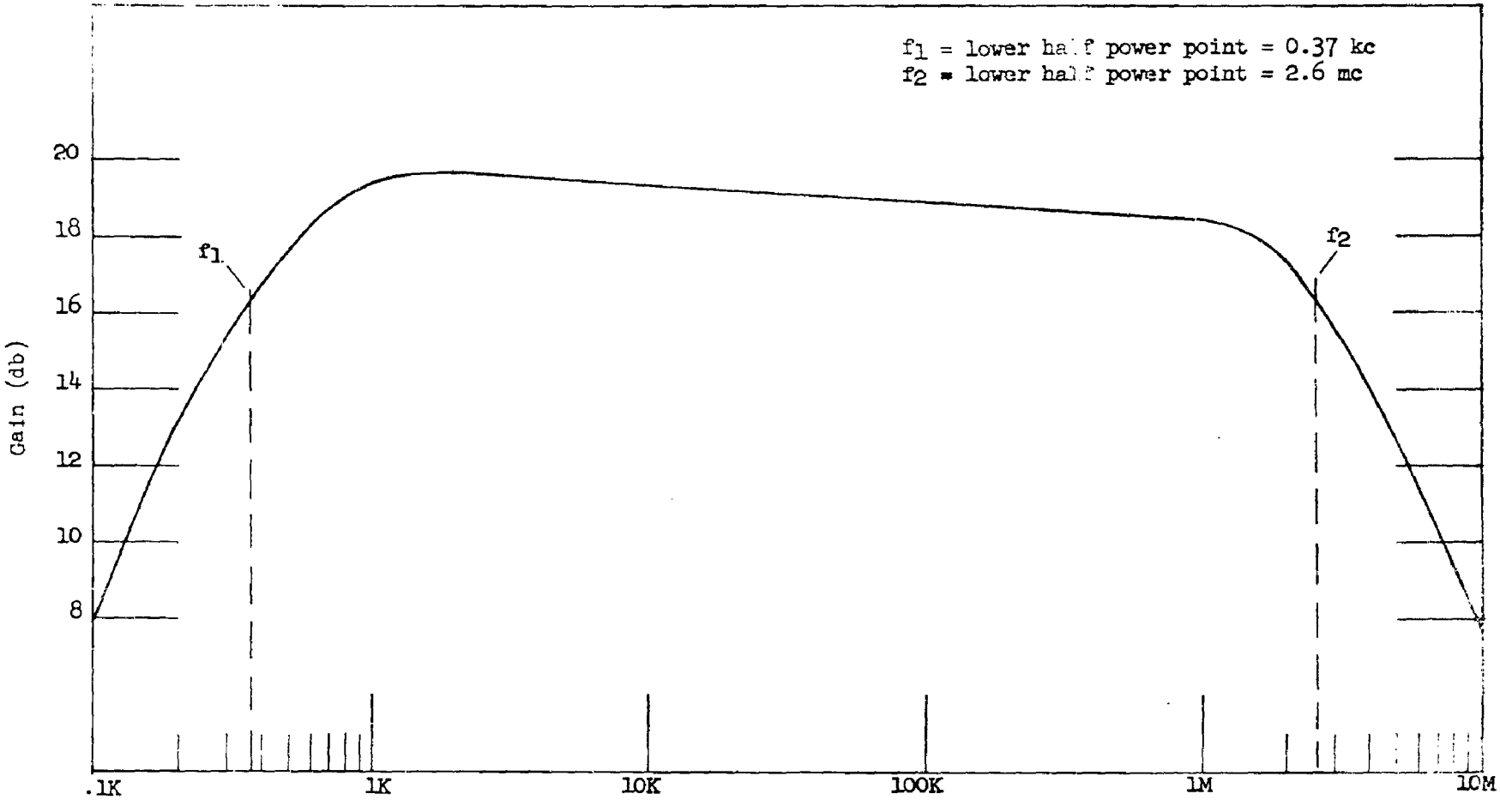

Figure 55

and C2 act as a voltage divider network. These capacitors, together with the input capacity of the triode and the inductor, will also determine the frequency of oscillations. Capacitor Cf is the feedback capacitor; the value being 100 pf. An RF choke should be utilized in place of resistor R_L, but inductors of this type have yet to be developed for the TIMM concept. Resistor Rg is simply the grid resistor whose value is near 20K ohms. The data shown in Table 13 was taken with an R_L = 15K ohms.

Case	E_{bb} Volts	ib ma	Triode No.	mu	gm μmhos	C_1 pf	C_2 pf	L μh	Q -	e_o (RMS volts)	Frequency Megacycles
1	100	2.0	5073	1100	25	20	10	1.0	60	6.0	30
2	100	2.0	5073	1100	25	56	20	0.6	80	4.2	41
3	100	2.0	5073	1100	25	160	33	6.0	65	28.0	18
4	150	3.8	5088	5000	42	56	20	1.0	60	15.0	30
5	100	3.3	5088	5000	42	60	10	1.5	84	16.0	30

TABLE 14

From the preceding data it can be seen that the output of the oscillator increases as the inductive to capacitive ratio increases. Since larger inductance values would increase the physical size of the TIMM inductor and since microminiaturization is a desirable feature of the TIMM concept, then the values of capacitance should be decreased. This in turn should increase the operating frequency of the oscillator. How much the values of C1 and C2 can be decreased has yet to be determined.

Shift Register

Improvements in the shift register performance have been realized by increasing the shift triggering sensitivity of the stages by a factor of at least three. Three circuit modifications (see Figure 57) were investigated. As noted in the last quarterly report, a portion of the shift trigger pulse was passed by the "closed" gating diode "D" to the "off" grid, counteracting to some extent the trigger pulse actually passed by the "open" gating diode "D." The undesired transmission of the trigger by the "closed" gating diode was [illegible] cathode to anode capacitance of the diode. Thus, it

SCHEMATIC OF
2-BIT SHIFT REGISTER MODULE

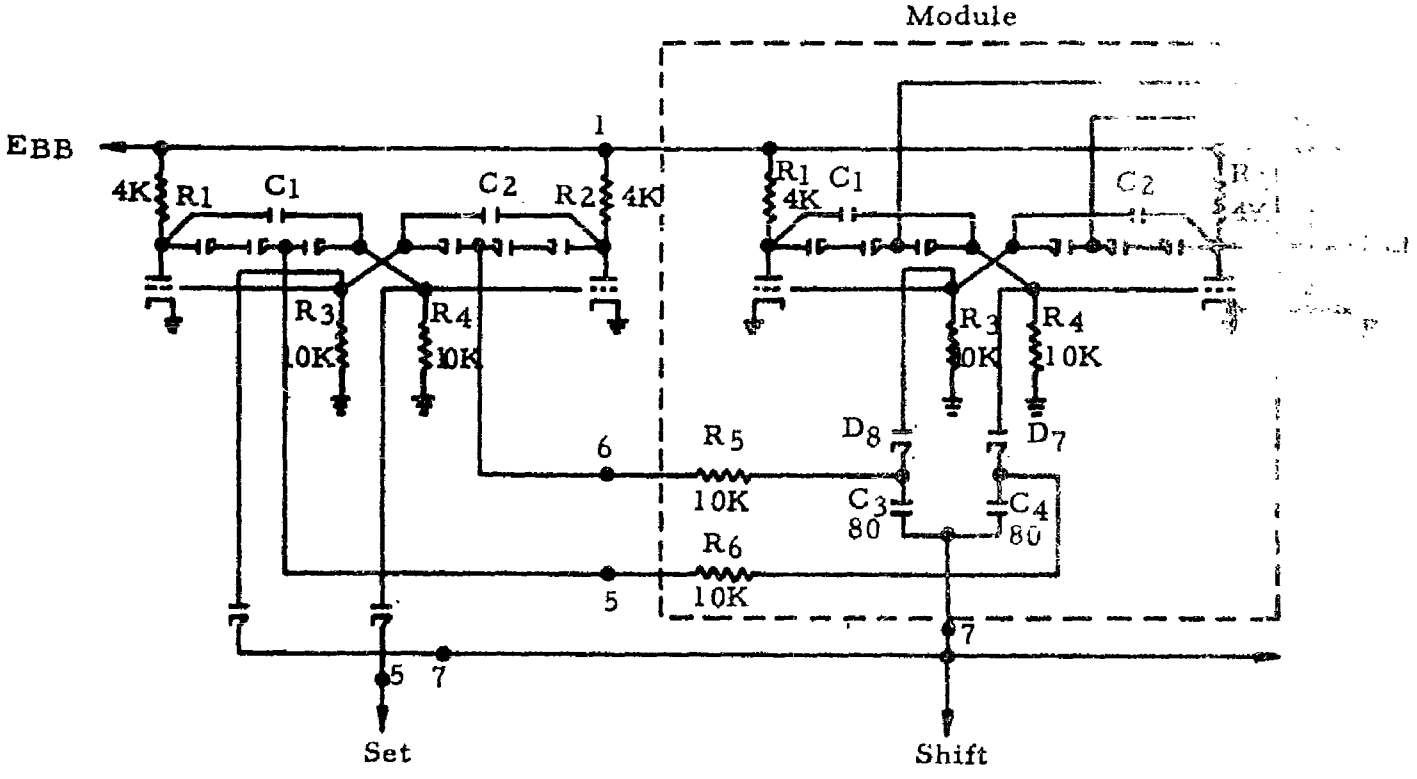

FIGURE 57

was apparent that the trigger sensitivity of the circuit could be increased by reducing the diode capacitance. Subsequently, low capacitance diodes, produced by the Tube Development group, were received, measured and found to exhibit a capacitance reduction of almost 50%. These low capacitance (4.0 pf at one megacycle) diodes were constructed with 0.035" anode-cathode insulators and with an 0.003" anode-cathode spacing.

The low capacitance diodes were inserted into the gating lead of the shift-register and the shift pulse amplitude required to trigger the circuit was measured. The minimum shift-pulse amplitude required was reduced from -16.0 volts to -8.0 volts, a definite, but insufficient improvement.

The second approach to the problem consisted of designing a gating circuit for positive instead of negative shift pulses. Such a circuit would block off positive 5.0 volt pulses to the negative grid of the flip-flop whenever the gating voltage was at +2.5 volts, and pass the positive 5.0 volt trigger pulse, with sufficient amplitude at the grid to trigger the stage, whenever the gating voltage was zero. It has the disadvantage, however, of passing all of the positive trigger pulse to the grid of the "on" tube. This would not result in undesired triggering but would again detract from the triggering sensitivity of the stage. Thus, it was decided that a positive triggering gate would not contribute significantly to the solution of the problem, and some other approach must be considered.

The shift register flip-flop circuit was again examined for any possible improvement in design. It was noted that the gating voltages were "picked off" at a junction of the coupling diodes of the preceding stage. This point had been chosen in order to allow the shift pulse a wider amplitude range than could be realized if the gating voltage were picked off at the grid. The voltage, as derived at the diode junction, ranged from +2.4 volts minimum to a maximum of -6.0 volts, a change of 3.6 volts. The grid, however, would range [illegible] volts. It had been

thought that the greater voltage change at the diode junction was desirable, but it was now apparent that it was objectionable from the standpoint of the high minimum value of the voltage. The shift trigger must be of sufficient amplitude to over-ride the minimum voltage by at least +2.6 volts t trigger the stage properly, even with a perfect gate. The circuit was, therefore, modified so that the gating voltage was picked off directly at the grid of the preceding stage. The triggering capacitors were thus allowed to discharge completely, enabling a lower shift trigger voltage to trigger the stage. The circuit was found to trigger reliably with a minimum trigger pulse amplitude of -5.0 volts. A combination of low capacitance diodes and lower gating potentials allowed the circuit to trigger with a shift trigger of -4.7 volts as compared to the -16.0 volts which had originally been required. The modifications then had afforded a very significant improvement in trigger sensitivity.

An effort was then made to improve the speed of the register. It was determined that the circuit speed was limited by the time spacing between the "set" and "shift" pulses. The input sequence generator currently being used would not allow the time between a "set" and the next "shift" pulse to exceed 10 per cent of the time between shift pulses. Thus, for the circuit to operate with a shift repetition rate of 1.0 megacycle, the input flip-flop must respond to a 10.0-megacycle bit rate, a speed in excess of the design capabilities of the circuit. The input flip-flop was found to operate satisfactorily at a bit rate of 1.3 megacycles, allowing the two-bit shift register to operate at speeds in excess of 100 kc. It was felt that the circuit would operate at greater shift repetition rates if the time between a "set" and "shift" pulse could be increased. In order to accomplish this, it is necessary to allow more delay between the "set" and "shift" generators than is obtainable with the generators now available. To remedy this situation, a variable delay line has been ordered, and work

will be resumed in this area as soon as the delay line is received.

Four-Input NOR

During this quarter, the four-input Nor circuitry was designed and te
A schematic diagram of the circuit is shown in Figure 58. The Nor circu
was designed to deliver up to 1.0 ma of current into a load. After the cir-
cuit configuration was decided upon, the component values and specifications
were determined as follows:

1. Assume a full load of 1.0 ma at output voltage of +2.5 volts.

2. Assume three coupling diodes in series, each with a built-in back bias of +2.35 volts and each capable of conducting not less than 1.0 ma of forward current when the anode-cathode potential is +3.0 volts.

3. To obtain +2.5 volts at the output, across a 2.5K ohm load, a diode current of 1.0 ma must flow, establishing a voltage drop of approximately 9.0 volts in the coupling diodes. Thus, E_p (max) of the Nor must be not less than 11.5 volts for a full logical "one" output.

4. Since the diodes will conduct a very small, but nevertheless significant current (50 μA), with an anode to cathode potential of 2.35 volts, the driving Nor should exhibit a full conduction Ep of not more than 6.9 volts. This figure should be from 6.0 to 6.5 volts for reliable operation of the Nor.

5. From 3 and 4 above it is evident that the plate potential of the Nor triode must not exceed a full conduction value of 6.5 volts; and, when the triode is not conducting, the plate potential must not be less than 11.5 volts.

6. Assume E_{bb} = 16 volts.

7. Assume a cutoff plate current (I_{co}) of 100 μA with E_p = 11.5 volts and E_g = 0 volts.

8. Then the total current through the R_L of the cutoff triode is $I_L + I_{co}$ = 1.1 ma. This current must produce a potential drop in R_L of not more than $E_{bb} - E_{p(co)}$ = 15.0V - 11.5V = 4.5V.

$$R_L < \frac{4.5}{1.1} \text{ K ohms.} \quad \text{Let } R_L = 4.0\text{K ohms.}$$

9. The full conduction current of the triode must be sufficient to drop 9.0 volts in R_L, thus lowering the plate potential to the 6.5 volt value specified in step #5.

$$\text{[illegible]} \quad i_p > \frac{(16.0-6.5) \text{ volts}}{\text{[illegible]} \text{ ohms}} = 2.4 \text{ Ma}$$

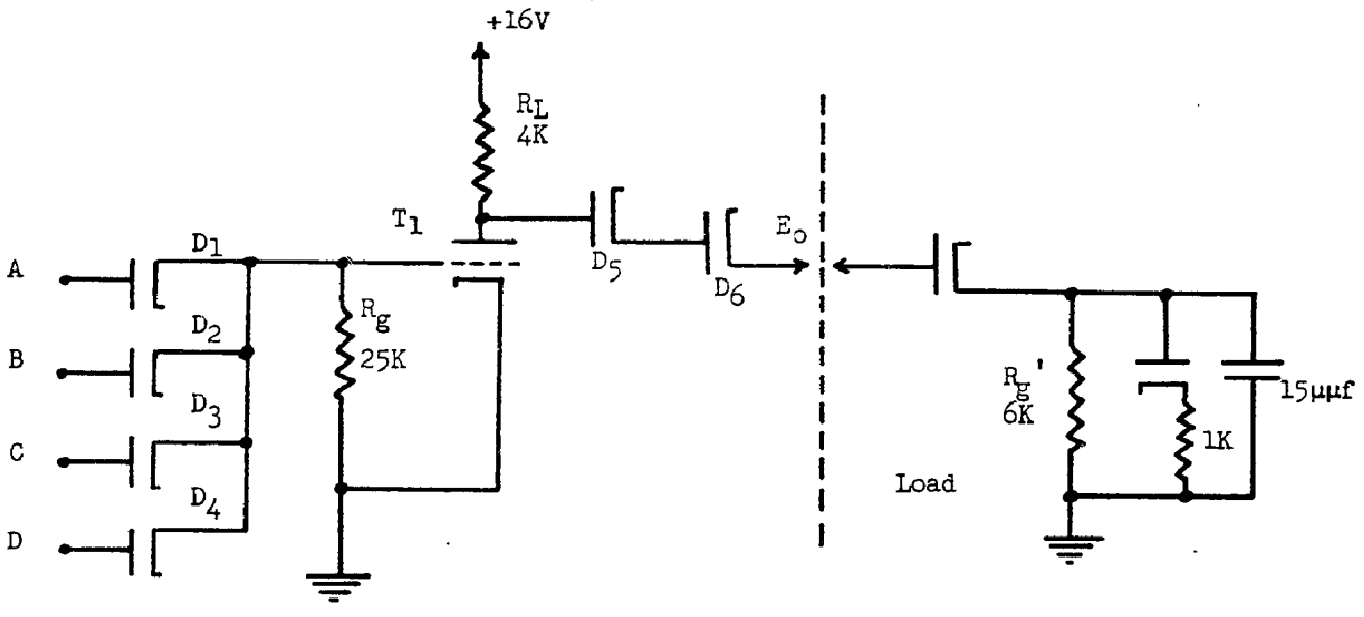

TIMM 4-INPUT NOR CIRCUIT

Figure 58

The triode then must be capable of conducting not less than 2.4 ma when the grid is at +2.5 volts and the plate at +6.5 volts.

The components which were specified for the Nor circuit are as follows:

Triodes $I_p \geq 2.4$ ma with $E_p = 6.5$ volts, $E_g = +2.5$ volts

$I_p \leq 100$ μA with $E_p = 11.5$ volts, $E_g = 0$ volts

$I_g \leq 150$ μA with $E_p = 6.5$ volts, $E_g = 2.5$ volts

Diodes A. Coupling diodes

$E_{pk} \geq 2.35$ volts when $I_d = 50$ μA

$E_{pk} \leq 3.0$ volts when $I_d = 1.0$ ma

Slope resistance ≤ 650 ohms

B. Grid circuit (input) diodes

$E_{pk} \geq 2.35$ volts when $I_d = 50$ μA

$E_{pk} \leq 3.0$ volts when $I_d = 300$ μA

Slope resistance ≤ 3200 ohms

Resistors $R_L = 4.0K \pm 10\%$

$R_g = 25.0K \pm 10\%$

The above information was submitted to the respective component development groups.

Some of the operating advantages of TIMM diode coupled Nor circuits are illustrated in Figures 59 and 60. Figure 59 shows the composite load line of a Nor circuit operating into a load which consists of another Nor circuit. The actual operating path for the tube is shown by the heavy lines. The portion of the load line to the left of point (1) has a slope of minus $\frac{1}{R_L}$. The tube will operate on that portion of the curve when its grid is clamped at its maximum positive value by its grid current; that is, when the tube is in a fully conducting state. As the grid potential is reduced, the operating point arrives at point (1). Here the plate potential has risen to a value sufficient to cause a current to flow through the coupling diodes and the load, [illegible] the grid resistor of the driven stage. The load R_L, which is now presented to the tube, consists of the plate load resistor R_L, in [illegible] combination of the diode resistance, R_D, and the grid

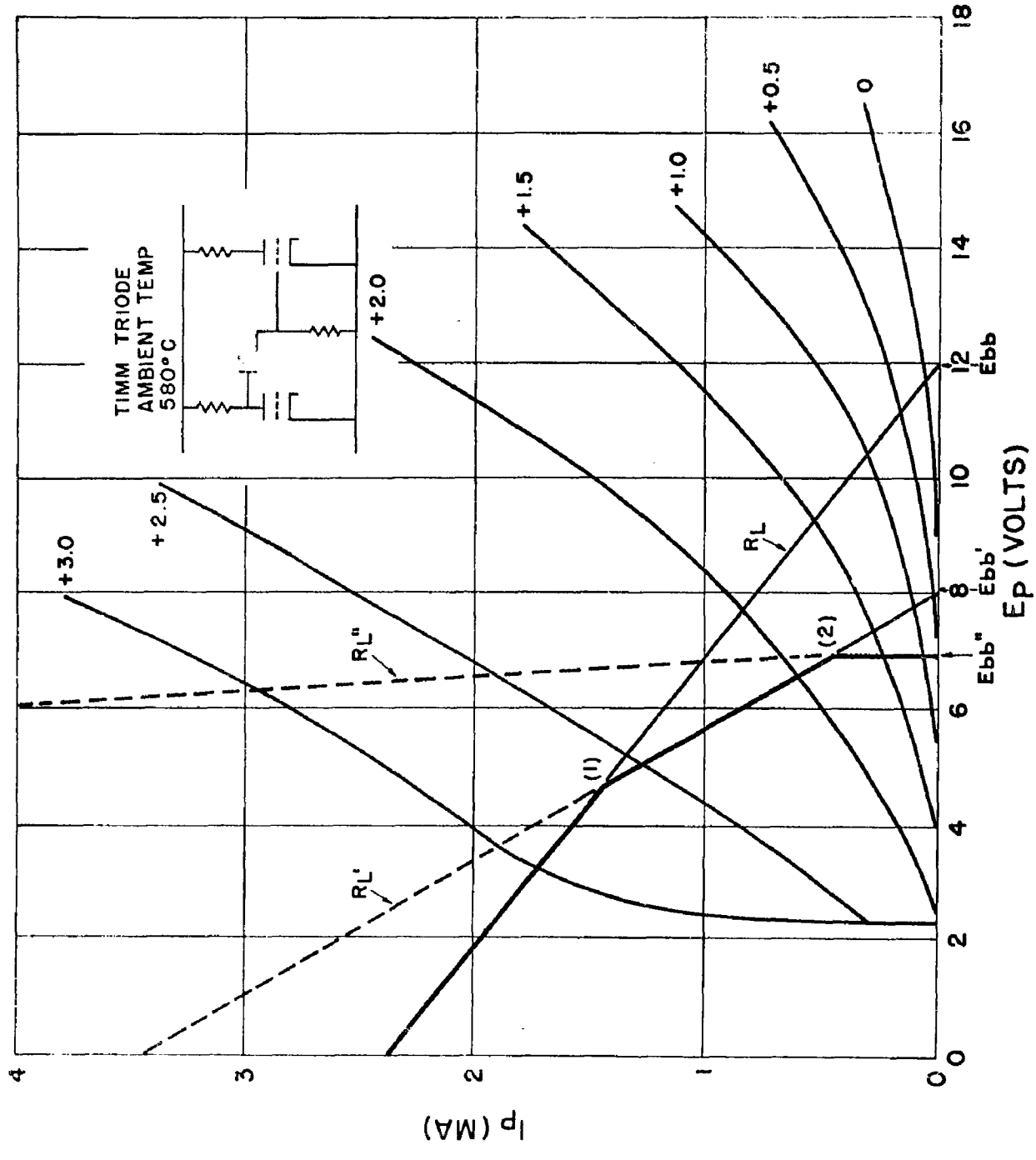
COMPOSITE STATIC OPERATING LOAD LINES FOR TIMM NOR
TIMM TRIODE
AMBIENT TEMP
580°C
+3.0
+2.5
+2.0
+1.5
+1.0
+0.5
0
RL
RL'
RL"
(1)
(2)
Ebb"
Ebb'
Ebb
Ep (VOLTS)
Ip (MA)
0
2
4
6
8
10
12
14
16
18
1
2
3
4

Figure 59

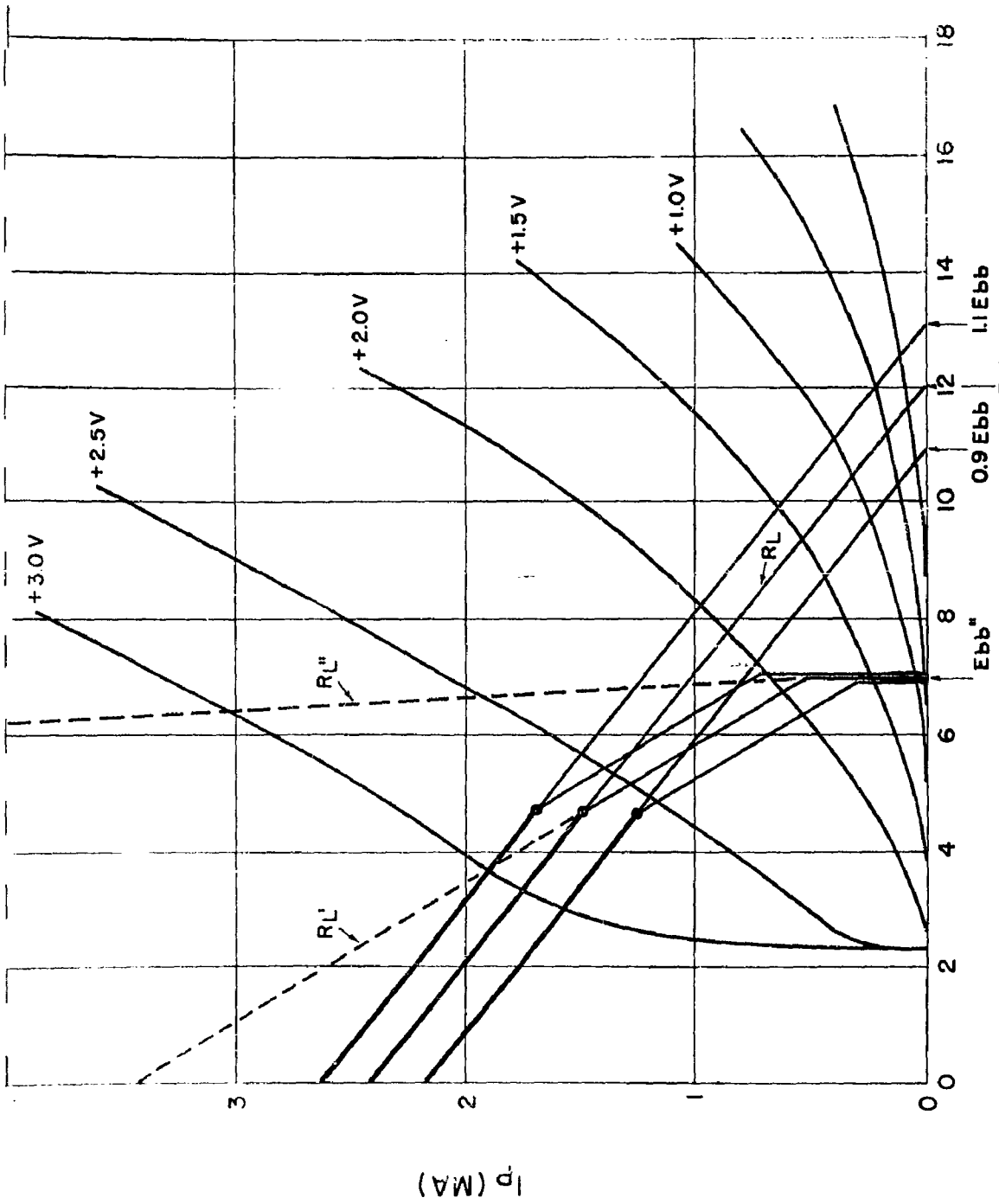
COMPOSITE STATIC LOAD LINES FOR TIMMS NOR SHOWING
CIRCUIT TOLERANCE TO VARIATIONS IN Ebb.
+3.0V
+2.5V
+2.0V
+1.5V
+1.0V
RL'
RL"
RL
Ebb"
0.9 Ebb
Ebb
1.1 Ebb
Ep (VOLTS)
Ip (MA)
0
2
4
6
8
10
12
14
16
18
1
2
3

Figure 60

resistor, R_g. R_L' then is given by the expression:

$$R_L' = \frac{R_L (R_d + R_g)}{R_L + R_d + R_g}$$

The load line from point (1) to point (2) then has a slope of minus $\frac{1}{R_L'}$.

At point (2) the voltage across the grid resistor of the driven stage has risen to a value sufficient to cause grid current flow, further reducing the load resistance seen by the driving stage. The new load resistance, R_L'', into which the driving tube operates, is given by the expression:

$$R_L'' = \frac{R_L (R_d R_x)}{R_L + R_d + R_x}$$

where $$R_x = \frac{R_g E_g}{R_g I_g + E_g}$$

The values of R_x refer to the grid circuit of the load Nor. The load line from point (2) to the E_p intercept then has a slope of minus $\frac{1}{R_L''}$. This latter slope is very steep, as can be seen in the figure.

The operating path described above is peculiar to a TIMM diode coupled stage, offering advantage to this type of operation from the resulting circuit tolerance to variations in the plate supply voltage. Figure 60 shows the composite load lines for a stage operating with a plate supply voltage E_{bb}. Shown on the same graph are the load lines which result when E_{bb} is varied to 0.9 E_{bb} or 1.1 E_{bb}, a supply voltage variation of $\pm$ 10 per cent. Note that the E_b intercept varies very little, indicating stable operation over a wide range of plate supply voltages.

The Nor circuit was breadboarded as designed using available components closely approximating those specified previously. It was not possible to obtain triodes having as high a plate current and as low a grid current as those specified. Since the input voltage could be derived from a supply source of low impedance, a high grid current triode was used that met fairly well the plate characteristics desired. The triode which was actually used

exhibited the following characteristics:

$I_{p(co)}$ = 130 μA at E_p = 11.5V, E_g = 0V
I_p = 2.7 mA at E_p = 6.5V, E_g = +2.5V
I_g = 550 μA at E_p = 6.5V, E_g = +2.5V

All other components were obtained having values as specified.

The breadboard Nor was loaded with the circuit shown to the right of the dotted line in Figure 59. The load is composed of TIMM components and is designed to simulate the actual maximum load the Nor is expected to drive. A pulse was applied to the input of the Nor and the resulting data are shown below:

Condition	Input	Output E_p	E_o	E_g'
Voltage, "Zero"	0 volts	+11.5 volts	+5.6 volts	2.3 volts
"One"	+2.3 volts	+ 6.0 volts	+2.0 volts	0 volts
Pulse rise	0.040 μsec	0.2 μsec	0.3 μsec	0.3 μsec
Pulse fall	0.040 μsec	0.1 μsec	1.0 μsec	3.0 μsec

The reason for the long fall time of the pulse at E_g' was investigated. It is caused by the relatively large R_g which was used in the load circuit coupled with the large grid-cathode capacitance of the load triodes. In addition, the grid resistor, R_g, presented a rather large capacitance in shunt with the grid circuit of the load triodes. This capacitance totals approximately 25.0 pf. The resulting time constant R_gC_t then is about 0.63 μsec., since 5 RC is the time the circuit will take to discharge to a value of 90 per cent E_{max}. This long fall time, if intolerable, can be shortened by reduction of R_g and interelectrode capacitances of the input of the load triodes. Work is being conducted by the tube and resistor group toward reducing these objectionable capacitances.

In an attempt to reduce rise and fall times evidenced above, it was decided to use speed-up capacitors across the coupling diodes. It was found that the fall time could be reduced by as much as 75 per cent of the original by the use of rather large (0.002 μf) capacitors across the diodes. It

was found, however, that this value of capacitance was too large for the circuit since it rendered ineffective the isolation afforded by the diodes. At the present time, without speed-up capacitors, the Nor will respond well to pulse repetition rates up to 20 Kc. If Rg is reduced to 10.0K ohms, the maximum frequency is increased to 50 Kc. Low capacitance resistors will further increase the operating speed to nearly 100 Kc. These changes, in addition to appropriate speed-up capacitors, could raise the frequency limit to the megacycle range if desired.

The design for component lug arrangement and component placement within the shift register and Nor circuit modules was completed this period. The arrangement of the Nor module is, however, tentative since it has not been decided what geometrical form the input diodes will take.

A scaled outline drawing of the shift register module is shown in Figure 61. The component lugs are not shown on this drawing, only the relative position of the module components. Figure 62 shows a schematic drawing of the module indicating lug placement and internal module wiring. Note that the entire shift register module is constructed in such a way that only two insulating spacers are required. This module arrangement necessitates the use of components with both radial and tangential lugs to facilitate wiring the module without crossing wires. The required component and lug configurations are shown in Figure 63. All input and output connections are made to the lower rows of tangential lugs so that the leads connecting the module to its circuit board may be kept as short as possible.

Since each shift register circuit consists of ten modules, it is planned to integrate modules to a ceramic printboard capable of withstanding the same high ambient temperature to which the TIMM module is exposed. Design of the printboard is complete and drawings have been submitted to the Ceramic and [illegible] group. The printboard will eliminate long intermodule connecting

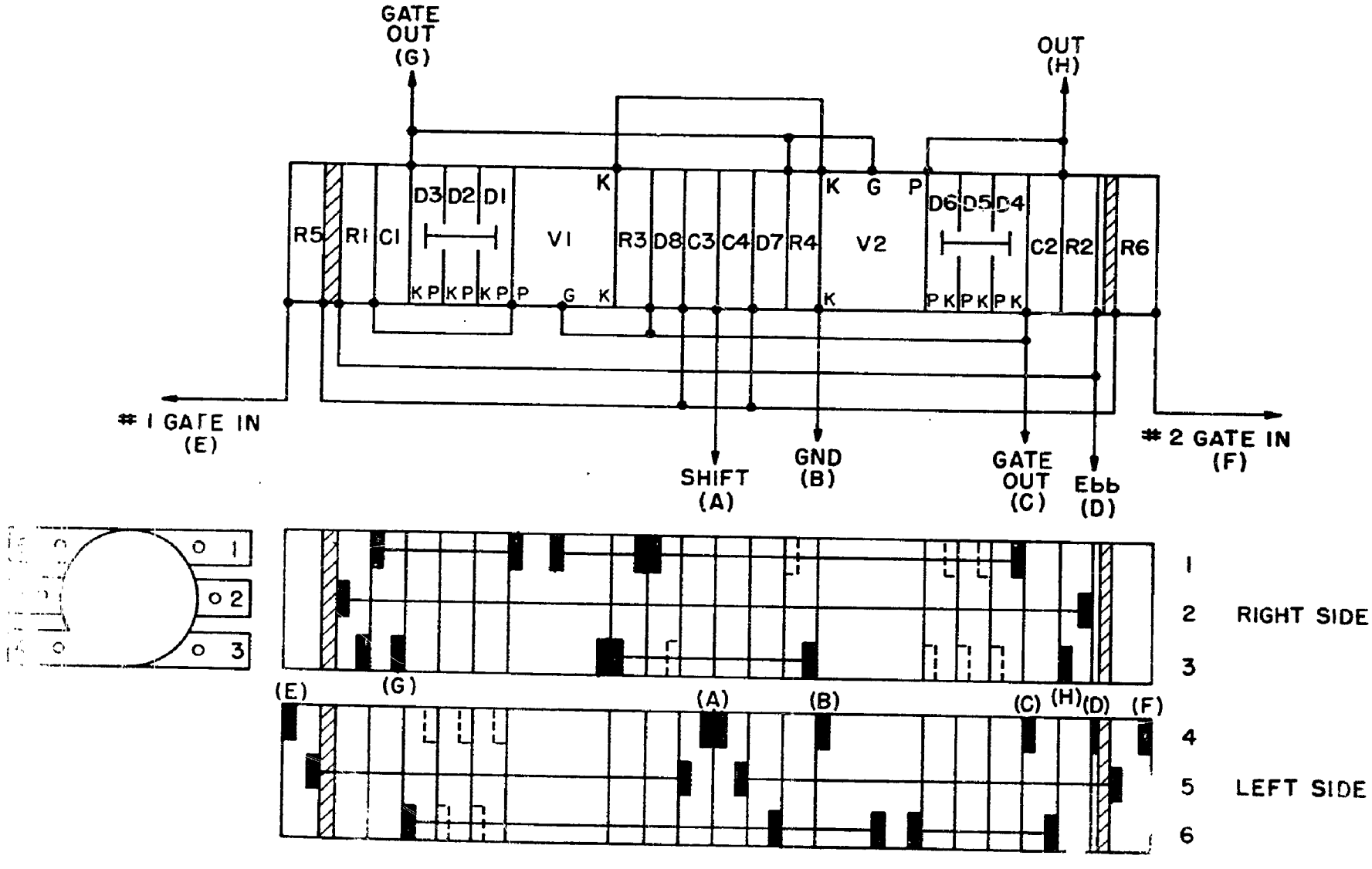

STACKING AND WIRING DIAGRAM FOR TIMM
IO-BIT SHIFT REGISTER MODULE

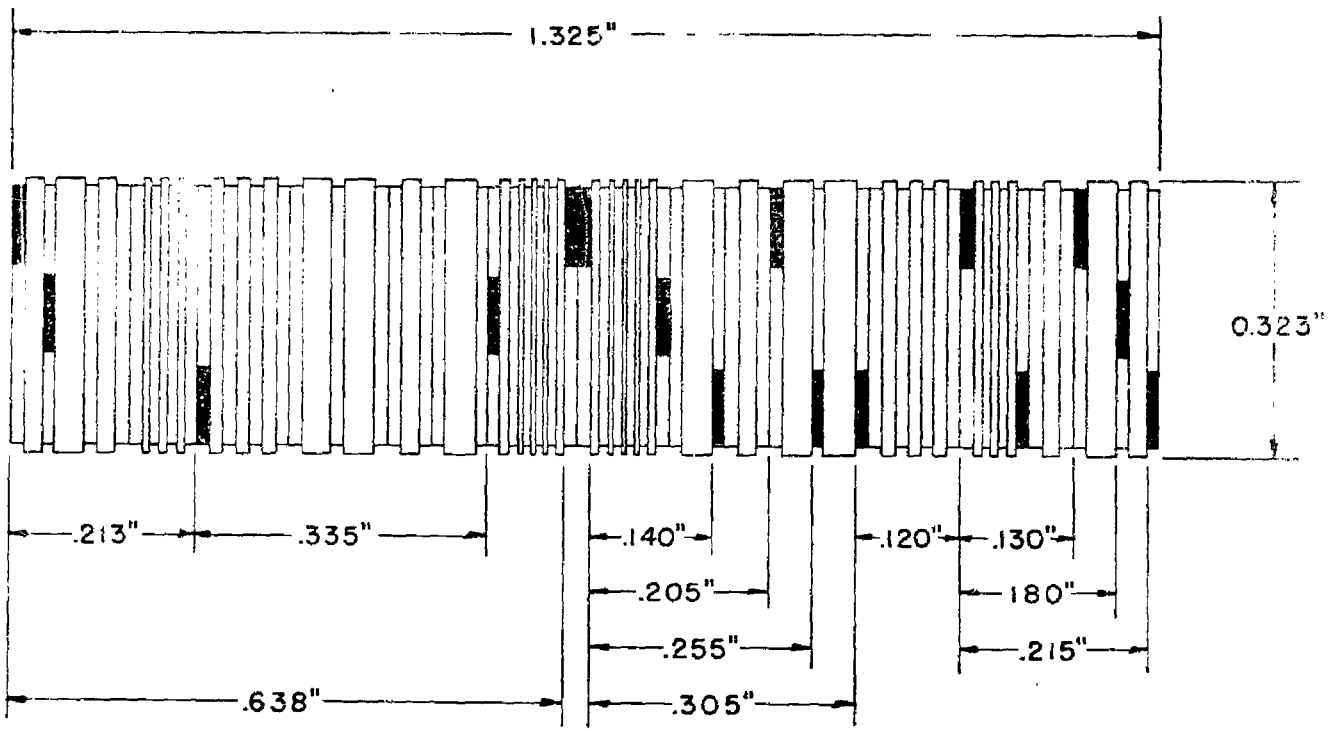

SHIFT REGISTER MODULE

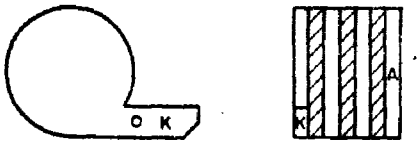

SERIES CONNECTED "TRIPLE" DIODE
TYPE B

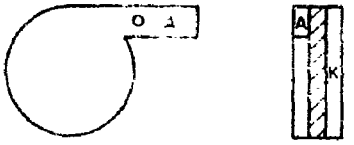

DIODE
TYPE F

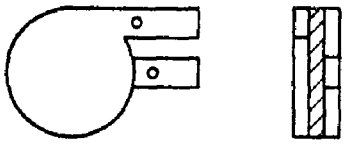

RESISTOR
TYPE G

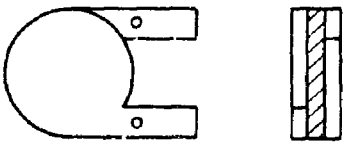

RESISTOR
TYPE B

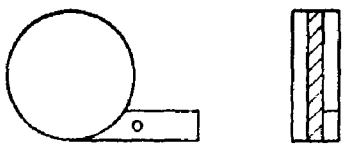

RESISTOR
TYPE C

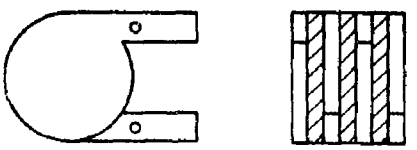

CAPACITOR
TYPE D

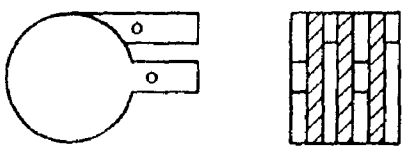

CAPACITOR
TYPE F

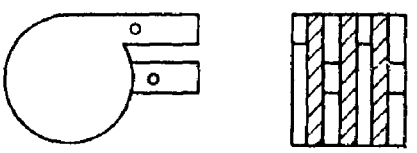

CAPACITOR
TYPE G

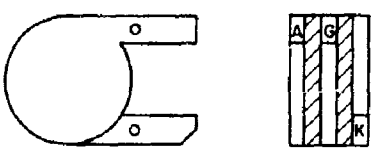

TRIODE
TYPE A

TIMM 10-BIT SHIFT REGISTER
COMPONENT CONFIGURATIONS UTILIZING
RADIAL AND TANGENTIAL LUGS

Figure 67

leads which may be subject to vibration and shock damage. Only extremely short leads will be necessary for module interconnections. Thermal expansion characteristics of the ceramic board will match those of the module.

In order to present maximum resistance to shock and vibration, the modules will be mounted on the board as shown in Figure 64. Note that the center of gravity is maintained at a low point by this method of mounting. Each module will be secured to the board by leads welded to the lugs. These leads are passed through holes in the board and welded to connecting pins on the bottom of the board. The leads will consist of 0.002" thick by 0.050" wide Inconel ribbon, doubled and welded for strength. The modules will be held a short distance (about 0.015") from the board by the titanium supports brazed to the end of each module, also shown in Figure 64. This is done to allow for any slight misalignment of the components within the module. It is anticipated that this method of module mounting will permit the units to withstand large acceleration forces. Some of these forces have been calculated and are presented at the end of this section.

Since the entire Nor circuit can be included within one module, it is not necessary to provide a mounting board for that circuit. The Nor module arrangement is shown in Figure 65.

The logic design for a TIMM demonstration unit to be presented at Wright Field was completed this month. This unit is intended to demonstrate the ability of TIMM components to operate in essential computer logic circuits.

Dynamic Display Unit

It was proposed that a Binary Word Simulator be constructed to demonstrate feasibility of TIMM components and TIMM circuitry for computer applications. This [illegible] circuit was chosen because it is self-contained, needing only primary (battery) power for input and an oscilloscope for display of the output. [illegible] basic circuits are utilized: free running multivibrators, flip-flops,

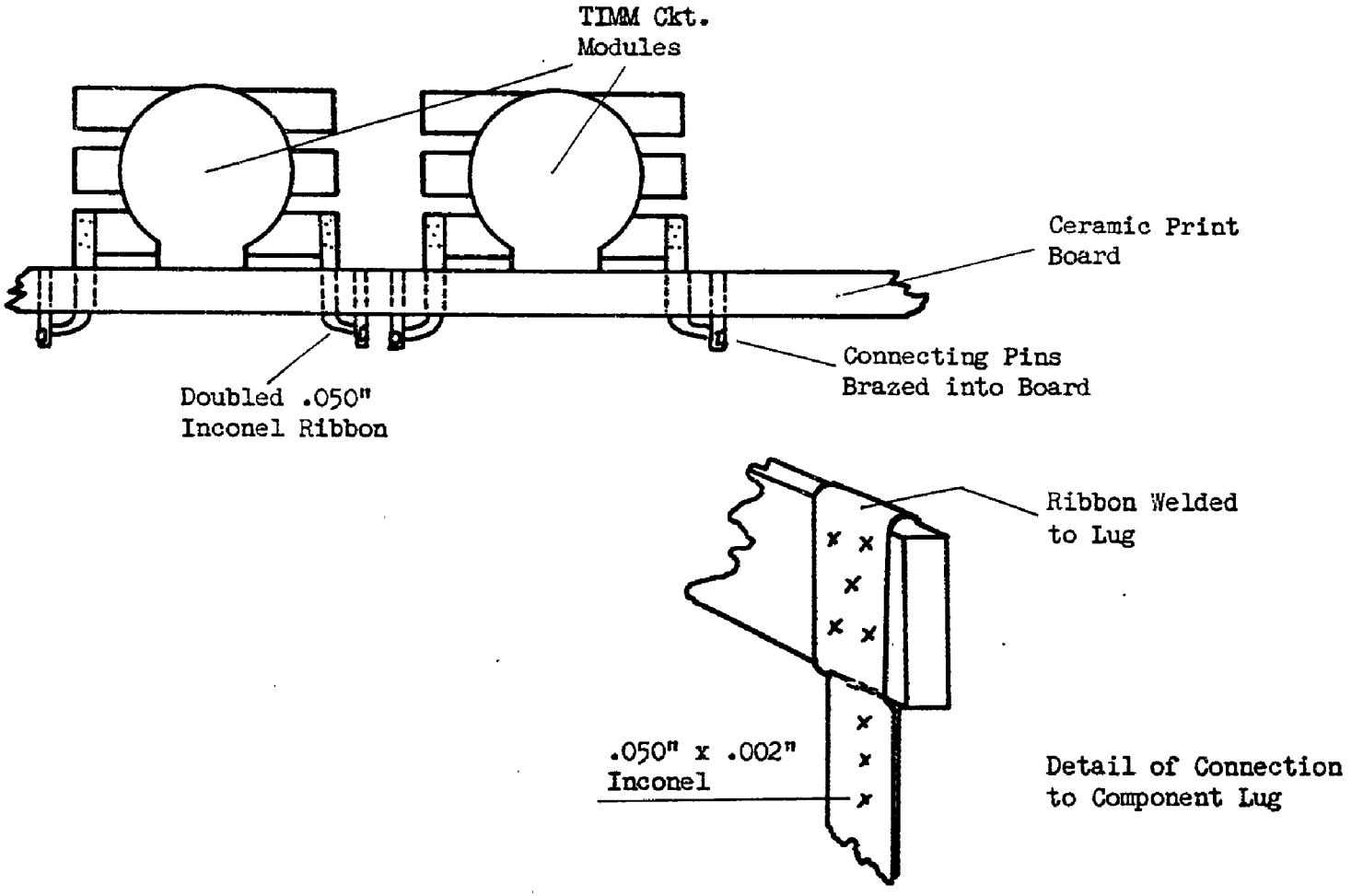

METHOD OF MOUNTING AND FASTENING
MODULES TO CIRCUIT BOARD

Figure 64

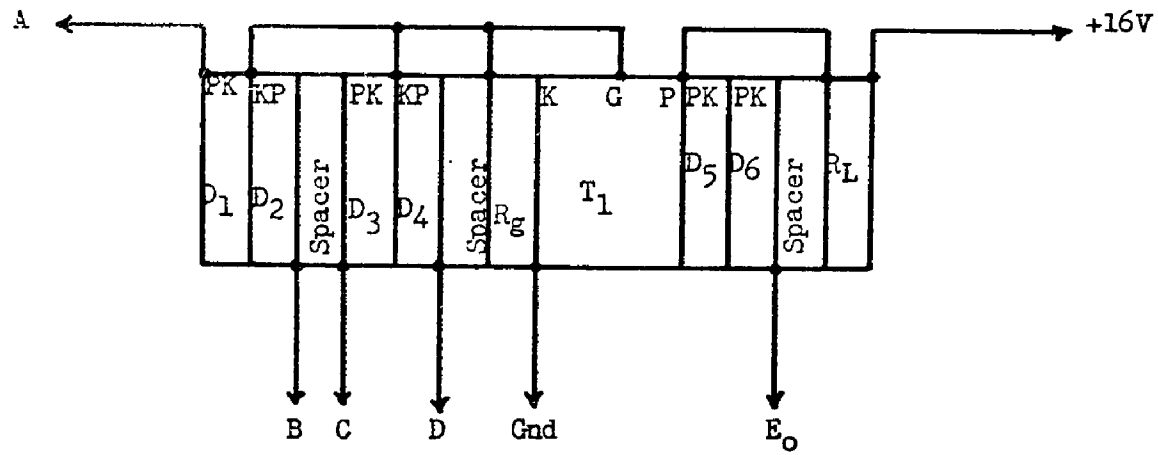

Note: Module Length
0.55"

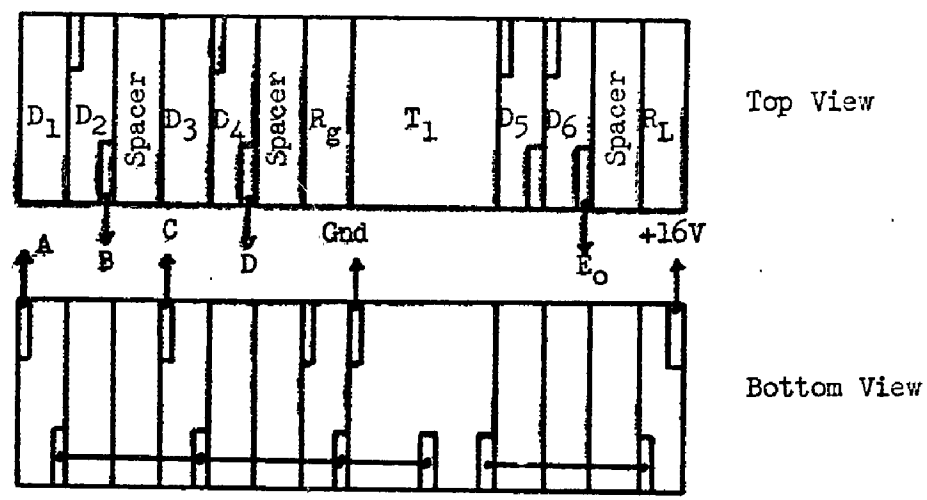

STACKING AND WIRING DIAGRAM
FOR TIMM 4-INPUT NOR MODULE

Figure 65

And gates and Nor gates. The block diagram for the circuit is shown in Figure 66.

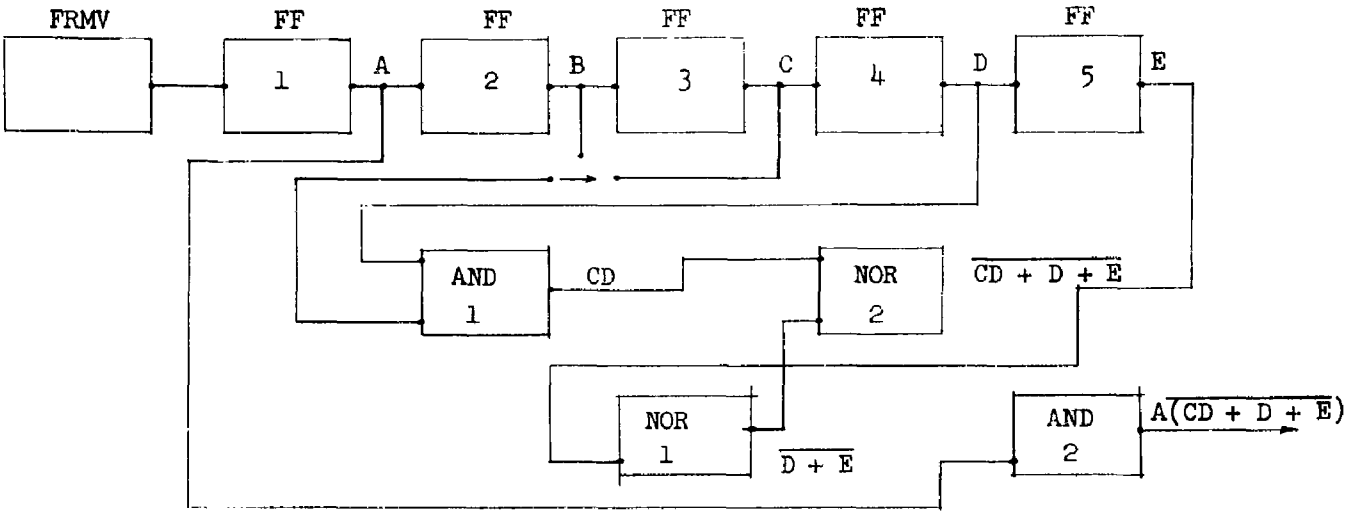

Word Simulator Block Diagram
Figure 66

It was planned that each circuit would be breadboarded, optimized, stacked and sealed into modules and the modules arranged on a section of ceramic board in such a manner that the entire unit may be operated in an 8.0" long x 1 1/2" (ID) Vycor oven. Interconnections will be nickel wire (0.015" dia.) with ceramic spaghetti being used where necessary.

The output of the display unit will be as shown in Figure 67.

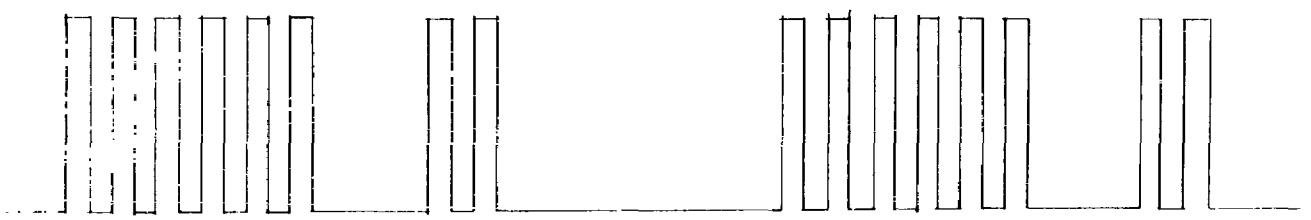

Word Simulator Output Waveform
Figure 67

The duration of the pulses will be determined by the rate of the free-running multivibrator circuit, which in turn will be determined by the characteristics of the triodes available for the display unit.

Component requirements are as follows:

Circuit	Triodes	Diodes	Resistors	Capacitors
1 FRMV	2	0	5	3
4 FF	8	24	20	12
2 And	0	4	2	0
2 Nor	2	8	4	2
Total/unit	12	36	31	17

The efforts devoted to the display unit this period were mainly those of the Circuit Development group. Most of the individual circuits were designed, breadboarded and optimized electronically. Stacking diagrams were designed for optimum component placement in the module and several circuits returned to the Tube Development group for sealing into modules. Several experimental modules were constructed and subsequently nickel and chrome plated for oxidation protection of the titanium. Comparison of data taken prior to plating and after the plating process showed no changes in electrical or mechanical characteristics.

Additional work performed by the Circuit Development group for this quarter consisted of calculating the mass center of a TIMM Shift Register module and the stresses developed in the module and ceramic circuit board due to an acceleration of 500 g's in each of three mutually perpendicular planes.

Location of Module Mass Center

Due to the symmetry in the TIMM shift register module, the module's mass center (center of gravity) is very close to the module's centroid (physical center). Calculations carried out on the module showed that the maximum deviation of the mass center was less than 0.0011" in any one of the three mutually perpendicular planes (Figure 68). Because of this small deviation, the torsional shearing stress will be very small and will not be the critical stress involved when the module is subjected to an acceleration of 500 g's.

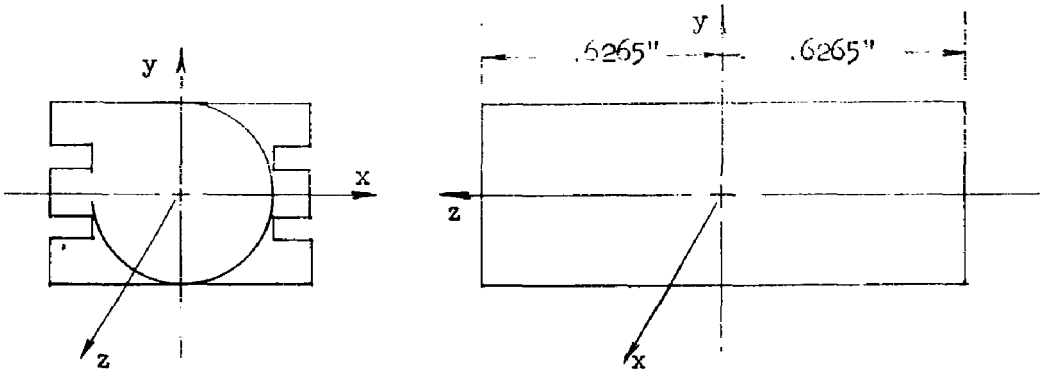

Centroid	Mass Center	Estimated Weight
x = 0	$\bar{x}$ = -.00108"	
y = 0	$\bar{y}$ = -.000623"	6.06 grams (.0134 lbs.)
z = 0	$\bar{z}$ = -.00103"	

Location of Mass Center of
TIMM Shift Register Module

Figure 68

Module Seal Stresses

If the completed module is supported only on its ends, then an acceleration upward on the unit (Figure 69) will tend to put a tensile stress on the center seals. By assuming the module is a homogeneous cylinder subjected to a 500-g acceleration, a stress of 824 psi was found to exist at the bottom edge of a nickel seal ring at the mid point of the module. Experimental seal strengths range from 8,000 to 13,000 psi. These values are in general less than the modules of rupture of the ceramic material.

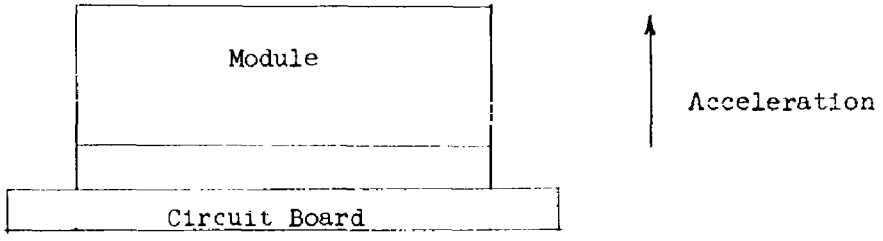

Integral Module - Circuit Board Arrangement

Figure 69

Circuit Board Stresses

Although there is not any definite agreement as to the final module mounting, a suggested configuration is shown in Figure 70. When the complete unit with its 10 modules is accelerated in a direction perpendicular to the plane of the ceramic board, analytical calculations show the tensile stress at the center of the board to be 24,500 psi. Suggested modules of rupture for ceramic material is between 20,000 and 24,000 psi. If mounting holes are to be taken into account, the calculated stress would be higher for a given acceleration. The maximum calculated stress when the board alone is accelerated at 500 g's is 7860 psi.

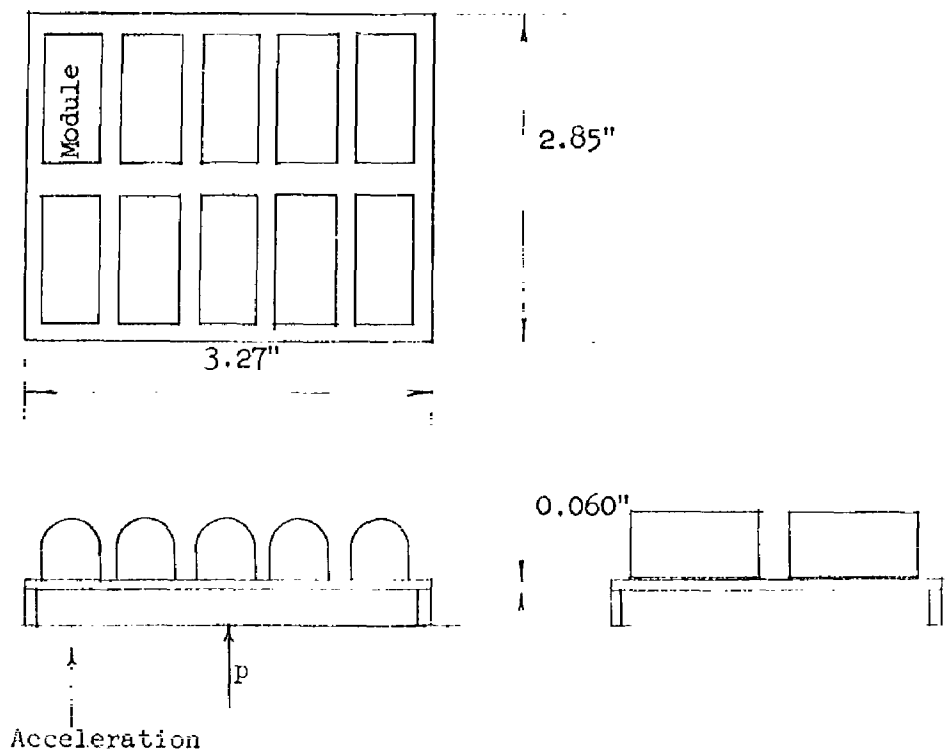

Physical Module Arrangement - 10 Bit Shift Register

Figure 70

MATERIALS INVESTIGATION

Protective Coatings

Non-Metallic Coatings - The stacked capacitors spray coated with "No-Scale" or "No-Carb," as reported in the Second Quarterly Report, were exposed in air for one week at 600 C and retested for capacitance and resistance. As a result of further deterioration of resistance values, as shown in the summary in Table 14, these materials were dropped as potential protective coatings for TIMM circuits.

Protective Coating "CR-NET" - manufactured by Markal Company, was evaluated as a coating for Ti at 580 C. The manufacturer reported this material as composed of a synthetic resin vehicle which decomposed at 550 F, an aromatic solvent (xylol) and silicone and boro-silicate pigments. Preliminary tests showed that the coating melted during heating to 580 C, and produced a brittle, water soluble glass coating when cooled to room temperature. Since the material behaved like a conventional water-glass composition, further tests were conducted to determine the physical nature of the coating at 580 C. Testing disclosed the material to be a viscous fluid at operating temperature which will readily wet other surfaces with which it comes in contact. Several titanium strips 0.25" x 1.50" x 0.020" were subsequently coated and suspended vertically in a furnace at 580 C. Examination after one week exposure showed that the coating had flowed to the lower end of the strip, and micro-examination indicated inadequate protection against scaling and oxygen diffusion even in areas where the coating was intact. No further investigation of this material will be conducted.

Electroplating - The investigation of electroplated chromium and nickel for protection of titanium from air contamination was continued with primary emphasis on techniques applicable to components and stacked modules. The effectiveness of electroplated chromium and nickel in preventing scaling and

Sample No	Uncoated	As Coated	1 Wk at 600 C.
	Leakage Current at 90V DC Amps		
No-Scale			
1	5.5×10^{-2}	1.4×10^{-5}	1.5×10^{-5}
3	3.6×10^{-11}	-	-
5	2.6×10^{-12}	2.3×10^{-5}	1.8×10^{-6}
7	2.2×10^{-12}	1.3×10^{-5}	short
9	1.3×10^{-11}	1.2×10^{-5}	9.2×10^{-4}
11	2.8×10^{-12}	1.3×10^{-5}	2.1×10^{-5}
13	2.1×10^{-12}	9.2×10^{-6}	4.4×10^{-5}
No-Carb			
2	1.8×10^{-12}	4.7×10^{-7}	3.0×10^{-5}
4	2.0×10^{-12}	6.4×10^{-7}	3.2×10^{-6}
6	2.0×10^{-12}	1.1×10^{-6}	short
8	3.3×10^{-10}	1.8×10^{-6}	short
10	4.8×10^{-12}	1.1×10^{-6}	3.0×10^{-4}
12	2.5×10^{-11}	6.8×10^{-7}	short
	Average Cp, picofarads		
No-Scale	85.5	88.6	89.0
No-Carb	90.7	94.1	95.0
	Average Tan		
No-Scale	.0017	.0176	.0278
No-Carb	.0015	.0040	.0270

Effect of "No-Scale" and "No-Carb" on Room Temperature Properties of Stacked Capacitors Cp and Tan δ Measured at 500 Kc.

Table 14

contamination of titanium, at temperatures to 700 C in air, was demonstrated and reported earlier, but detailed procedures and techniques must be developed and evaluated for application to TIMM circuits.

The tendency toward cracking of the chromium plate has been recognized for some time; and, although such cracks have apparently not been detrimental, a commercial proprietary crack-free chromium plating electrolyte was evaluated to determine if a ductile, crack-free deposit would be advantageous. Three titanium electrodes were plated at each of three current densities (2.0, 3.0 and 4.0 amps per sq. in.) in Metal and Thermit Corporation's "Unichrome CF-500" electrolyte and examined metallographically for uniformity of deposit. All samples exhibited a discontinuous powdery-type deposit - more characteristic of an unsintered cataphoretic deposit than an electroplate. Because of the poor initial results with the proprietary electrolyte and because all earlier results were based on chromium deposition from a standard Cr_2O_3 electrolyte, no further work with this proprietary formula is anticipated.

A group of 25 mechanical sample triodes were plated under the following conditions:

Chromium: 21° Be electrolyte; 60 C; 20 min at 2.5 amps per sq. in.
Nickel Strike: Woods electrolyte; room temperature; 3.0 min at 0.07 amps per sq. in.
Nickel: Watts electrolyte; 60 C; 30 min at 0.25 amps per sq. in.

All samples were prepared for plating by sandblasting the surfaces with S.S. White No. 1 abrasive. Micro-examination of the as-plated samples showed a distinct lack of adherence between the titanium and chromium and, in some cases, between the chromium and nickel. Air exposure at 600 C, however, caused no blistering or flaking of the plating. Recognizing that the as-plated adherence on titanium is poor as compared with more conventional base metals, and that good adherence is achieved only after some diffusion occurs at operating temperature, it was determined that the separation between plating and base metal noted in the as-plated samples was a result of stresses resulting

from mounting, sectioning, and grinding.

Visual and micro-examination of the plated triodes showed excessive plating build-up at the electrode edges, at points the greatest distance from the point of electrical contact during the plating cycle. This was particularly pronounced in the high current density chromium bath. Sample electrodes were therefore evaluated after chromium plating at an electrolyte temperature of 54 C and current densities of 1.0, 2.0, and 2.5 amps per square inch. The average plating thickness on the sample surfaces and at the point of maximum edge build-up were as follows:

Time Minutes	Current Density Amps Per Square Inch	Avg. Plating Thickness, Inches	
		Surface	Edge
20	1.0	0.00010	0.00025
13.5	2.0	0.00015	0.00042
8	2.5	0.00011	Nodules

The low average plating thickness obtained with the highest current density schedule is probably a result of reduced efficiency in the bath. Pronounced "nodule" formation, however, was noted at the edge of the sample. Based on the above results, the current density for chromium plating was reduced to 1.0 amps per square inch at 54 C in order to limit the plating build-up at points of maximum current density.

The electrical characteristics of three "And" and two "Nor" circuit modules were measured before and after plating in order to determine the effect of the plating process. The components were stacked and brazed with aluminum filler and the modules operated at 580 C to establish performance characteristics. They were then sandblasted and auxiliary nickel wire leads were spotwelded to all electrodes to which electrical contact was not made through the module interconnections. The modules were plated as follows:

Chromium: 54 C, 1.0 amps per sq. in., 20 minutes
Nickel Strike: room temp., 0.7 amps per sq. in., 3.0 minutes
Nickel: 60 C, 0.25 amps per sq. in., 30 minutes

The two "Nor" modules were nickel-plated at an excessively high current density

as a result of an error in calculating total bath current, and four electrodes in one module were not plated because of failure to attach one of the auxiliary leads. Despite these changes from the planned procedure, the circuit showed no change in electrical characteristics after plating. The "And" circuits were all plated per the above schedule. Two of the three circuits showed no change after plating, and the characteristics of the third one indicated an air diode. The physical location of this diode in the stack makes it susceptible to mechanical damage, however; and the change could not be attributed directly to the plating process.

Welding and Brazing

A limited amount of investigation had indicated early in the program that TIMM components could be stacked and brazed with aluminum filler for module assembly. Previous work in connection with the application of aluminum as a protective coating for titanium had also shown the formation of the intermetallic compound $TiAl_3$ when these two elements in intimate contact are heated to 580 C or higher. Since the properties of the compound are relatively unknown, and since changes in the electrical resistance of the brazed joints in a module may affect the circuit performance, a test was conducted to determine the change in joint resistance with time.

Four pairs of 0.015" thick titanium electrodes were vacuum brazed for 2.0 minutes at 730 C with a 0.005" thick aluminum foil shim as filler material. Nickel wire leads were resistance welded to each electrode lug so that the total circuit resistance measured would include the resistance of the brazed joint. Two control samples were assembled by resistance welding nickel leads to each of two single titanium electrodes. The six assemblies were placed in an air furnace with the leads brought out to fixed terminals, and the resistance of each sample was measured at intervals with a Wheatstone Bridge. The change in resistance with time at 580 C is shown in Figure 71. The data show no

Aluminum Brazed Titanium
Resistance
Vs
Time at 590 C

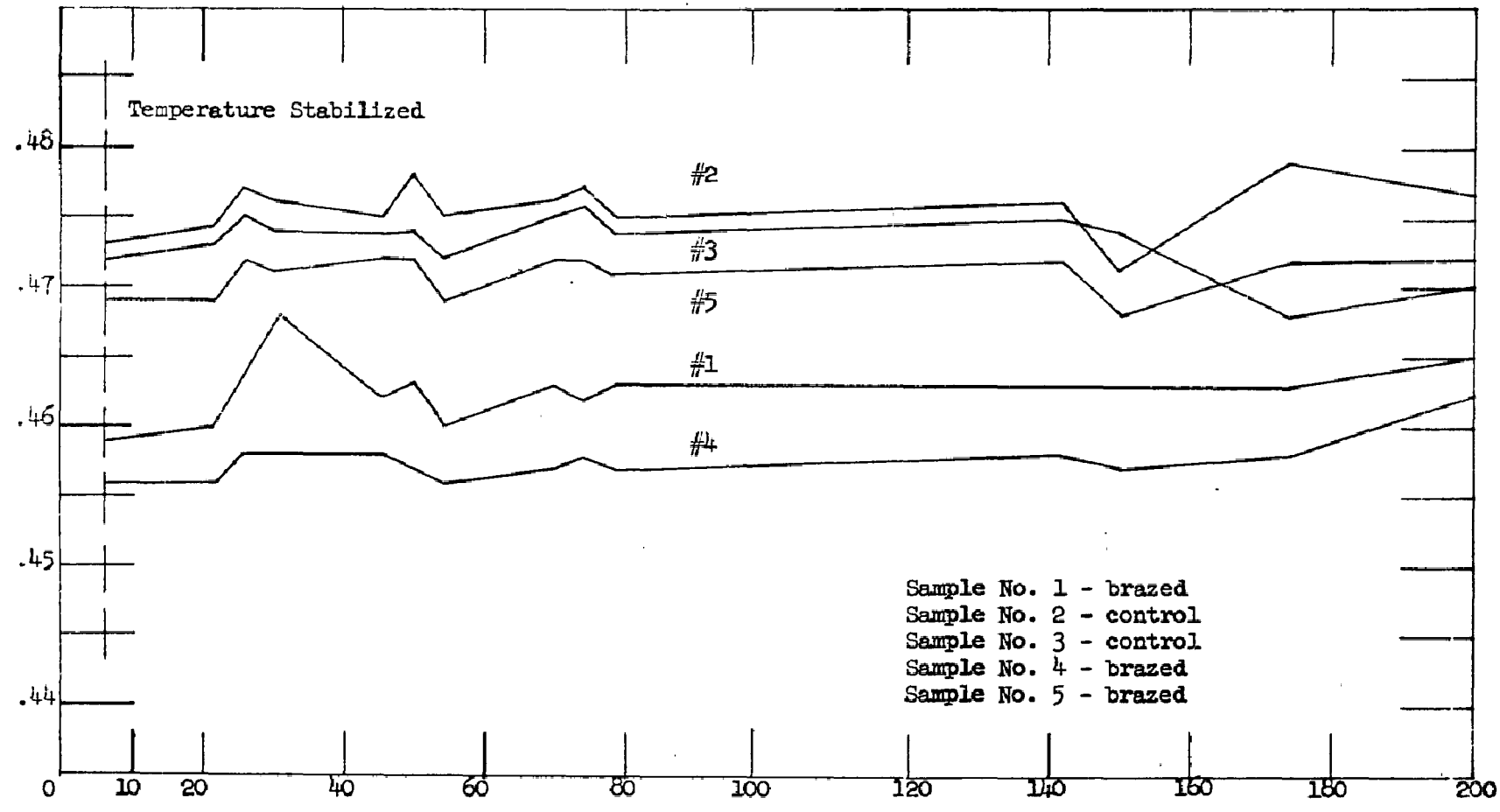

Figure 71

significant change in resistance in either the brazed samples or the control samples of 200 hours.

X-ray diffraction studies of brazed surfaces of reperesentative as-brazed samples and of the 200-hour resistance test samples showed no difference in the phases present. This indicates a stable structure in the as-brazed condition; and therefore no significant change in resistance would be anticipated during exposure at temperatures to 590 C.

The mechanical strength of aluminum brazed titanium joints obtained to date has been erratic, and a more intensive investigation of the process will be undertaken during the next quarter. A reliable quantitative test method has not yet been developed, but efforts toward this goal will be increased. The tensile and shear strength values of butt joints as used in module assembly are relatively unimportant during service because joint failure will occur most readily as a result of forces imposed by a bending moment on the module. It is expected therefore that the most realistic test method will require assembly of a special test specimen to be tested as a simple beam, loaded at mid-span.

Several experimental interconnecting lead joints were also attempted with aluminum brazing. A 0.025" diameter Inconel wire was inserted through the holes in the lugs of standard titanium electrodes, and a ring formed from 0.012" diameter aluminum wire was preplaced at each joint. Brazing was performed in vacuum at temperatures from 700 C to 800 C. Examination of the joints indicated that the aluminum alloyed with both the Inconel and titanium, but that very little flow took place. The limited flow of the aluminum filler at the temperatures used is understandable since the addition of small amounts of either nickel or titanium to molten aluminum cause a steep rise in the liquidus temperature. The joints exhibited reasonable strength despite the small bond area resulting from the poor flow and properties can probably be improved by more precise preplacement of the filler metal. Further study of this method will

be conducted in connection with the investigation of module brazing techniques.

A qualitative study of resistance welded interconnecting and external leads confirmed that the strongest welds may be achieved between the titanium electrodes and titanium wire leads. For long time service at 580 C, however, titanium leads will require surface protection to avoid severe embrittlement from air contamination. For external leads reliable connections can be achieved by spot welding annealed, 0.002" thick Inconel ribbon to both sides of the electrode lug and then spot welding the two strips of ribbon together over their entire length. Nickel has adequate oxidation resistance at 580 C and has been used successfully in wire form by welding to bare and electroplated titanium surfaces. For example, on the module mentioned above in the discussion of electroplating, the interconnecting leads were 0.015" diameter titanium wire welded in place prior to plating, and the external leads were 0.015" diameter nickel wire welded after plating. This method provided oxidation protection for the titanium leads and an oxidation resistant material for all unplated leads. Full annealed wire, particularly for the external leads, is desirable to reduce the strain imposed on the weld during handling.

Coated Grids

Twelve 0.001" thick photoetched molybdenum grids were coated with a titanium-iron composition for evaluation in triodes. The grids were cataphoretically coated for 8.0 seconds at 200V in a suspension of the following composition:

240 ml	nitromethane
40 ml	isopropanol
10 ml	of a mixture of 70 parts by volume isopropanol and 30 parts nitromethane saturated with zein
10 gms	325-mesh titanium powder
1 gm	carbonyl iron powder

After coating the parts were fired in a vacuum induction furnace by heating to 1400-1500 C in 15.0 seconds. A typical coated grid element is illustrated in the photomicrograph in Figure 72.

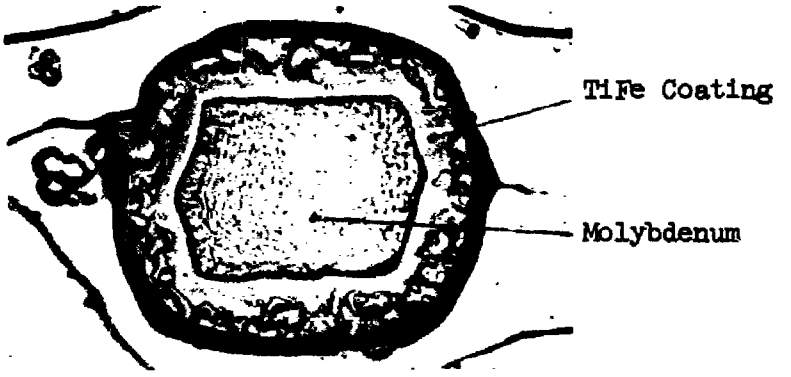

Figure 72

Cross Section of Photoetched Molybdenum Grid Element Coated with Titanium Iron

Mag. - 1000X

All of the coated grids were bowed after coating and firing, and were also quite brittle as a result of partial recrystallization of the molybdenum and the inherent brittleness of the coating. Considerable difficulty was encountered therefore in assembling the grids into tubes, and several were lost because of distortion and fracture. During processing of the tubes that were assembled, the grids warped and shorted to the plates. For test purposes, the grid was electrically connected as the anode; and contact potential and emission current were compared against similar tubes having uncoated molybdenum and titanium grids. The average values are summarized below:

Grid	Contact Potential Volts	Emission, ma
Coated molybdenum	1.0	0.2
Uncoated molybdenum	0.2	> 3.0
Titanium	2.0	> 3.0

The low emission with the coated grid may be a result of the formation of molybdenum oxide during processing of the coating, but this theory has not been evaluated experimentally.

An investigation of the process for coating molybdenum and tungsten with titanium, by electrodecomposition from a molten salt bath, has been initiated. G. E. Electronics Laboratory, Syracuse, N. Y., personnel and facilities will be utilized. The feasibility study is to be completed by March 1, 1962.

Oxidation Resistant Electrodes

The substitution of a material with good oxidation resistance at 580 C for TIMM component electrodes would eliminate the concern for a protective coating for titanium and might also reduce the problems encountered in making high reliability welded and brazed connections. To evaluate the feasibility of this approach, several diodes with type 430 stainless steel electrodes were assembled and tested. The type 430 alloy was selected because of its excellent oxidation resistance and because of the availability of a ceramic insulator (OW-116) with closely matching expansion characteristics.

In order to retain the tube characteristics afforded by titanium, a titanium stud was secured to the plate electrode by spot welding. This operation can also be accomplished by assembling the titanium and 430 parts and heating in vacuum to a temperature above the Ti-Fe eutectic temperature of 1080 C. Figure 73 illustrates typical joints obtained when a titanium stud in contact with a type 430 electrode is heated in vacuum for two minutes at 1130 C. Note in Figure 73A the extremely large grain size in the stainless steel over the area in contact with the titanium. A study of many similar samples and a number of special control samples indicated that the excessive grain growth is a result of a localized temperature increase caused by the heat released during the exothermic Ti-Fe eutectic reaction. The excessive growth can be controlled to some extent with a heat sink in contact with the surface of the stainless electrode.

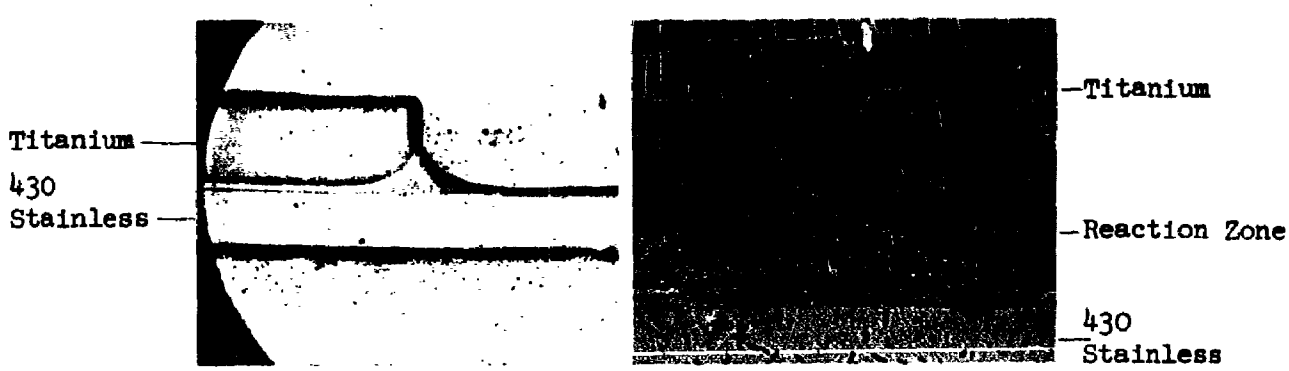

73A
Fillet Formation

73B
Interface Structure

Figure 73

Typical Structure of Ti-430 Stainless Steel
When Heated Two Minutes at 1130 C in Vacuum

Figure 74, which is an enlarged view of the fine grained stainless steel in Figure 73A, shows that partial alpha to gamma phase transformation occurred during the vacuum heating cycle. Such transformation may be undesirable since it causes a discontinuity in the thermal expansion curve and a resultant mismatch with the ceramic insulator. The transformation can be suppressed, however, by selecting a modified alloy such as titanium stabilized 430 stainless steel.

Figure 74
Phase Transformation in 430 Stainless Steel Mag. - 750X

The test diodes were assembled with a 0.0013" thick titanium shim and a 0.0005 thick nickel shim at each ceramic-to-metal seal area, and sealed in

accordance with the standard sealing schedule used for titanium electrodes. All of the diodes went air when tested at 580 C. Several dummy units were subsequently assembled and sealed with just the stainless electrodes and the ceramic insulator, and these also were not vacuum tight.

A metallographic study of the ceramic-to-metal seal structure showed a variation in structure within a single seal, and little or no eutectic formation over most of the seal area, illustrated in Figure 75. Figures 75A and 75B are typical of the seal structure over most of the area, and C and D are representative of a small area at the inner edge of the seal. Note the relatively smooth, straight-line ceramic interface in the former as compared to the latter, indicating that the ceramic-to-metal bond in 75A and 75B is not satisfactory. Severe cracking in the sealing alloy typified by Figures 75A and 75B was also noted in most assemblies. Based on these observations, it is concluded that the titanium-nickel ratio of the sealing shims and/or the sealing schedule used must be modified to produce a vacuum-tight seal.

An alternative sealing method may also be applicable to 430 stainless steel electrodes. By utilizing the Ti-Fe reaction, as illustrated above in joining Ti to 430 stainless, an active alloy seal can be made by using only a titanium shim in the joint. This would, of course, require a higher sealing temperature than is used at present for the Ti-Ni seal and may not be compatible with some components.

Further investigation in this area is planned for the next quarter.

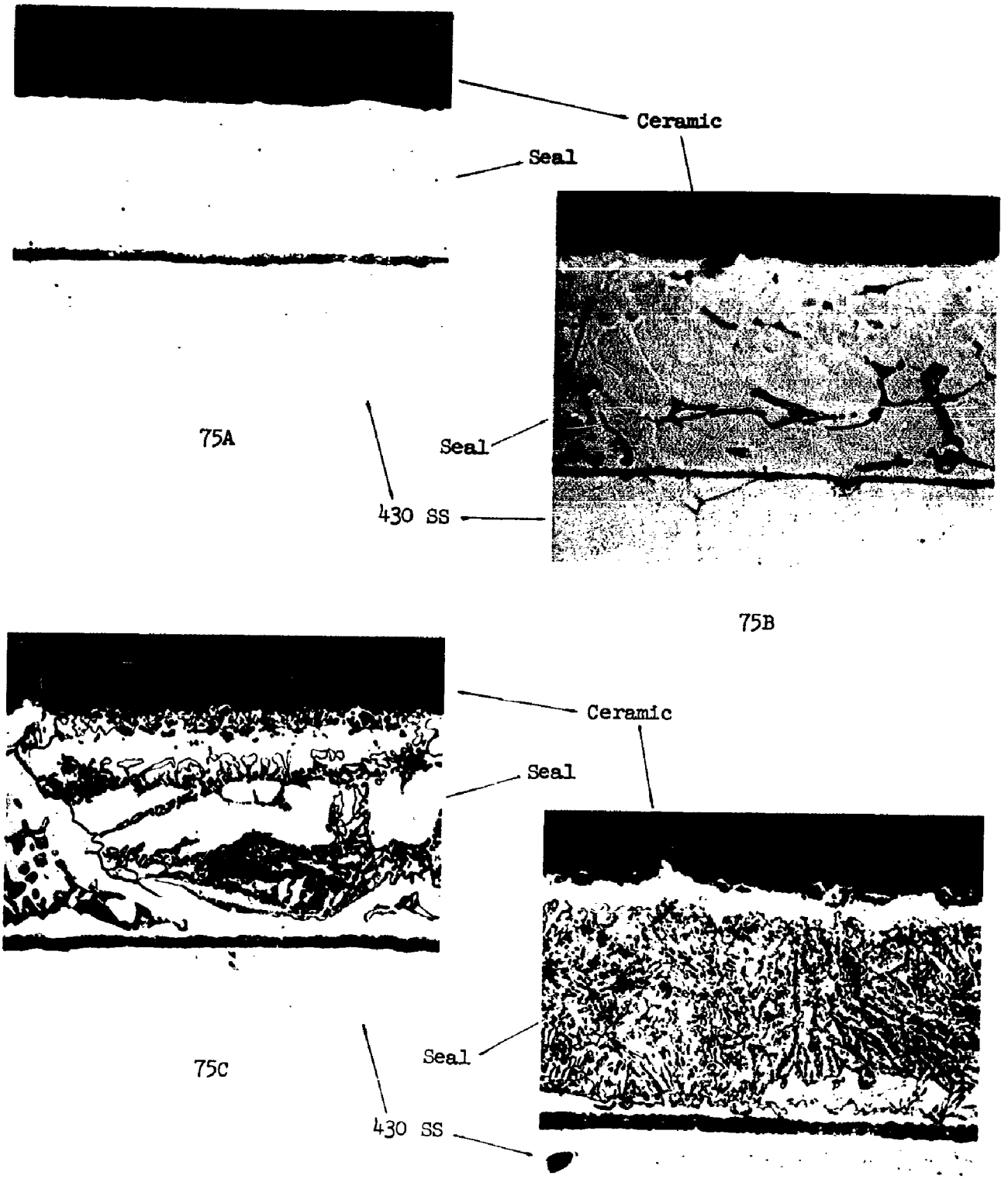

Figure 75

Typical 430 Stainless-to-CW-116 Ceramic Seals. Mag. 1000X

TEST EQUIPMENT DEVELOPMENT

Life Test Ovens

The status of component life test ovens, at the end of the third quarterly reporting period, is as follows:

Capacitor - Three, 20-position capacitor life test ovens have been constructed and are now in operation. These ovens are heated by a constant a-c current transformed directly from a regulated line. Temperature measurements have been extended to past 100 hours operation with fluctuation remaining within plus or minus three degrees of the pre-set, desired temperature.

The operational status of these ovens is as follows:

Oven #1 - 200 volts d-c applied to ten capacitors, 300 volts d-c applied to the other ten. Capacitors have been on life for approximately 5000 hours.

Oven #2 - 300 volts RMS, 60 cycle, applied to all capacitors. Capacitors have been on life approximately 500 hours.

Oven #3 - Square wave 40 volts peak-to-peak, 15 kc applied to all capacitors. Capacitors have been on life approximately 500 hours.

Triode - One, 72-position triode oven has been completed and placed into operation. This oven utilizes the "metal block" with individual chambers principle as used for resistor life testing and described in previous reports. Temperature monitoring during operation of this type oven construction shows deviations of less than plus or minus two degrees from the pre-set desired temperature. Small, two triode life test ovens are still being utilized for special testing where characteristics of components are being evaluated under conditions of reduced and elevated temperature.

Diode - One 144-position life test oven has been completed and placed into operation. This is the second resistor oven of this construction fabricated under the contract.

Test Equipment

Triode-Diode-Resistor Test Set - This item of test equipment was completed during the quarter and is now being utilized for testing TIMM components at operating temperatures. The test equipment was designed and fabricated to be portable and capable of being transported to the components under test. This eliminates the undesirable situation of removing components from the 580 C environment during the process of conveyance to the test equipment.

The unit will perform the following tests on the components referred to above:

a. Resistance measurements - These measurements will be made on a Wheatstone Bridge. The lower limit of resistance measurements is between 25-50 ohms, determined by the resistance of the wiring and the switch contacts. The upper limit is 10 megohms. Readings are to four significant places.

b. Diode measurements - The power supplies for diode and triode measurements are two low voltage regulated supplies. The set will perform the following measurements on diodes: insulation resistance, contact potential and two separate emission tests.

c. Triode measurements - This set will measure plate current, grid current, zero plate current, contact potential, and emission current. In the measurement of grid current, provision is made to introduce into the measuring circuit a "zero" resistance current meter to compensate for the grid current meter voltage drop.

Shock Testing

Construction of a shock test oven has been completed. The oven consists of a stainless steel plate 1/8-inch thick and two inches in diameter, mounted to the shock machine plate by four steel stand-offs 3/4 inches long. A nichrome heater wound on a mica form is placed directly under the plate. The plate and heater are sandwiched between two 1.0-inch thick x 3.0 inch diameter pieces of Du Pont "Tipersul" insulation. Components to be shocked must be furnished with 4-40 stainless steel studs brazed to one end. The oven will accommodate three such components at one time. Voltages can be applied to the components during shock. The equipment used for shock testing components is a high impulse device, capable of hammer angles in excess of 60 degrees (900 g's).

Environmental conditions, applied voltages, hammer angles (g's), and results achieved from shock testing TIMM triodes are included in the Tube Development portion of this report.

Vibration

A variable frequency vibration test jig has been designed, built and is being evaluated. This setup consists of a stationary oven which is positioned above the shake table. The component under test is fastened to a 2 1/2 inch stainless rod by means of a 4-40 stud brazed to the component. The rod is fastened to the shake table and extends through a hole in the bottom of the oven.

This test method appears to be practical for frequencies up to 2000 cps. Testing will be time-consuming,as the setup accommodates only one tube at a time. testing will be done on the Unholtz-Dickie Shaker rather than on the Ling system, as had originally been planned. The Unholtz-Dickie is a more refined system and is equipped for tracing curves of output versus frequency.

SUMMARY

Tube Development

Electrical design work has been concentrated primarily on grids to improve the uniformity of tube characteristics. Theoretical calculations, as well as experimental data, have shown that unless grids can be etched to more exacting tolerances, it may be necessary to inspect grids for correct transparency using an optical device designed for the purpose. Investigation was made of the factors governing triode grid contact potential since this is one of the variables that must be rigidly controlled to insure good uniformity of tube characteristics, especially in tubes having high transconductance.

New one-piece electrode studs for both anode and cathodes have been designed. This design incorporates both a vapor trap and a solder trap. Tests are being conducted to determine if these studs can be machined to close tolerances, thereby eliminating the resizing operations.

A grid tensioning electrode of the type reported last quarter has been successfully used to tension and hold flat the grids now in use. Although some interelectrode shorts still occur, it is expected that a refinement of the basic principle of this design will be completely successful in positioning and holding flat, thin, pure titanium grids.

A new oil-free vacuum system employing an ion pump was put into use for both tube sealing and parts firing. Tests indicate that tubes processed in this system are generally superior to tubes processed in systems employing oil diffusion pumps. Tubes processed in both systems are being evaluated on life test.

Additional shock testing of TIMM triodes has been completed. These tests, conducted at 580 C and under typical operating conditions, showed no instances of grid failure. Some cases of slight characteristic change were noted, but this is not believed to be a serious problem.

Module fabrication using aluminum as a brazing material was investigated. There has been some difficulty in obtaining sufficient braze strength, but the nature of the problem is under investigation. It is expected that better results will be obtained using different techniques of applying the aluminum braze material to the titanium surfaces.

Resistor Development:

1. Attempts to produce tungsten film resistors failed due to difficulties encountered in deposition of WO_3. Two methods of deposition were used: 1) evaporation from oxidizing tungsten wire, and 2) spraying of WO_3 suspended in amyl acetate. In both cases, the film was soft, fluffy and peeled from the substrate on removal from the mask.

2. High value evaporated platinum film resistors were made and are now on life.

3. Evaporated rhodium film resistors were of such high value (> 2 megohms) that no practical value would be derived from life testing insofar as the TIMM contact circuitry is concerned.

4. Several batches of evaporated carbon resistors were made utilizing ground surface substrates. Forty of these units have been put on life test; however, no data are available at this time.

5. Approximately 75 low capacitance resistors have been built. Room temperature measurements indicate a reduction in capacitance of from 65-70% over the regular design.

6. Sixteen evaporated carbon film units utilizing OW-129 ceramic substrates are now on life. There were no significant differences noted between this material and OW-102 at initial testing.

7. Several pyrolytic and evaporated carbon film units have been sent to the Test Lab for shock and vibration testing.

8. A considerable amount of time was devoted to building special value resistors for use in building modules for the contract review, dynamic display unit.

9. At the end of 5000 hours, carbon film resistors operating at loads of from 0.25 to 0.40 watts show a change in resistance of 13.8% for the pyrolytic type and 7.3% for the evaporated type.

10. Carbon film resistors operating over a range of load levels from 0.1 to 1.0 watts show very different life characteristics from one level to another. Both types show very rapid degradation at 0.5 watt and above with the fastest change occurring in the pyrolytic type. At the end of 1000 hours, pyrolytic type resistors operating at 0.5 watts have changed by 15.5%, while the

evaporated type shows a change of 6.0%. There were no significant differences noted between the two types operating at 0.1 and 0.25 watts at the end of 1000 hours.

11. Molybdenum and nichrome film resistors show some change during early life but have remained relatively stable from that point to the end of 1500 hours.

Capacitor Development

A measurable voltage can be obtained from a stacked ceramic capacitor after subjecting the unit to operating temperature and voltage. It is reversible with applied voltage. The unit can be shorted, loaded, or cooled down and reheated and still show an emf, although at a reduced level. The present work indicates a boundary layer is formed at the ceramic-metal interface by the injection of titanium into the ceramic during the sealing cycle. Ti or TiO_2 may prove to be the cause of more than one of the characteristics encountered in completed capacitor configurations. The properties of TiO_2 were discussed in the last report with a reference to the literature (Physical Review, Vol. 120, pp. 1631-1637, December 1, 1960). The properties discussed in the article included a rapid increase in dielectric constant as frequency is decreased, spontaneous polarization, reversible polarization, residual voltages, and open hysteresis loops.

Spontaneous polarization and polarization reversal were verified for stacked ceramic capacitors. A very small but measurable d-c voltage can be obtained from a capacitor while it is being subjected to operating temperatures. The magnitude and polarity of this voltage can be modified by application of an external voltage.

Open hysteresis loops of polarization versus an applied field can be shown over long measuring time intervals. The area enclosed decreases with increasing frequency so as to approach a straight line at approximately [illegible].

The change of dielectric constant has been previously reported for these units.

Conductivity data has revealed a change in the slope of conductivity versus the reciprocal of absolute temperature which corresponds to a change in the conduction mechanism between 400 C and 500 C for at least three of the ceramic bodies tested in the completed capacitor configuration. This change has not been evident in tests performed on platinized ceramic discs.

There is some indication that titanium is being injected into the ceramic during the sealing cycle. The boundary area at the ceramic-metal interface can then act as a Ti. concentration cell. The estimated activation energies fit the requirements for the Ti-TiO_2 cell theory. A maximum of about 2.0 volts could be expected from a Ti-TiO_2 half cell. The value obtained is not unrealistic.

Inductor Development

A ceramic "spool" has been designed and fabricated on which inductor coils may be evaluated. These units can be hermetically enclosed by encasing in a ceramic cylinder and sealing with metal end electrodes.

Inductor units have been fabricated using copper magnet wire encased with Secon "D" insulation. Encapsulation was achieved by metallizing the ends of a OW-116 ceramic cylinder and subsequently applying a copper plate. Sealing to copper-clad Telemet end electrodes is accomplished using Nicoro #80 braze material.

Data are presented for values of inductance and "Q" over a temperature range from 25 C to 580 C. At 30.0 megacycles and 580 C, Q's > 50 have been achieved with values of inductance between 0.5 - 0.6 μh.

Circuit Development

A new Half adder circuit was designed, breadboarded, and maximized; the stacking and lug arrangement of the entire module was completed but will have to be revised due to changes in the type lugs that will be used in the future.

Using a Schmitt trigger circuit, an attempt was made to reshape a distorted pulse; however the rise times obtained were not those desired.

Work was initiated on the r-f portion of the contract. An r-f amplifier (grounded-grid) circuit and a Colpitts oscillator circuit were constructed using simulated TIMM inductors. Both circuits were designed to function at 30 megacycles. The amplifier circuit yielded a gain of 20 db; the oscillator produced an output signal of 16.0 volts rms at the desired frequency.

A frequency response curve of an RC amplifier was obtained using a TIMM triode; the upper half power point occurred at 2.6 megacycles. The midband gain was 17.4 db.

The trigger sensitivity of the shift register was increased by a factor of three. This was accomplished by using improved components and by slight circuit modifications. The speed of the circuit was also improved, but limitations of the input generator equipment make it impossible to measure the maximum repetition rate at the present time.

The circuit for the Nor unit has been designed. The design procedure is described as well as the results of breadboard tests.

Work was also done on module arrangement and layout of the shift register and Nor circuits. This work resulted in some changes being made in component lug configurations. A printed circuit board has been designed and drawings submitted to the ceramic group.

Materials Investigation

Evaluation of protective coatings for titanium was continued, and experience has been gained in electroplating circuit modules with chromium and nickel. Aluminum brazing of titanium for module assembly was investigated, and the electrical resistance of brazed joints was measured for times to 200 hours at 580 C. Photoetched molybdenum grids, coated with a titanium-iron composition, were tested in standard triodes, but produced

units exhibiting low contact potential and low emission. A study of type 430 stainless steel as a substitute for titanium electrodes was initiated; however, efforts to produce a vacuum-tight ceramic-to-metal seal have been unsuccessful.